US Army Corps
of Engineers
Construction Engineering
Research Laboratories

USACERL Technical Report 98/03
December 1997

CONSTRUCTION PRODUCTIVITY ADVANCEMENT RESEARCH (CPAR) PROGRAM

Design and Performance Testing of Prestressed Precast Reinforced Concrete Double-Tee Beams With Web Openings

by

Mohsen A. Saleh, Pamalee A. Brady,
Amin Einea, and Maher K. Tadros

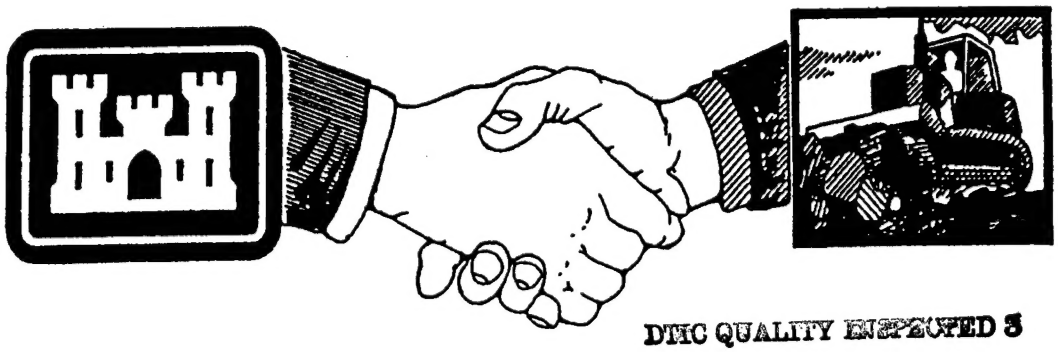

**A Corps/Industry Partnership To Advance
Construction Productivity and Reduce Costs**

The contents of this report are not to be used for advertising, publication, or promotional purposes. Citation of trade names does not constitute an official endorsement or approval of the use of such commercial products. The findings of this report are not to be construed as an official Department of the Army position, unless so designated by other authorized documents.

DESTROY THIS REPORT WHEN IT IS NO LONGER NEEDED

DO NOT RETURN IT TO THE ORIGINATOR

USER EVALUATION OF REPORT

REFERENCE: USACERL 98/03, *Design and Performance Testing of Prestressed Precast Reinforced Concrete Double-Tee Beams With Web Openings*

Please take a few minutes to answer the questions below, tear out this sheet, and return it to USACERL. As user of this report, your customer comments will provide USACERL with information essential for improving future reports.

1. Does this report satisfy a need? (Comment on purpose, related project, or other area of interest for which report will be used.)

_____

_____

_____

2. How, specifically, is the report being used? (Information source, design data or procedure, management procedure, source of ideas, etc.)

_____

_____

3. Has the information in this report led to any quantitative savings as far as manhours/contract dollars saved, operating costs avoided, efficiencies achieved, etc.? If so, please elaborate.

_____

_____

4. What is your evaluation of this report in the following areas?

   a. Presentation: _____

   b. Completeness: _____

   c. Easy to Understand: _____

   d. Easy to Implement: _____

   e. Adequate Reference Material: _____

   f. Relates to Area of Interest: _____

   g. Did the report meet your expectations? _____

   h. Does the report raise unanswered questions? _____

i. General Comments. (Indicate what you think should be changed to make this report and future reports of this type more responsive to your needs, more usable, improve readability, etc.)

5. If you would like to be contacted by the personnel who prepared this report to raise specific questions or discuss the topic, please fill in the following information.

Name: _____

Telephone Number: _____

Organization Address: _____

_____

_____

6. Please mail the completed form to:

Department of the Army
CONSTRUCTION ENGINEERING RESEARCH LABORATORIES
ATTN: CECER-TR-I
P.O. Box 9005
Champaign, IL 61826-9005

REPORT DOCUMENTATION PAGE

Form Approved
OMB No. 0704-0188

1. AGENCY USE ONLY *(Leave Blank)*	2. REPORT DATE	3. REPORT TYPE AND DATES COVERED
	December 1997	Final

4. TITLE AND SUBTITLE
Design and Performance Testing of Prestressed Precast Reinforced Concrete Double-Tee Beams With Web Openings

5. FUNDING NUMBERS
CPAR
LT3

6. AUTHOR(S)
Moshen A. Saleh, Pamalee A. Brady, Amin Einea, and Maher K. Tadros

7. PERFORMING ORGANIZATION NAME(S) AND ADDRESS(ES)
U.S. Army Construction Engineering Research Laboratories (USACERL)
P.O. Box 9005
Champaign, IL 61826-9005

8. PERFORMING ORGANIZATION REPORT NUMBER
TR 98/03

9. SPONSORING / MONITORING AGENCY NAME(S) AND ADDRESS(ES)
Headquarters, U.S. Army Corps of Engineers
ATTN: CERD-C
20 Massachusetts Ave. NW
Washington, DC 20314-1000

10. SPONSORING / MONITORING AGENCY REPORT NUMBER

11. SUPPLEMENTARY NOTES
Copies are available from the National Technical Information Service, 5285 Port Royal Road, Springfield, VA 22161.

12a. DISTRIBUTION / AVAILABILITY STATEMENT
Approved for public release; distribution is unlimited.

12b. DISTRIBUTION CODE

13. ABSTRACT (Maximum 200 words)

Conventional precast reinforced concrete double-tee joists may be made more structurally efficient by incorporating large openings in the web to accommodate environmental pipes and ducts. Double-tee joists with web openings may also reduce the total required building height, which would significantly lower costs for labor and materials during new construction.

This report presents a method for designing prestressed precast reinforced concrete double-tee joists with web openings. Alternative designs were investigated by varying parameters such as prestressing strand layout, opening pier width, and pier reinforcement. Test results from six prestressed concrete joists are presented to substantiate finite element analysis results. The effect of web openings on beam behavior is discussed, and a simple method for designing the beams is presented.

It is concluded that double-tee joists can be designed and manufactured with many web openings without jeopardizing beam strength. However, due to the effect of concentrated loading on shear failure modes in the tests, double-tee designs with web openings are recommended only floor and roof applications where only uniform loading will occur. Material costs associated with this design are slightly higher than for conventional double-tee members, but the design promotes an overall reduction in new construction costs.

14. SUBJECT TERMS
Construction Productivity Advancement Research (CPAR)
concrete testing
prestressed concrete
precast concrete

15. NUMBER OF PAGES
144

16. PRICE CODE

17. SECURITY CLASSIFICATION OF REPORT	18. SECURITY CLASSIFICATION OF THIS PAGE	19. SECURITY CLASSIFICATION OF ABSTRACT	20. LIMITATION OF ABSTRACT
Unclassified	Unclassified	Unclassified	SAR

Foreword

This research was performed for Headquarters, U.S. Army Corps of Engineers, under Construction Productivity Advancement Research (CPAR) Work Unit LT3, "Optimization of Prefabricated Joists." The technical monitors were Daniel Chen, CEMP-ET, and Stanley Green, CEMP-CE.

The work was performed by the Engineering Division (FL-E) of the Facilities Technology Laboratory (FL), U.S. Army Construction Engineering Research Laboratories (USACERL). The USACERL Principal Investigator was Pamalee Brady, CECER-FL-E. The CPAR research and development partner was the Center for Infrastructure Research at the University of Nebraska, Omaha. The University of Nebraska Principal Investigator was Dr. Maher K. Tadros. Larry M. Windingland is Acting Chief, CECER-FLE, and L. Michael Golish is Acting Operations Chief, CECER-FL. The USACERL technical editor was Gordon L. Cohen, Technical Information Team.

The contributions of the following individuals to this research are gratefully acknowledged:

- Mr. Larry Fischer of Concrete Industries, Inc., a CPAR industry participant
- Mr. Ervell Staab of Missouri River Division, a Corps of Engineers participant in this CPAR work.

COL James A. Walter is the Commander of USACERL and Dr. Michael J. O'Connor is the Director.

Contents

List of Figures and Tables

Figures

Tables

1 Introduction

Background

Existing precast concrete double-tee beams, which are widely used as floor and roof members, may be made structurally and economically more efficient by taking advantage of concepts used for steel truss joist systems. One means of increasing the economy of precast concrete joists is to add large web openings in the joist to permit the passage of mechanical ducts through the webs instead of under them. This approach reduces the floor-to-floor height in a building, and reduces wind and earthquake forces on the building through weight optimization. Cost savings may therefore be achieved in structural and foundation systems, and mechanical and electrical systems.

There are other potential advantages to such a configuration. Increasing the flange width of the double tee from a maximum of 8 ft to 10 ft or 12 ft may provide greater efficiencies. Making the double tee wider would reduce the weight of the double tee per square foot (square meter) by using only two webs for a width of 12 ft (versus two webs for a width of 8 ft). Furthermore, the erection time of a structure may be reduced because fewer double tees would be needed to support a given area. Also, fewer trips would be needed to haul double tees to the job site, fewer crane picks would be required to place the double tees, and fewer double tees would need to be leveled and connected in the field.

The U.S. Army Construction Engineering Research Laboratories (USACERL) investigated designs for reinforced concrete double-tee beams with web openings under the U.S. Army Corps of Engineers Construction Productivity Advancement Research (CPAR) program. The CPAR Partner in this study was the University of Nebraska, Omaha.

Objectives

The first objective of this CPAR work unit was to modify the existing precast concrete double-tee shape, which is widely used as floor and roof members, to make it more structurally and economically efficient. The project was to focus on

adding the largest web openings possible, which will allow passage of mechanical ducts through the webs instead of under them. The addition of web openings in double tees will reduce the floor-to-floor height in a building and reduce wind and earthquake forces on the building through weight optimization. Cost savings may therefore be achieved in structural and foundation systems, and mechanical and electrical systems.

Increasing the width of the double tee from a maximum of 8 ft to 10 ft or 12 ft was another modification to be investigated. This change in width may be possible in part through the use of high-strength concrete. Making the double tee wider will reduce the weight of the double tee per square foot (or square meter) by using only two webs for a width of 12 ft versus two webs for a width of 8 ft. Also, the increased width will reduce the erection time of a structure because there will be fewer double tees to erect. This approach would require fewer trips to bring double tees to the job site, fewer crane picks to place the double tees, and fewer double tees to be leveled and connected in the field.

The second objective of the program involved the relatively "high-risk, high-reward" development of a new hybrid joist that combines benefits of both the steel bar joist and the concrete double tee. This hybrid joist could be used for either floor or roof framing. The working ideas for the new joist involve using a truss configuration of precast concrete, with steel tendons in the top and bottom chords of the member.

This report encompasses the first objective of the CPAR project only. Documentation of the second objective is available in USACERL Technical Report 98/04, *Design and Performance Testing of Prestressed Precast Reinforced Concrete Hybrid Joists* (Saleh et al., December 1997).

Approach

The program approach stated in the CPAR Cooperative Research and Development Agreement (CPAR-CRDA) encompasses the following steps:

1. Information on the state-of-the-art technology in the areas of steel joists, precast concrete framing systems, prestressed beams with web openings, and emerging structural materials such as high-strength concrete, lightweight concrete, high-strength steel, and fiber-reinforced plastics for possible use in the hybrid joist will be compiled for documentation. The performance of existing systems will be

evaluated, standard designs will be assessed, and methods of testing both the modified tees and the hybrid joist will be reviewed.

2. Material strengths, opening size and placement, and reinforcement details will be refined for double-tee joist designs. Effects of span length and widening the double tees will be evaluated. Analysis of the modified double tees will be conducted, and design guidelines will be developed.
3. Two different systems of the hybrid joist will be developed. Prototype materials and joist configurations will be selected for the new joist designs. Analysis of prototype designs will be conducted for a number of spans and loading conditions. The designs will be optimized and final designs will be prepared for testing.
4. Double-tee specimens with web openings and hybrid joist specimens will be manufactured. These specimens may be full scale or small scale. For the hybrid joist, the components of the joist and the full joist itself will be tested. A test program will be defined, and the equipment and instrumentation requirements will be assessed.
5. Experimental tests to evaluate the performance of the hybrid joist components will be conducted. Double tees with web openings and complete hybrid joists will also be tested to determine their structural performance. Test data will be collected. The specimens will be produced by industry with input from both NTDC and USACERL. Testing of the double tees will be conducted by NTDC; testing of the hybrid joists will be conduced by USACERL.
6. Detailed analysis will be conducted on the experimental test results to evaluate the performance of the modified double tee and the hybrid joist. Further analysis, design and testing of the final joist designs will be demonstrated in a field project. USACE-MRD will assist in identification of an appropriate filed demonstration project.
7. The industry design method for elements of each type of joist will be established. Design aids in the form of tables or charts will be developed. The design philosophy will be articulated for structural engineering designers.
8. A final report will be prepared that documents the joist development, test verification, final prototype design, design procedure, plans for commercialization and technology transfer and conclusions as to the extent of the products' application and benefits to the U.S. construction industry.

This approach was followed in the conduct of this CPAR project. The current report documents work related to double-tee designs. As noted above, a separate report (USACERL TR 98/04) reports on the work related to hybrid joist designs.

Units of Weight and Measure

U.S. standard units of measure are used throughout this report. A table of conversion factors for Standard International (SI) units is provided below.

SI conversion factors

1 in.	=	25.4 cm
1 ft	=	0.305 m
1 sq in.	=	6.452 cm^2
1 sq ft	=	0.093 m^2
1 lb	=	0.453 kg
1 kip	=	453 kg
1 psi	=	6.89 kPa
1 psf	=	4.88 kg/m^2

2 Existing Joist Systems

Introduction

This chapter reviews currently available joist systems and research conducted to modify the designs of these systems as they relate to the design of a double tee with web openings. Several floor/roof framing systems are available for building construction. The most commonly used systems are *cast-in-place* concrete systems, *prestressed precast* concrete, and *steel joist* systems. Each of these systems offers specific construction advantages.

Cast-in-Place Concrete Systems

Several floor and roof framing systems use cast-in-place (CIP) concrete. These systems are known as flat slab, flat plate, waffle flat slab, and joist systems. The *flat slab* is usually 6 to 12 in. thick and spans up to 35 ft. The *flat plate* system is 5 to 10 in. thick and spans up to 30 ft. The *waffle flat slab* is 11 to 16.5 in. thick and spans up to 38 ft. A concrete *joist system* consists of closely spaced beams supporting a thin slab. A joist system is usually 11 to 24.5 in. in depth and spans up to 45 ft. The CIP concrete systems are advantageous as they require no fireproofing and have a higher stiffness than joist systems made of other materials thereby reducing deflections and vibrations in application. Their disadvantages include the following:

1. They require a large amount of field work for forming, placing the reinforcement, and pouring and finishing the concrete.
2. Quality varies widely.
3. Their construction is affected by weather conditions.
4. For the same span, deeper sections are required than for some other systems.

Also, these systems have heavy sections that require larger columns and foundations.

Precast Prestressed Concrete Joist Systems

Precast prestressed joist systems are used as either floor or roof members. The most popular sections in these systems are solid flat plates, hollow core sections, and double-tee sections. *Solid flat plates* have a depth range of 4 to 8 in. and the span range is from 10 to 35 ft. The depth of *hollow core sections* ranges from 6 to 15 in. and spans range from 12 to 50 ft. *Double-tee sections* are between 12 to 36 in. in depth and span between 40 and 90 ft. The main advantages of these systems are:

1. They are made under controlled conditions, so their quality is high.
2. Steel reinforcement is protected against corrosive and fire environments.
3. The sections have high stiffness, which reduces vibrations and deflections.
4. Using these systems reduces the amount of field labor required for erection.

However, these systems have some disadvantages. They, like CIP systems, are relatively heavy compared to the steel joist systems, so they require stronger structures and foundations for their support. This will lead to higher seismic loads. They also do not allow passage of service ducts through their webs.

Open Web Steel Joist Systems

The open web steel joist system (OWSJ), or *bar joist* system, consists of top and bottom chords constructed of steel double-angles with diagonal steel bars welded to the angles. This joist system is used to support cold-formed corrugated steel sheets with a cast-in-place slab. Different series of OWSJs are available on the North American market, such as K-Series, CS-Series, LH-Series, DLH-Series, and SLH-Series (Vulcraft 1995), for example.

The *K-Series* is designed to support uniformly distributed loads. The design of this series is based on a yield strength of 50,000 pounds per square inch (psi). The depth of K-Series joists ranges from 8 to 30 in. covering spans from 8 to 60 ft. *The CS-Series* was introduced to address concentrated or nonuniform loading. For the chords, uniform design moment and shear diagrams are used. That is, the moment and shear capacity are constant throughout the span. Also, all webs are designed for 100 percent stress reversal.

The *LH-* and *DLH-Series* were developed to address longer spans. The LH-Series is suitable for the direct support of floors and roof decks in buildings, and the DLH-Series is suitable for the direct support of roof decks in buildings. In

the design of LH- and DLH-Series, the chord or web sections are based on a yield strength of at least 36,000 psi. The depth of LH-Series ranges from 18 to 48 in., which can cover spans from 21 to 96 ft. The DLH-Series has a range of depth from 52 to 72 in., covering spans from 61 to 144 ft. The SLH-Series are "Super Longspan Steel Joists." This term refers to open web, load-carrying members utilizing hot-rolled steel shapes. The SLH-Series is suitable for the direct support of roof decks in buildings. The joists have a range of depth from 80 to 120 in., which can cover spans from 80 to 240 ft.

However, open web steel joists have low overall stiffness, which may result in excessive vibrations and deflections. The low stiffness and light weight of this structural system also requires that effects of uplift loads be examined in design. Furthermore, steel joist systems have very low resistance to fire and corrosion, and the systems require intensive labor to erect.

Web Openings in Concrete Joists

To address a major disadvantage in precast concrete double tees several studies have been undertaken since 1967 to develop precast prestressed concrete beams with web openings. The research has focused on designing for flexural failure, preventing shear failure, limiting deflections, and optimizing shape, size, and location of web openings. The following paragraphs provide a summary of these research studies.

Experimental Research

Ragan and Warwaruk (1967) conducted the first experimental study on pre-stressed concrete T-beams with large web openings. Four model beams and two full-size T-beams were tested in the program. All model beams were subjected to two-point loads while the loading of full-size beams was approximately uniform. The results showed that the failure moment was two to three times that at which cracking was first observed. The researchers concluded that sizable web openings could be accommodated without sacrificing strength and that deflections of beams with openings were not significantly greater than for beams without openings.

Suave (1970) conducted experimental work on prestressed concrete T-beams with large web openings. He investigated varying two-point load positions, shear reinforcement, and additional longitudinal reinforcement in the shear spans. He tested nine beams, one of which was solid and the rest with eight openings, 8 in.

tall by 16 in. wide, separated by 8 in. wide posts. Suave drew the following conclusions:

1. Additional shear reinforcement served to increase the load-carrying capacity of a beam with large web openings.
2. Increasing the supplementary longitudinal reinforcement did not significantly increase the shear capacity of the beams.
3. Additional vertical reinforcement placed in the posts gave these posts the capacity required to localize the failure in the lower chord if this chord had no vertical reinforcement.
4. The reinforcing of both the posts and the lower chord resulted in a redistribution of stresses in the shear span such that all sections were more equally stressed in diagonal tension.

LeBlanc (1971) conducted tests on prestressed T-beams. He investigated the behavior of beams with different opening shapes, number of prestressing strands, and amount of shear reinforcement. Ten beams were tested. Six contained 8 in. tall x 16 in. wide parallelogram-shaped openings, three contained rectangular openings of the same overall dimensions, and one beam had no openings. He concluded that beams with parallelogram-shaped openings performed better than the beams with rectangular shaped openings. Increasing the number of prestressing strands required an increase in shear reinforcement to ensure that the beam failed in flexure.

Barney, Corley, Hanson, and Parmelee (1977) expanded on the work done by Ragan and Warwaruk (1967). They tested 5 short span and 13 long span full-size precast prestressed concrete T-beams. Figure 2.1* shows the details of the long-span beam sections; Figure 2.2 shows the loading location for the tested beams. The variables investigated were size and location of opening along the span, type and amount of shear reinforcement, and amount of primary flexural reinforcement. The capacity of specimens with openings in high shear regions was limited by an unrestrained shear crack extending from the lower side of the opening toward the support. These cracks normally propagated along the prestressing strands. In some beams, the cracks extended into the region required for strand embedment causing the strand to slip. The variables having greatest effect on beam strength and behavior were the location of web openings along the span and the amount of web shear reinforcement. The behavior of these beams was similar to a Vierendeel* truss. Barney et al. recommended that

* Figures are presented at the end of the first chapter in which they are discussed.

* Vierendeel truss: a Pratt truss without diagonal members having rigid joints between the chords and verticals.

adjacent web openings be separated by web elements (posts) having overall width-to-depth ratios of at least 2.0, where the width of the post is the distance between adjacent stirrups. The authors concluded that large web openings can be placed in prestressed concrete beams without sacrificing strength or serviceability. However, openings must be located outside the required strand embedment length and adequate shear reinforcement must be provided adjacent to openings. They developed a design procedure for prestressed double-tee beams with multiple web openings.

Salam and Harrop (1979) studied the effects of circular web openings on the performance of prestressed concrete beams. The parameters studied were opening size, location, and reinforcement. Consideration was given to the prediction of beam strength and to different methods of reinforcement around the openings. It was concluded that beams with multiple circular openings had peak stresses below those for beams with a single hole. Also, compensation for the presence of the holes is best provided by vertical stirrups at the sides of the holes. This reinforcement resists the horizontal splitting due to prestress and diagonal tensile stress at working load. The researchers concluded that a perforated beam can be as strong as a similar solid beam provided the holes do not protrude into the ultimate rectangular stress block required to produce flexure failure.

Kennedy and El-Laithy (1982) investigated both theoretically and experimentally the behavior of prestressed concrete beams with rectangular openings. They were particularly interested in behavior at the prestressing force transfer stage. Eighteen post-tensioned concrete beams were used for the experimental program. The main parameters studied were the depth of the opening and its horizontal and vertical location. The results indicated that the depth and the vertical location of the opening were the two parameters that significantly affected the stresses around the opening. The horizontal location of the openings did not have an appreciable influence on the stresses at the transfer stage. The analyses also revealed that the maximum vertical tensile stress occurs at or near the mid-depth of the opening, and this stress increases linearly with the increase in the prestressing force until a horizontal crack is formed. The presence of the opening also gives rise to significant shear stresses near the four corners of the opening. The influence of transverse reinforcement on the cracking load was also studied. It was found that reinforcing against the vertical tension force was effective in increasing the cracking load by approximately 30 percent for both rectangular and T-beams. It was concluded that:

1. The presence of an opening gives rise to a potential splitting-tension field, followed by a compression field, whose distances are functions of the depth and vertical location of the opening.
2. The assumption of plane sections remaining planar does not apply in the vicinity of the opening.
3. The presence of an opening increases the deflection only slightly at the transfer stage.

Dinakaran and Sastry (1984) conducted tests on T-beams with openings. The variables considered were the size of opening, location of openings, and type of reinforcement around openings. The openings were positioned both in the shear span as well as in the interior of the span. The results showed that the first crack appeared from the side of the opening closest to the support for beams having openings in the shear span due to the shear concentration at the opening corners. This crack propagated toward the support. Beams having openings in the constant moment zone did not exhibit crack propagation from the corner of the opening. The test results also revealed that the location of the opening has the greatest effect on the strength and the behavior of the beams. It was concluded that post-tensioned prestressed concrete T-beams with large openings behave similarly to a Vierendeel truss. Also, beams with openings in the high-moment region behave better than those having openings in the shear span, and their ultimate moment capacity is also greater. It was found that vertical stirrups and hooks provided adjacent to openings control cracking. Compressive struts and tensile struts carry external shear in proportion to their cross-sectional areas. The influence of openings on deflection is minor in properly reinforced beams.

Kennedy and Abdalla (1992) investigated the response of prestressed beams with openings for the purpose of developing a design procedure to overcome cracking at openings. This study focused on the potential splitting forces that may develop at the edges of the openings at prestressing force transfer stage and at the corners of the openings at service load stage. A parameter study of specific variables was also conducted analytically. These variables were horizontal and vertical locations of the openings, opening width and depth, and type of cross section. An experimental study of post-tensioned beams with web openings was also conducted to justify the proposed design process. Tests were carried out on 13 post-tensioned beams. Six of the beams were rectangular in section, five were T-section, and the remaining two were I-section. The layout of the specimens is shown in Figure 2.3. As shown in Figure 2.4, the experimental results revealed five critical locations for potential cracking of prestressed beams with openings:

1. the edges of the opening due to prestressing force
2. at the corners of the opening due to the framing action at the opening
3. in the opening chords due to the flexural stresses resulting from the secondary moments in these chords
4. in the tension chord due to the normal tensile stresses in that chord
5. in the opening chords due to shear.

The first of the above five types of potential cracking was assumed to occur at the transfer stage due to the prestressing force only. The rest of the cracking would occur at the service load stage due to applied vertical loads. The last two types of cracking may cause the complete collapse of the beam. Kennedy and Abdalla's design method was developed for beams with a single web opening.

Savage (1993) at University of Nebraska investigated variables including the effect of two prestressing strand depression points, opening size and location, and use of high-strength concrete on double-tee beams with openings. Figure 2.5 shows the typical dimensions of the test specimens. The design of the specimen, was based on finite element analysis and the design procedure by Barney et al. (1977). Four full-sized specimens were tested to failure. Figure 2.6 shows the reinforcement details of these specimens. They concluded that:

1. The ultimate strength of the beams was not affected by the presence of web openings.
2. The double tees with web openings behaved like Vierendeel trusses.
3. None of the compression chords above the openings exhibited buckling behavior.
4. The beams should be designed not to crack under service loads.
5. The addition of prestressing strands above the openings was effective in counteracting the tensile stress concentrations caused by end moments acting on the compression chord.

Analytical Methods

Several researchers have developed procedures for the analysis and design of prestressed concrete beams with web openings.

Barney et al. (1977) developed both a simplified and an iterative analysis procedure. Barney explains that primary stress results from the two chords resisting moment in unison; secondary flexural stresses in the chords are also created due to a statically indeterminate portion of the total shear force acting at the section. In the design method, hinges are assumed at the mid-length of each chord (Figure 2.7). Resulting equations for top and bottom chord compression

and tension are derived as a function of moment, prestress force, distance of prestress force from the neutral axis, and distance between centroidal axes of the chords. These equations assume no cracking has taken place and apply to load stages at transfer of prestress service.

With cracking, a redistribution of forces takes place and Barney presents a conservative iterative technique to find values for chord shear forces at ultimate load that are based upon a cracked section moment of inertia. This technique is valid for all loads up to those causing full-depth cracks in the bottom chord member of the beam. Barney's test results indicated that after full-depth cracking of the bottom chord, additional shear is carried entirely by the compressive (top) chord.

This analytical procedure is also applicable to beams with concrete toppings. It is necessary to distinguish between the loads that are applied to the beam itself and the loads applied to the composite system. In an uncracked state, the beam is assumed to carry all the dead load and prestress force. Once cracking ensues, some of the dead load and prestress force, along with all of the load applied after the concrete topping is cast is assume to be carried by the composite system. The models by Barney et al. are valid when the chords behave primarily as flexural members and for beams having straight prestressing strands.

Kennedy and Abdalla (1992) performed a theoretical study using a nonlinear finite element program. Based on the results from the finite element solution, which were substantiated by experimental tests, a simple method was developed to estimate the vertical tensile force around web openings due to the prestressing force. The model permitted placement of reinforcement at different locations (running in horizontal, vertical, and inclined directions) around the opening with various cross-sectional areas and arrangements. The concrete under compression was modeled by an elastic-plastic theory and isotropic hardening was accounted for. The model was a "smeared crack" model in that it did not track individual macro cracks. However, at each integration point of the finite element model, the presence of cracks was entered in the calculations by the way in which the cracks affected the stresses and the material stiffness associated with the integration point. The finite element model was an idealization and used to get an overall idea of beam behavior and stresses.

The most relevant analysis process for this particular study is that developed by Savage (1993). The objective of the model was to get an idea of the deflection characteristics of beams with web openings and the location and magnitude of stress concentrations. The method began with a working stress analysis for

critical sections at the beam end and at midspan through an opening. Variables included concrete strength, number of prestressing strands, and opening depth. This analysis was an approximation as secondary moments caused by shear in the chords, above and below the openings, were neglected. The working stress model was used as a basis to begin finite element analysis.

The finite element analysis produced estimations of axial stresses at transfer as well as service, and shear and principal tensile stresses at ultimate load. The longitudinal stresses were checked against American Concrete Institute (ACI) working stress limits (ACI 318, 1995). Shear and principal tensile stresses at ultimate load were used to aid in the design of shear stirrups. The finite element analysis showed areas of high stress concentration. The model is an elastic one and does not take cracking into account. Thus loads at ultimate load—and to a lesser degree, service load—are not exact.

Conclusions on Previous Studies

From previous research it can be concluded that the prestressed concrete beam with web openings behaves similarly to a Vierendeel truss. The deflection of these beams is similar to that of beams without web openings. The most common failure mode observed in the experimental tests of beams with web openings is the formation of a hinging mechanism in the posts. Web openings should be placed outside of the strand development length and the high shear zone. Vertical stirrups should be placed on each side of an opening to control cracking. The chord below an opening may crack at loads less than the service load.

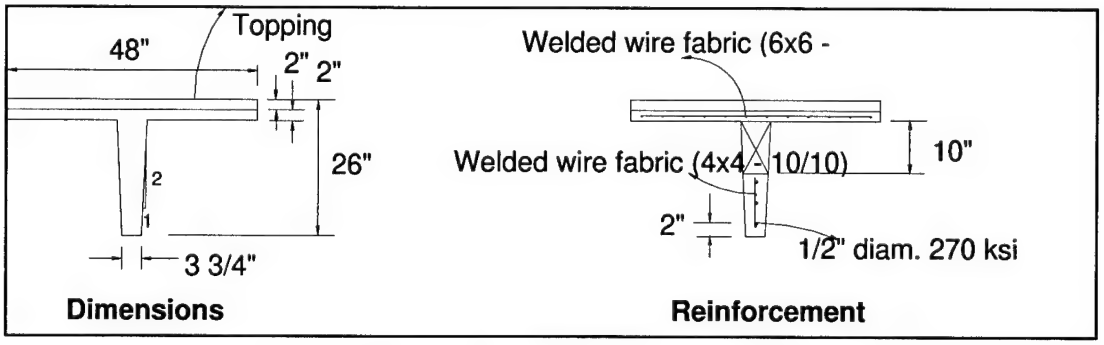

Figure 2.1. Long-span test beam sections from Barney et al. (1977).

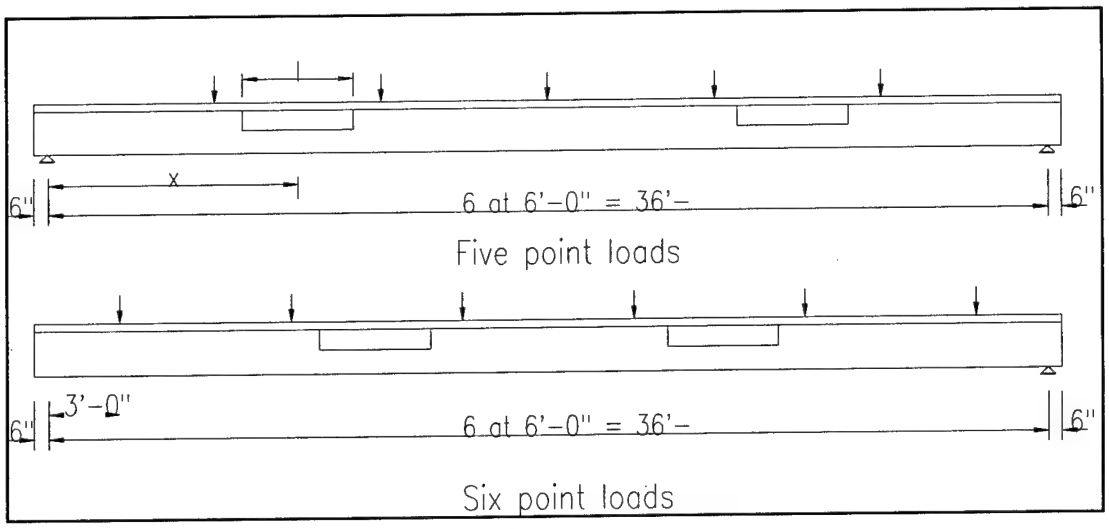

Figure 2.2. Loading location for test beams in Barney et al. (1977)

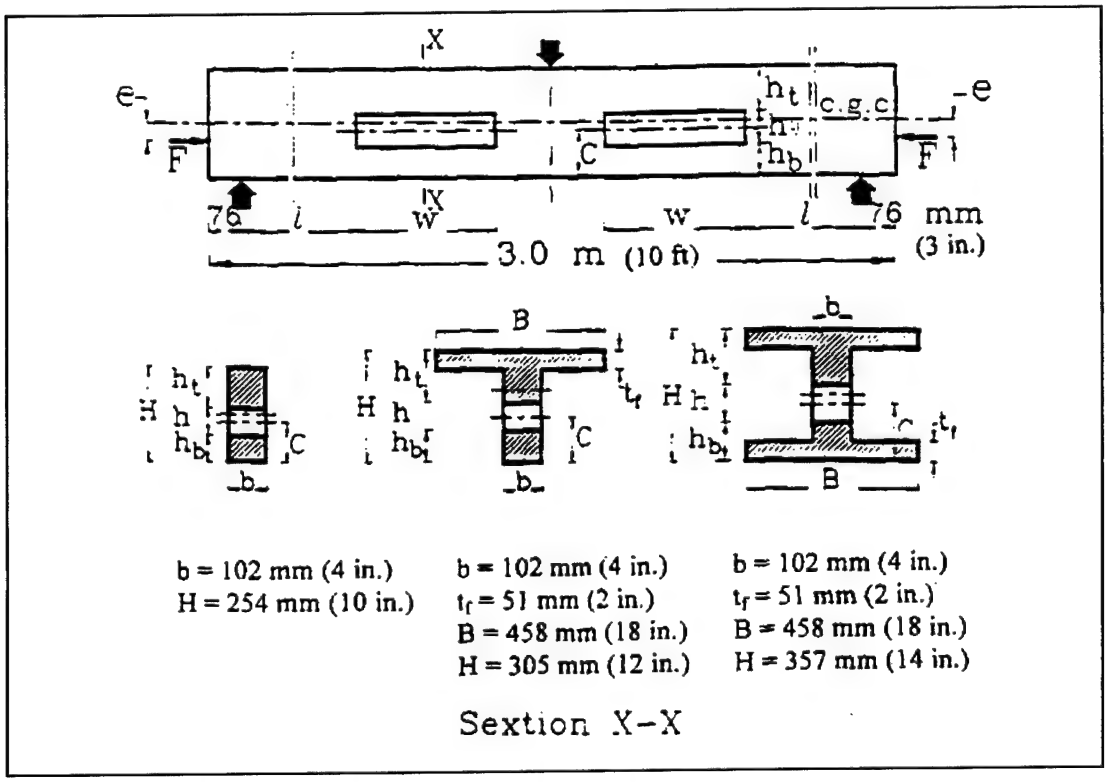

Figure 2.3. Layout of test beams adapted from Abdalla (1993).

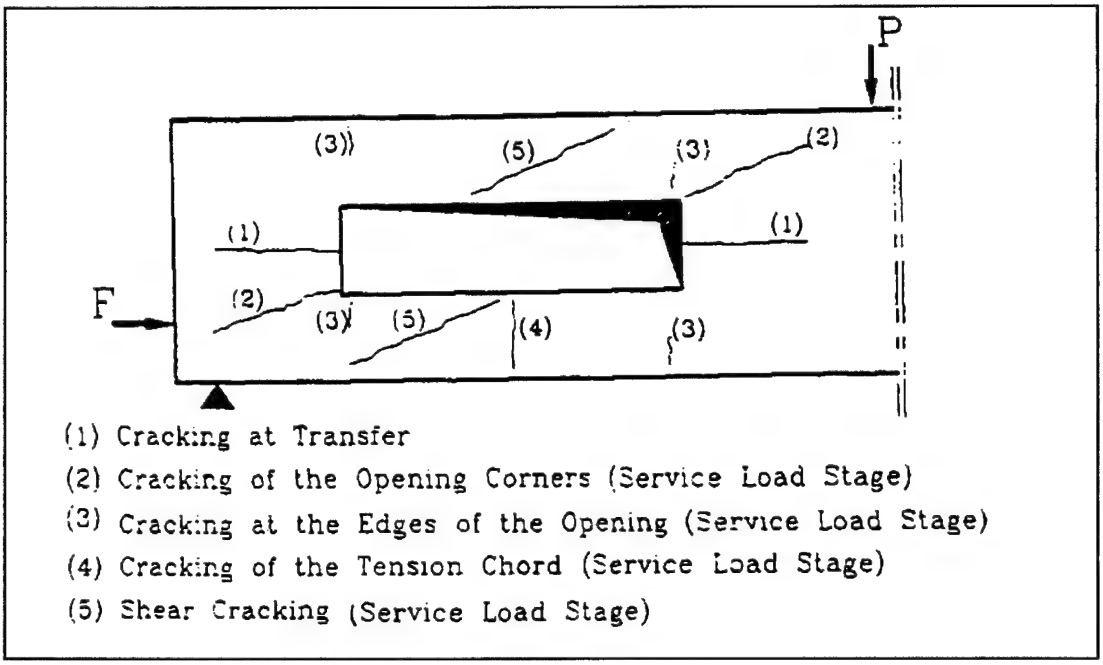

Figure 2.4. Different types of cracking around beam opening, adapted from Abdalla (1993).

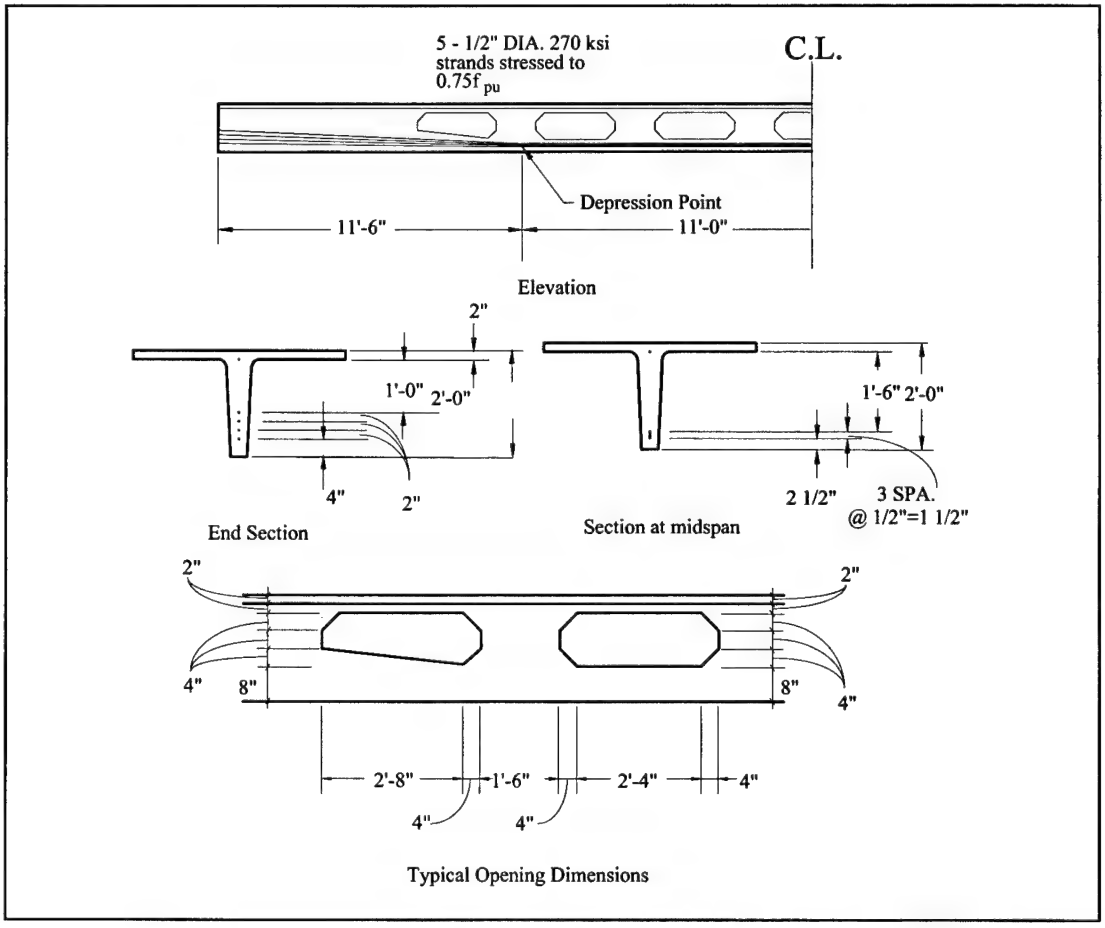

Figure 2.5. Concrete dimensions and strand profile by Savage (1993).

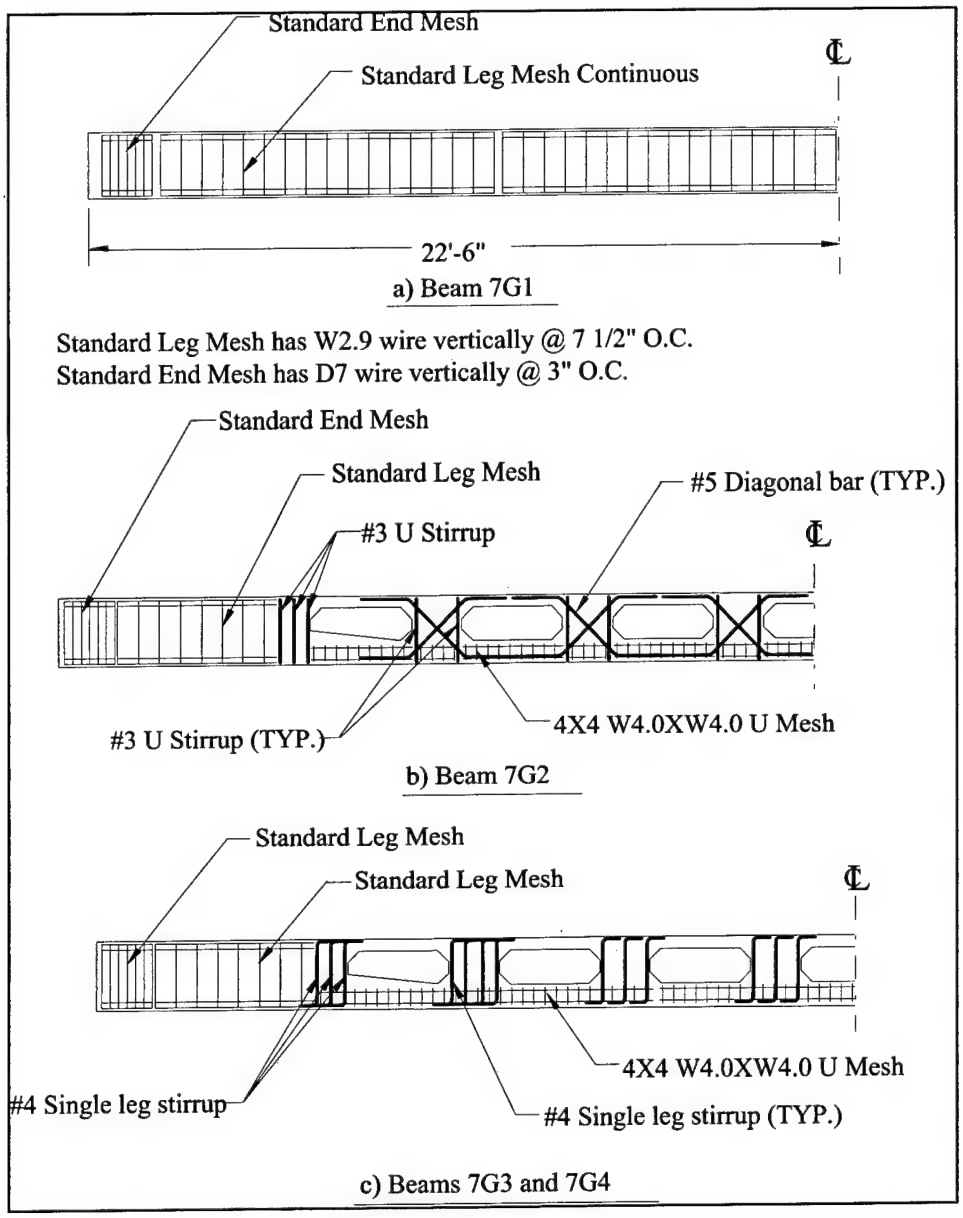

Figure 2.6. Reinforcement details by Savage (1993).

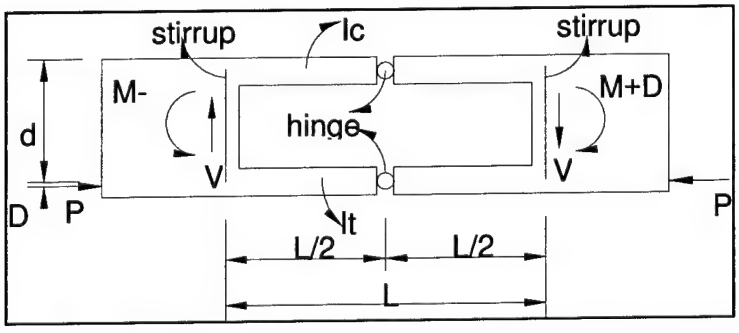

Figure 2.7. Idealized model of a beam with web openings adapted from Barney et al. (1977).

3 Joist Design

Introduction

This chapter describes the development of a prototype design for a prestressed precast concrete double-tee beam that has integral web openings. The research focused on modifying the beam developed by Savage (1993). The main variables investigated in the design were prestressing strand layout, pier width, opening size, shape and placement, and shear reinforcement at the openings. Design procedures developed by Barney et al. (1977) and Kennedy and Abdalla (1992) were modified for use in designing the beams.

Description of Proposed System

The double tees to be designed were envisioned for use in office and residential construction. A span of 45 ft and a tributary width of 8 ft were chosen for the design. Loads were 25 psf dead load to represent a 2 in. topping slab, 20 psf superimposed dead load, and 50 psf office live load. The total uniform superimposed service load was therefore 95 psf.

Based on the selected span and load parameters and the *PCI Design Handbook* (1992), a joist with an overall depth of 24 in., a 2 in. thick top flange, and a web tapering from 5.75 in. at the top to 3.75 in. at the bottom was selected (Figure 3.1). The test results of Savage (1993) showed that joists with a 24 in. overall depth required four prestressing strands for flexural resistance. Additionally, one strand should be placed at the bottom of the top flange to control the localized tensile stress concentration caused by end moments acting on the compression chord.

Two strand profiles were considered for the four strands in the bottom of the joist: a straight profile and a draped profile. In the straight profile, the strands were spaced at 1.5 in. apart along the entire beam span. In the draped profile, the strands are spaced at 2 in. apart at the end of the beam, and at 0.5 in. apart between the depression points. In the straight strand configuration the center of gravity of the strands is 2.75 in. from the bottom of the beam. The depression

points were placed at 7 ft, 2 in. from the beam ends. This was less than the length of 11 ft, 6 in. used by Savage (1993). In the draped configuration, the distance between the center of gravity of the strands to the bottom of the beams at the end section is 7.00 in.; this distance at midspan is 3.25 in.

A variety of shapes are possible for web openings, including ellipses, circles and rectangles. The ellipse and circle are the best shapes to reduce stress concentrations around the openings. However, these shapes are not highly flexible for service ducts. The shapes' bases are not level, permitting pipes to roll in the openings. Rectangular-shaped openings were used in the current analysis and design of the double tees because they provide greater flexibility of use than the other opening shapes. Although rectangular openings may produce a stress concentration at the corners of the opening, it was believed that this could be controlled with proper reinforcement.

Savage (1993) showed that the most promising web opening shape was rectangular with chamfered corners. Several alternative shapes were considered for the corners of the openings to reduce stresses concentrations, as shown in Figure 3.2. These included chamfered corners, curved corners, and circle ends. Analyses were conducted to optimize the corner shape of the rectangular opening to reduce stress concentrations. An opening size of 12 in. deep by 36 in. wide was used. The width of the pier between openings was 10 in. to permit a maximum number of openings. For the straight strand profile, seven complete openings were used and two small openings (12 in. by 30 in.) were used at each end. For the draped strand profile, eight complete openings were used and two small triangular openings (12 in. by 30 in.) were used at each end. The openings were placed at the center of the span, as shown in Figure 3.3. Based on the results of previous research, openings were not placed in high shear zones or in the length required for strand development.

Design Analysis

Based on the symmetry of the double-tee configuration, a single tee section with a flange width of 4 ft was used in all analyses. The shape of the joist was finalized based on several trial and error analyses. Using the preliminary designs described above, analysis in two stages was performed. First, working stress analysis was conducted to ensure the satisfaction of stresses at different construction and loading stages. Second, finite element modeling was carried out to predict the behavior of the joist and identify stress concentration regions.

In all analyses prestressing strands were assumed to be 0.5 in. in diameter with 270 kilopounds per square inch (ksi) ultimate strength and low relaxation properties. Mild reinforcing was assumed as Grade 60 deformed bars. Concrete with a compressive strength of 5500 psi at prestressing force transfer and 7000 psi at 28 days was assumed.

A working stress analysis was undertaken to check the stresses at different stages. Critical sections were determined to be at the beam end and at midspan through an opening. Several variables were investigated with the working stress models, including strand profile and shear reinforcement. Working stress analyses neglected secondary moments in the chords above and below the openings caused by shear. However, these analyses provided an overall indication of stresses and behavior of the beam for the different loading stages.

Finite element analysis was conducted using ANSYS50A finite element software (ANSYS, Inc., Canonsburg, PA 15357). To understand the overall behavior of the joist, the double tee was modeled as a two-dimensional structure. Several element types from the element library were evaluated to determine the appropriate elements for concrete and prestressing strands. A rectangular plane stress element, PLANE82 in ANSYS50A, was used to model the concrete. This eight-node element is defined by two degrees of freedom, UX and UY, at each node. An element thickness of 4.75 in. simulated the web of a single tee (i.e., half of the symmetrical double tee) and an element of 48 in. thickness simulated the top flange. A two-dimensional span element, LINK1, was used to model the prestressing strands. The two-node element is a uniaxial tension-compression element with two degrees of freedom at each node (UX, UY). As in a pin-joined structure, no bending of the element is considered. The element is defined by two nodes, the cross-sectional area, an initial strain, and the material properties. The initial strain in this element was used to present the prestressing forces on the element. The element was used to simulate the four strands in the bottom of the joist and the single strand in the bottom of the top flange.

The finite element model designated *Model 1* represented the 45 ft long single tee with eight rectangular web openings and two triangular openings. It had a pier width of 10 in. and a draped strand profile. The critical results from the finite element analyses were axial stresses, principal tensile stresses, and shear stresses at transfer of prestressing force, service loads, and ultimate loads. The final finite element analysis indicated several stress concentrations. There was a compressive stress concentration near the depression points at transfer of the prestressing force. Also, the analysis indicated tensile stresses in the posts between openings at transfer. For both service and ultimate loads, the highest

tensile and compressive stress concentrations occurred in the chords above and below the first full opening at each end of the beam. There were also stress concentrations at the corners of the openings and a stress concentration extending from the edge of the end openings toward the supports. The analysis indicated a compressive shear stress that ran diagonally through the posts between openings in a direction toward the supports.

A second model, *Model 2*, was developed to evaluate the effects of reducing the pier width to 6 in. This model had 11 openings measuring 12 in. tall by 36 in. wide. The finite element analysis showed that reducing the pier width to 6 in. increases the stress concentration around the openings. However, the performance of the beam was still acceptable.

Finite element models using straight strand profiles with a spacing of 1.5 in. were also evaluated. Results from the analysis showed stress concentrations at transfer at the ends of each strand. Longitudinal stresses in each model were checked against ACI code working stress limits. The shear and principal tensile stresses at ultimate load aided in the design of the shear stirrups.

Selection of Test Designs

The finite element models were used to analyze overall beam behavior rather than to derive exact values of stresses and deflections. The method involved some approximations that can affect the results. In each case, the web of the double tee was modeled as a constant 4.75 in. thickness. This constant thickness produces conservative stress values. Also, as an elastic model, cracking is not considered.

Three single-tee joist configurations were selected for further study in an experimental program. Two designs incorporated straight strands; one of these designs had 10 in. wide piers at the openings and the other had 6 in. wide piers at the openings. One design incorporated draped strands. Based on the uniform loading of the analytical models, a deflection capacity greater than three times the allowable deflection limits at service loading may be anticipated. Ultimate uniform loading also would produce a flexural failure mode in both the draped and straight strand tee beams.

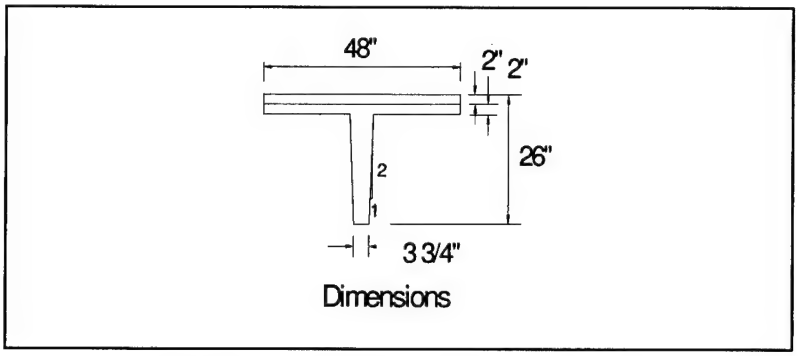

Figure 3.1. Dimensions of analytical model for single-tee.

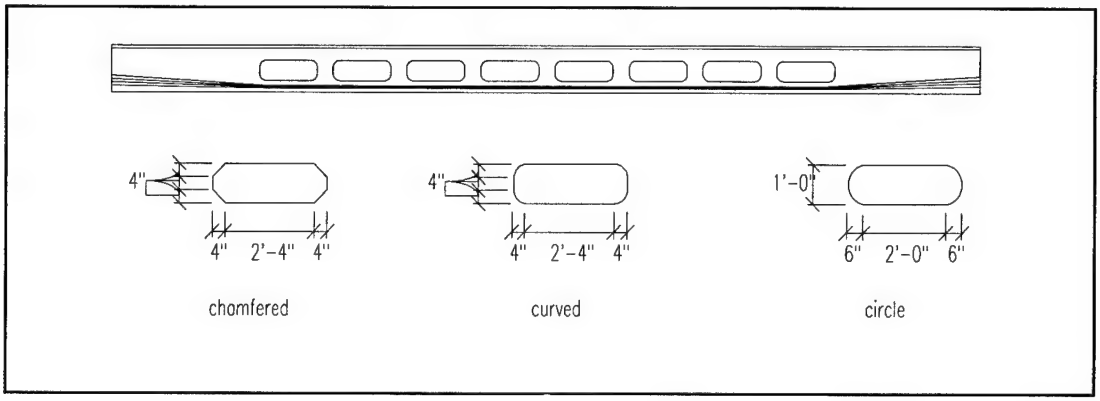

Figure 3.2. Alternative opening shapes.

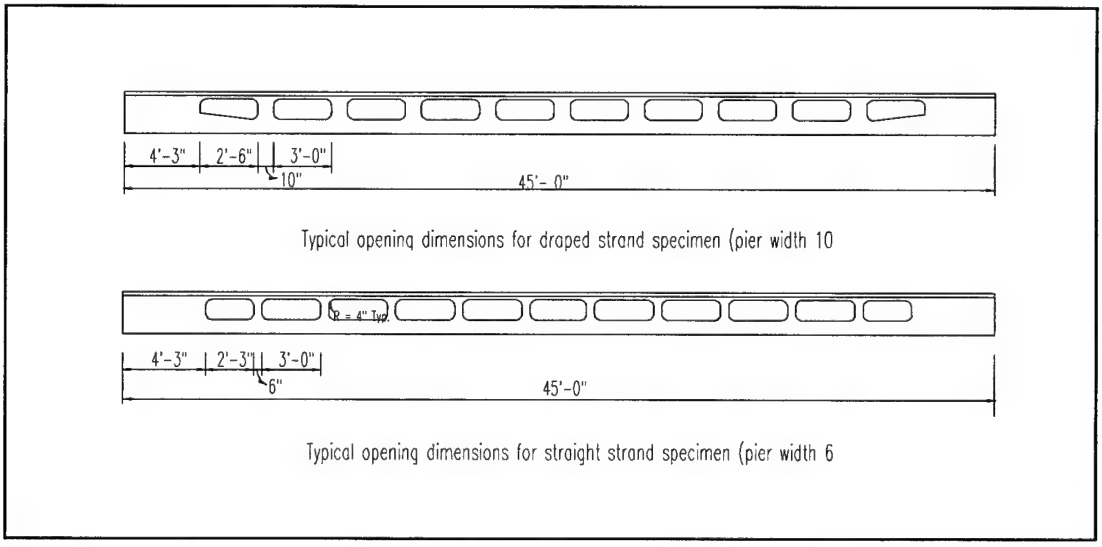

Figure 3.3. Opening locations in single-tee with straight and draped strands.

4 Experimental Test Specimens

Introduction

This chapter describes the six full-scale prestressed reinforced concrete single tee joists (i.e., half of a symmetrical double tee) fabricated for the experimental tests. Two series of joists were constructed by Concrete Industries, Inc., of Lincoln, NE. Series 1 comprised four joists to evaluate such variables as the number of openings, strand profile, pier width, and the reinforcement details around the openings. They were configured as follows:

- two draped strand specimens with different shear reinforcement
- one straight strand specimen with a 10 in. web pier
- one straight strand specimen with a 6 in. web pier.

The two joists comprising Series 2 were configured as draped strand specimens with specific shear reinforcement and 10 in. web piers.

Description of Specimens

The design of the joists was based on the preliminary analysis described in Chapter 3. As in the design analysis, test structures used cross-sectional symmetry in that one half of a double-tee joist was constructed. One web supported one half of the normal slab width. Joists in Test Series 1 were designated D10R, D10W, S10W, and S11P. Their designations are explained in the following paragraphs and summarized in Table 4.1. The overall shapes and dimensions of all joists were the same. The joists had a typical tee-shaped cross-section with a web thickness that tapered from 5.75 in. at the top to 3.75 in. at the base. Overall depth of the specimens was 24 in. (Figure 4.1). The 2 in. thick top flange of all the specimens was similarly reinforced; welded wire fabric—4x4-W4.0xW4.0—was placed at slab mid-depth.

Two specimens had draped strand profiles with two depression points at 7 ft, 2 in. from each end of the specimen. The spacing between the strands was 2 in. at the end of the specimen and 0.5 in. at the center of the specimen. Two specimens

had straight strand profiles. The spacing between strands was 1.5 in. to maximize the prestressing force contribution. This is not in conformance with ACI 318-95, Section 7.6.7, which requires the clear distance between pretensioning strands to be not less than 4 d_b of the strand, or 2 in. for 0.5 in. diameter strand. To resist the stresses caused by reducing the strand spacing, spiral reinforcement was provided around the end of each strand. Reinforcement was #2 with a 2 in. diameter spiral and 1 in. spacing. In both configurations, four strands were placed at the bottom of the specimen and one strand was placed at 22 in. from the bottom of the specimen, above the openings. Profiles are shown in Figures 4.2a and 4.2b for the draped and straight strand arrangements, respectively. The first letter of each specimen designation denotes the strand profile: D for draped strands and S for straight strands.

The second number of the joist designation indicates the number of web openings in the specimen. The draped strand specimens, D10R and D10W, had 10 openings. Eight openings, 12 in. deep by 36 in. wide, were placed between the strand depression points. One additional opening, 12 in. deep by 30 in. wide, was placed at each end of the specimen outside of the depression point. Pier width at each opening was 10 in. The opening sizes and locations for draped strand specimens are shown in Figure 4.3.

Straight strand specimens had either 10 or 11 openings. Specimen S10W was designed with 10 openings 12 in. deep by 36 in. wide located in the middle of the joist length. Specimen S11P was designed with nine openings in the middle of its length and an additional opening at each end of the specimen with dimensions of 12 in. deep by 30 in. Pier width in S10W was 10 in., and a 6 in. wide pier was used in specimen S11P. The opening sizes and locations for the straight strand specimens are shown in Figure 4.4.

Shear reinforcement in the bottom chord of specimens D10R, D10W, and S10W was provided by a U-shaped 4x4-W4.0xW4.0 welded wire fabric mesh 6 in. tall. This U-shaped mesh was designed to control cracks extending from the bottom corners of the openings and to control shear cracking in the tension chords. Shear reinforcement in the piers around web openings was designed for high stress concentrations that extend from the opening sides. Different configurations of shear reinforcement were investigated in each of the four specimens. The last letter of the joist specimen designation represents the type of shear reinforcement in the piers of the web openings: W for welded wire fabric mesh, R for rebar reinforcement, and P for the strap plate. The shear reinforcement of specimen D10R in the area of the openings was provided by U-shaped stirrups. A #5 U-shaped stirrup was placed on both sides of the openings. Two additional #5

U-shaped stirrups were placed at the end of the last openings. In this specimen the #5 U-shaped stirrups on each side of the openings did not allow the U-shaped mesh below the openings to run continuously. The U-shaped meshes were therefore spliced at the middle of the openings. Shear reinforcement in the solid sections at the ends of this specimen was standard leg mesh (Figure 4.5). The reinforcement details of Specimen D10R are shown in Figure 4.6.

The objective of the design of the shear reinforcement for specimen D10W was to simplify the stirrup details by using mesh. Shear reinforcement at the solid ends of specimen D10W was U-shaped 4x4-W4.0xW4.0 welded wire fabric mesh. This mesh extended the entire depth of the specimen and to the middle of the bottom chord of the first opening at each end. The shear reinforcement in the area opening piers was also U-shaped 4x4 W4.0xW4.0 welded wire fabric mesh. The mesh in each pier consisted of three wires, one wire at each end of the pier and one in the middle (Figure 4.5). This mesh extended from the pier edge under the opening to the middle of the bottom chord. The reinforcement details for Specimen D10W are shown in Figure 4.7. Shear reinforcement for specimen S10W was the same as for D10W. The reinforcement details for this specimen are shown in Figure 4.8.

In specimen S11P the shear reinforcement in the solid ends of the joist was a U-shaped 4x4-W4.0xW4.0 welded wire fabric mesh, as used for specimens D10W and S10W. The shear reinforcement in each opening pier was a 3/8 in. x 4 in. x 5 ft, 8 in. steel strap plate, Grade 36. It was placed at the middle of the pier with 1 in. cover on each side of the plate (Figure 4.9). The design of this strap plate was based on the results of finite element analysis and the PCACOL program (version 2.20, Portland Cement Association, Skokie, IL) to check the pier capacity. Twenty 1 in. diameter holes at a spacing of 3 in. were made in the plate to increase its confinement with surrounding concrete. Unlike all other specimens, there was no other reinforcement in the bottom chord below the openings in S11P. The reinforcement details of Specimen S11P are shown in Figure 4.10.

A second series of test specimens—two joists of identical design—was configured to verify the performance of the final design for a single tee with web openings. The specimen designations were D8R1 and D8R2, and details of both are described in Table 4.1. They had an overall depth of 24 in., with the draped strand profile using depression points at 7 ft, 2 in. from the end of the specimens. The strand spacing at joist ends was 2 in., and it was 0.5 in. in the center of the joist between depression points. The distance between the strand center of gravity and the bottom of the specimen was 7 in. at the ends and 3.25 in.

between depression points. The 2 in. thick top flange was reinforced the same way as specimens in the first series, with welded wire fabric 4x4-W4.0xW4.0 placed at slab mid-depth.

The specimens had eight openings measuring 12 in. deep by 36 in. wide. The two triangular openings present in the previous specimens D10R and D10W were eliminated to simplify joist production. To reduce stress concentrations at the openings, the corners were curved with a radius of 4 in. Figure 4.11 shows the overall joist dimensions and the number and placement of openings. Shear reinforcement at the specimen ends was standard leg mesh with details shown in Figure 4.5. Shear reinforcement in the bottom chord of the openings was U-shaped 4x4-W10xW10 wire fabric mesh. This mesh was spliced at the middle of selected openings, as illustrated in Figure 4.12. Pier shear reinforcement consisted of three bundled #3 U-shaped stirrups placed at the opening edges (Figure 4.13). Two continuous #4 bars in the joist top flange supported the legs of these U-shaped stirrups.

Construction

Specimens in the first series were constructed at Concrete Industries, Inc., in December 1994. The four specimens were formed on two prestressing lines. Strain gages were first placed on selected shear reinforcement. All shear reinforcement was then placed in the forms (Figure 4.14). Next, prestressing strands were run and stressed. The opening blockouts were then placed. In these specimens the openings were formed using expanded polystyrene foam (EPS). These blockouts did not stay in place well, and this resulted in misplaced openings. Following placement of the openings, the top flange wire mesh was placed (Figure 4.15).

Concrete casting for the four joists occurred at one time (Figure 4.16). Ten 4 in. diameter by 8 in. tall cylinders were taken from the concrete batches. All cylinders were cured with specimens until the specimens were removed from the forms. The specimens were moist-cured and left in the forms for 5 days. The prestressing strands were released when the concrete had achieved the desired strength, as monitored by tests of cylinders. Some initial cracks on each specimen were noticed after releasing the strands (Figure 4.17). These were small cracks approximately 1 in. or less in length extending horizontally from the corners of the first openings. The same kinds of cracks were reported by other researchers (Barney et al. 1977; Savage et al. 1996). Specimen D10R had fewer cracks than the other specimens. The specimens were then removed from the

forms and stored in Concrete Industries' yard. After 3 months of storage, the specimens were shipped to the University of Nebraska laboratory on the Omaha campus.

The second series of specimens was constructed at Concrete Industries, Inc., in April 1996. The two specimens were formed on one prestressing line. Strain gages were placed on selected shear reinforcement and rebar that was to be attached to prestressing strands. The standard end mesh and bottom chord mesh were placed, followed by the placement of bundled reinforcement at the opening edges in the piers. The opening blockouts, using EPS, and top flange mesh were then placed. Concrete was cast and the specimens were steam-cured for 24 hours. The strands were released when the concrete had reached the desired strength, which was monitored through tests of representative cylinders cast from the same batch of concrete. The specimens were then removed from the forms and stored at Concrete Industries, Inc. At this time it was noticed that there was little or no cover above some openings in D8R1 due to the floating of the blockouts during casting. Also, due to a lack of vibration in the web there was a void in the bottom chord at the first opening of specimen D8R2. (The effects of these fabrication flaws are discussed in Chapter 8.) Casting and release dates for all specimens are shown in Table 4.2.

Material Properties

Concrete

The concrete used for all six specimens was designed to have a strength of 5500 psi at release of prestressing force and 7000 psi at 28 days. Ten cylinders were taken from the batches and tested at different times. Table 4.3 shows the strength values from 5 to 79 days. Figure 4.18 is a graph of concrete strength over time. Strength and stiffness of the double tees may be less than assumed in the design, however, because the specimens' concrete strength did not reach 7000 psi at 28 days.

Reinforcement

Reinforcement strands were manufactured by the American Spring Wire Corporation. These strands were 0.5 in. diameter with an ultimate strength of 270 ksi and low relaxation properties. Three tests were performed on strand samples to obtain the stress-strain curve; an average stress-strain curve for these strands is shown in Figure 4.19. Test results showed an average strength

of 270 ksi and average modulus of elasticity of 30,000 ksi. The shear reinforcement in the webs consisted of No. 5, Grade 60 bar reinforcement or Grade 75 welded wire fabric mesh. The average yield stress determined from four test specimens was 65.0 ksi, and the average modulus of elasticity was 28,000 ksi. The stress-strain curve for these bars is shown in Figure 4.20. Spiral reinforcement was provided around the ends of strands in joists with straight strand profiles. No. 2, Grade 36 bars were used. Testing of three specimens resulted in an average yield stress of 56.0 ksi and an average modulus of elasticity of 27,300 ksi (Figure 4.21).

Table 4.1 Specimen descriptions.

Specimen	Strand profile	Number of openings	Details of shear reinforcement
D10R	Draped	10	# 5 rebar
D10W	Draped	10	4x4-W4.0xW4.0 mesh
S10W	Straight	10	4x4-W4.0xW4.0 mesh
S11P	Straight	11	Strap plate
D8R1	Draped	8	3 Bundled #3 rebar
D8R2	Draped	8	3 Bundled #3 rebar

Table 4.2. Casting and release dates for test specimens.

Specimen	Casting Date	Prestress Release Date
D10R	Dec. 22, 1994	Dec. 27, 1994
D10W	Dec. 22, 1994	Dec. 27, 1994
S10W	Dec. 22, 1994	Dec. 27, 1994
S11P	Dec. 22, 1994	Dec. 27, 1994
D8R1	Apr. 17 1996	April 22, 1996
D8R2	Apr. 17 1996	April 22, 1996

Table 4.3. Average concrete strength, Test Series 1.

Time (days)	Average stress from 3 cylinder (psi)
5	4662
6	5779
9	5889
14	6154
28	6247
79	6697

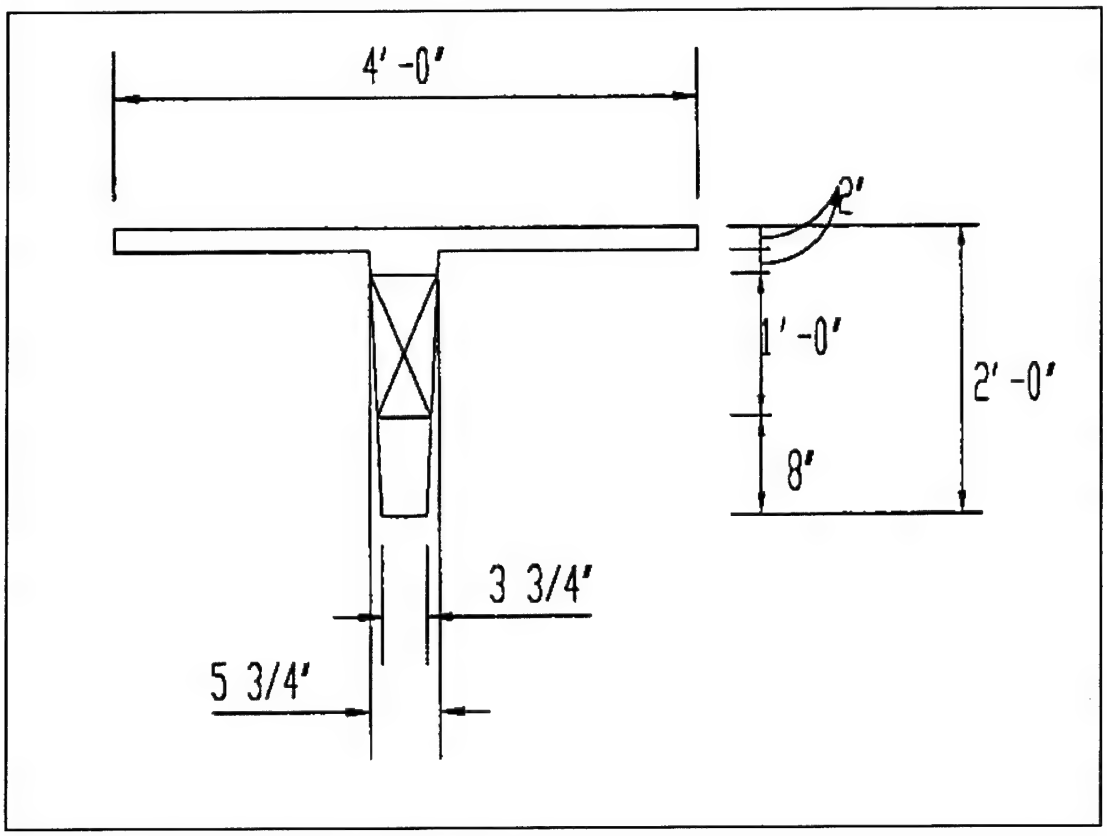

Figure 4.1. Single-tee specimen dimensions.

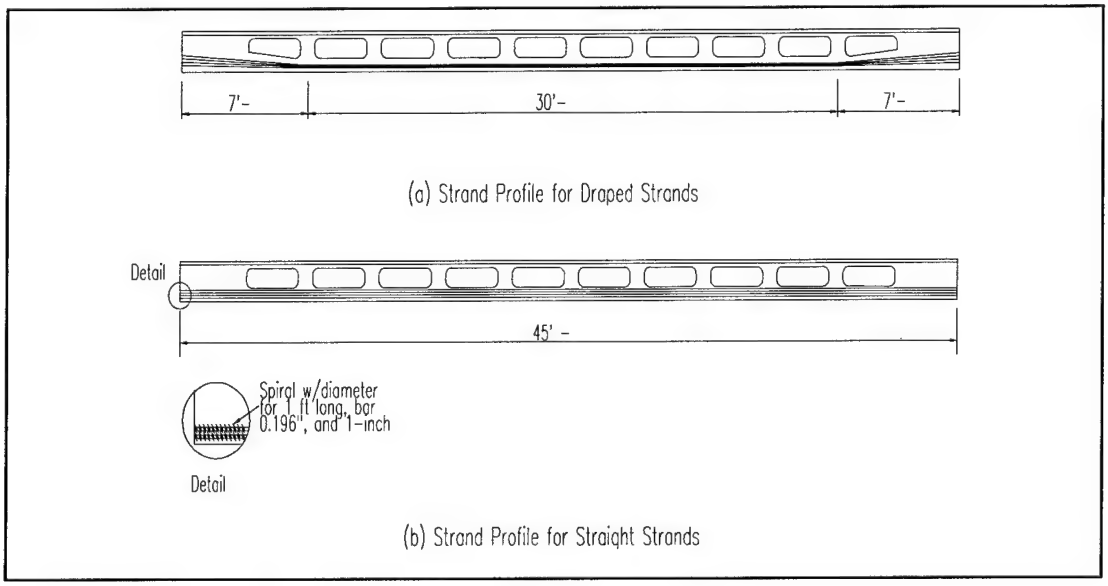

Figure 4.2. Single-tee specimen strand profiles.

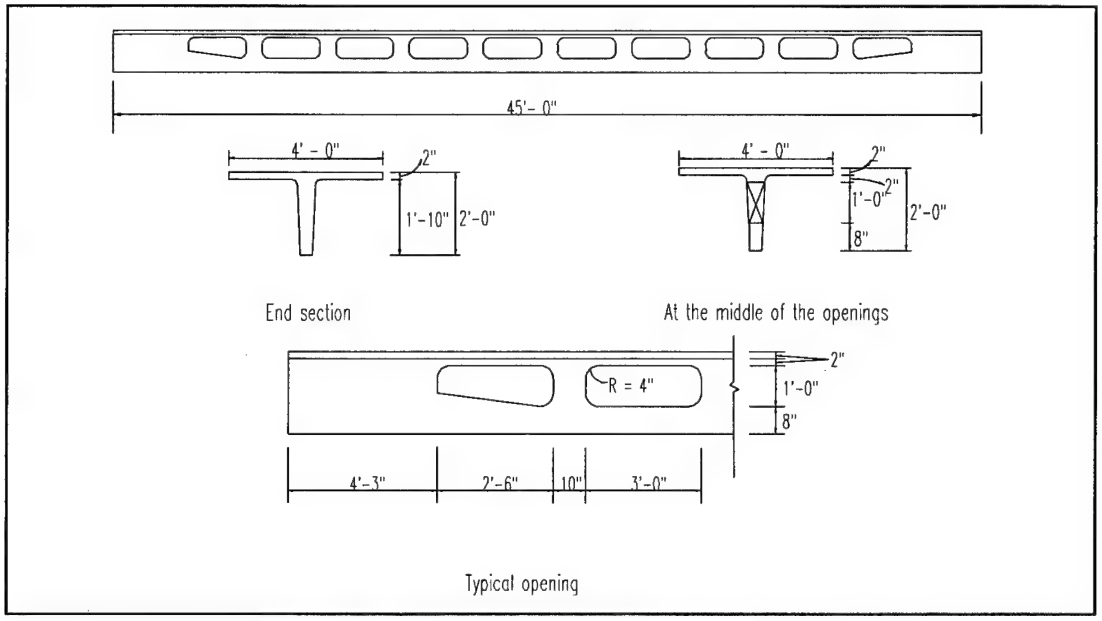

Figure 4.3. Web opening locations and sizes for draped strand profile specimens.

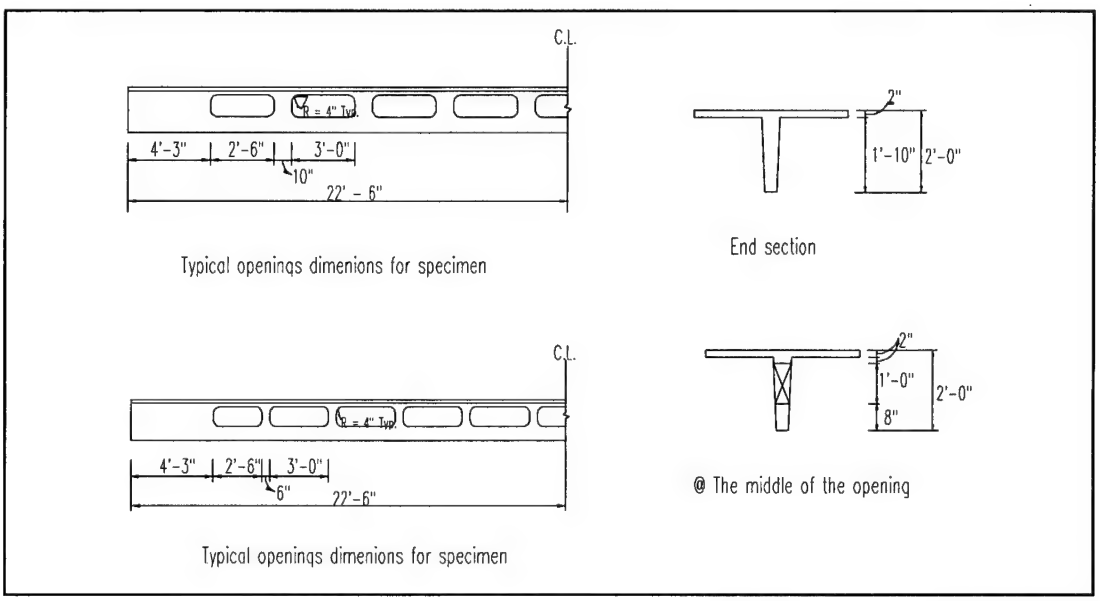

Figure 4.4. Web opening locations and sizes for straight strand profile specimens.

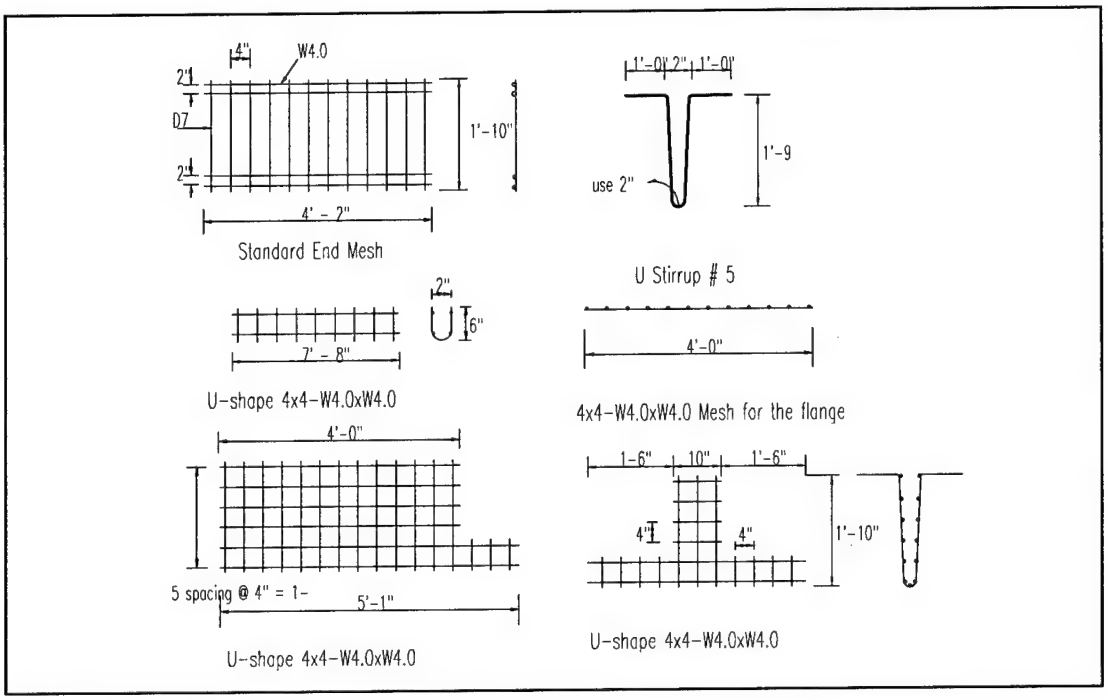

Figure 4.5. Web reinforcement details.

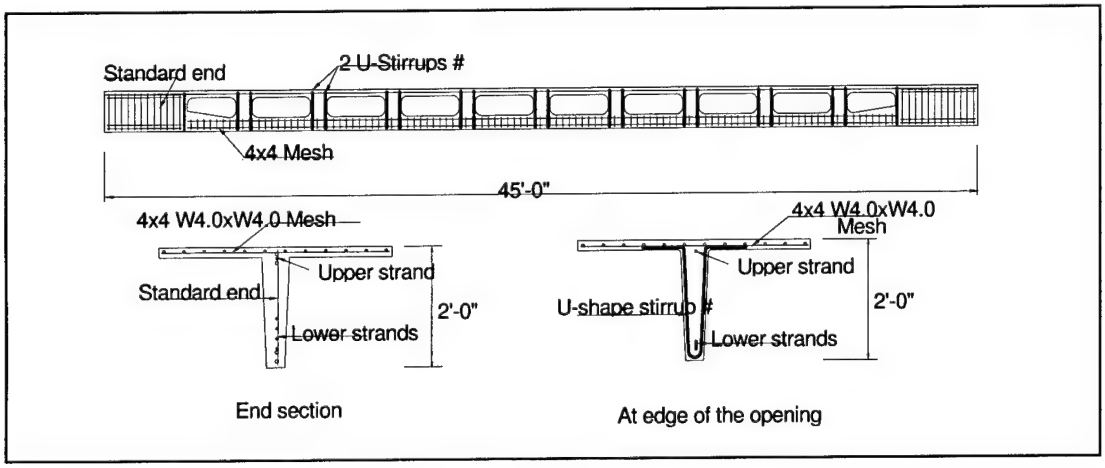

Figure 4.6. Reinforcement details for Specimen D10R.

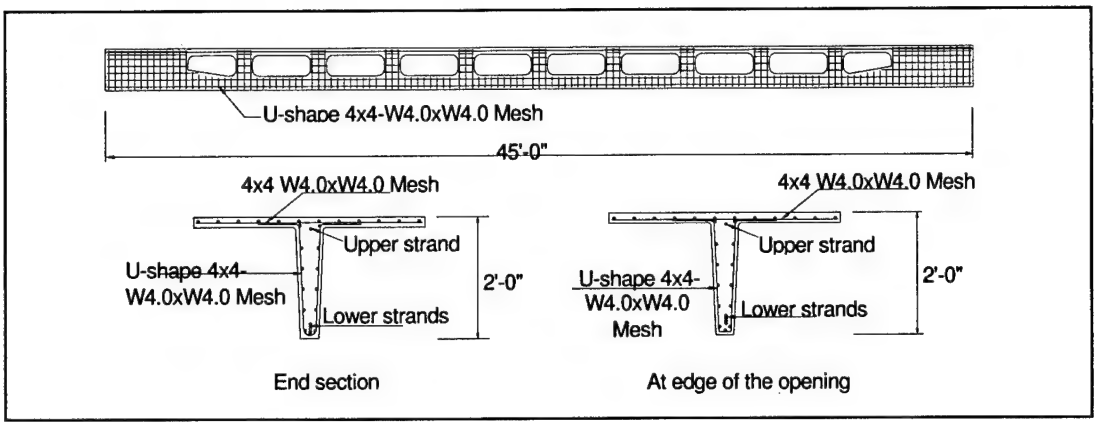

Figure 4.7. Reinforcement details for specimen D10W.

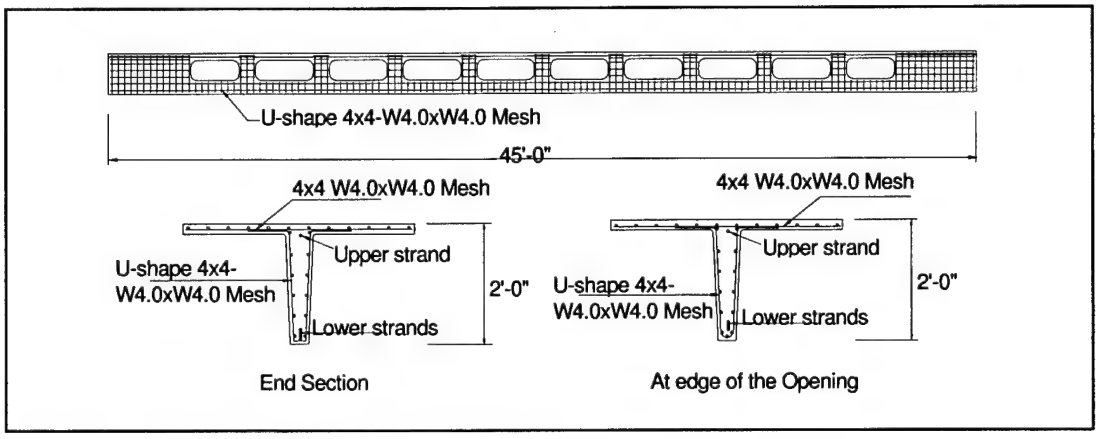

Figure 4.8. Reinforcement details for specimen S10W.

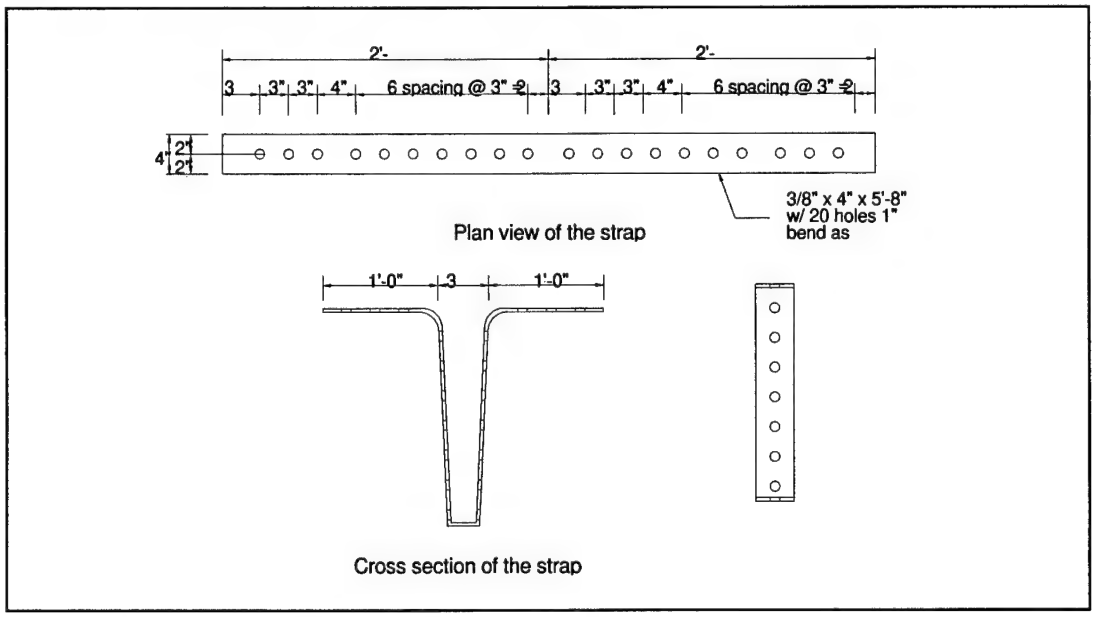

Figure 4.9. Strap plate details for Specimen S10W.

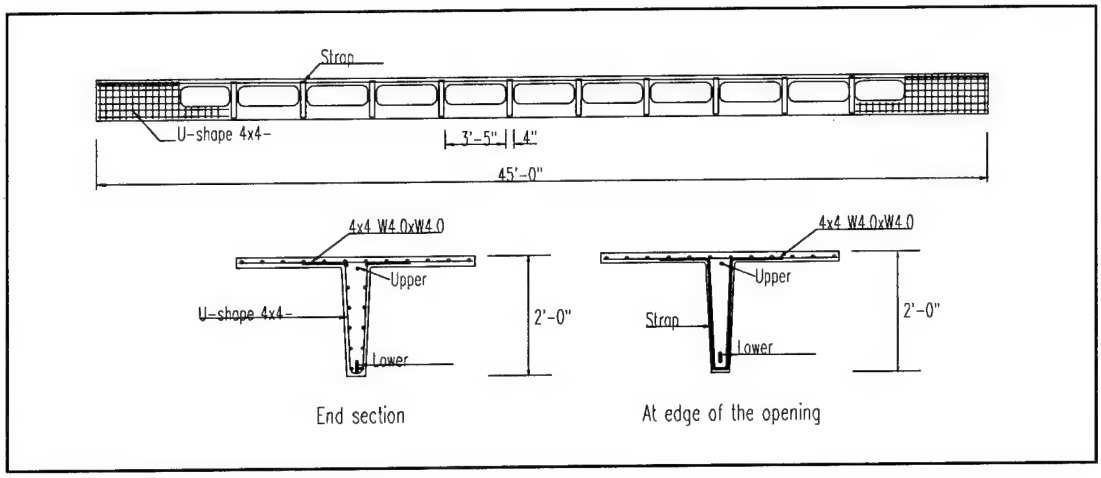

Figure 4.10. Reinforcement details for Specimen S11P.

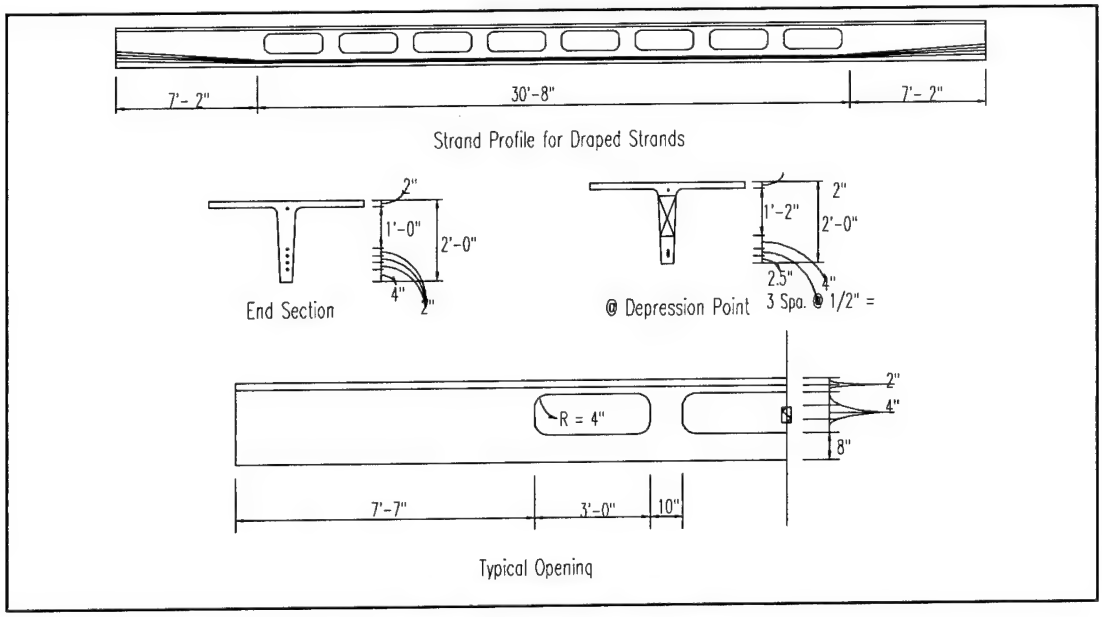

Figure 4.11. Strand profile and web opening dimensions for Series 2 specimens.

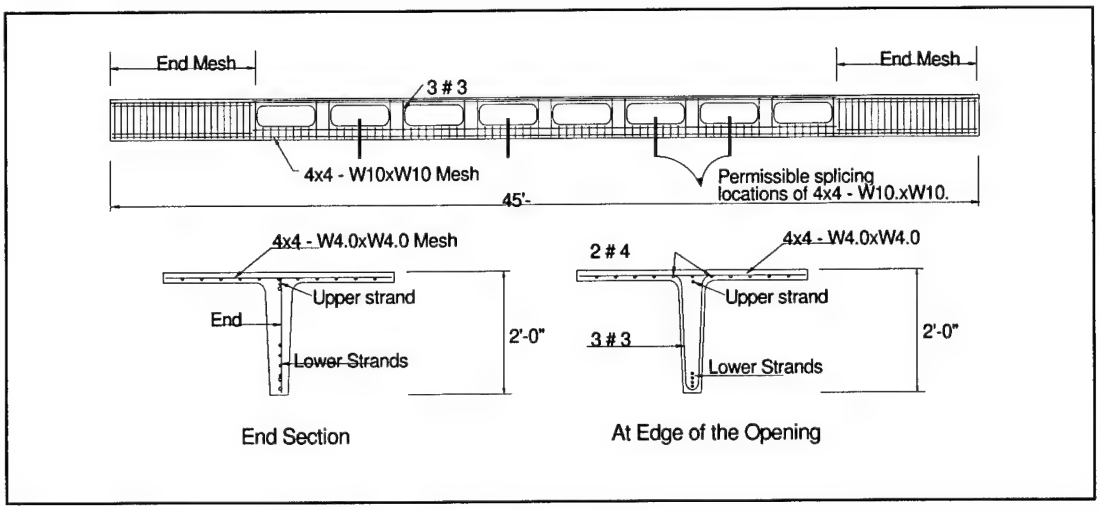

Figure 4.12. Reinforcement details for Series 2 specimens.

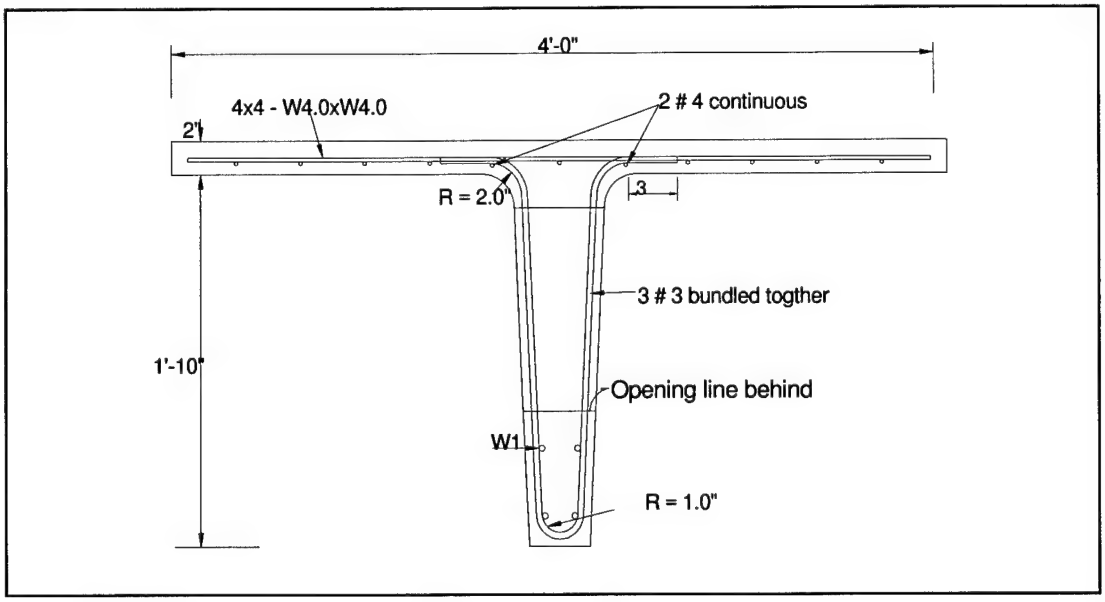

Figure 4.13. Reinforcement details at opening edges of Series 2 specimens.

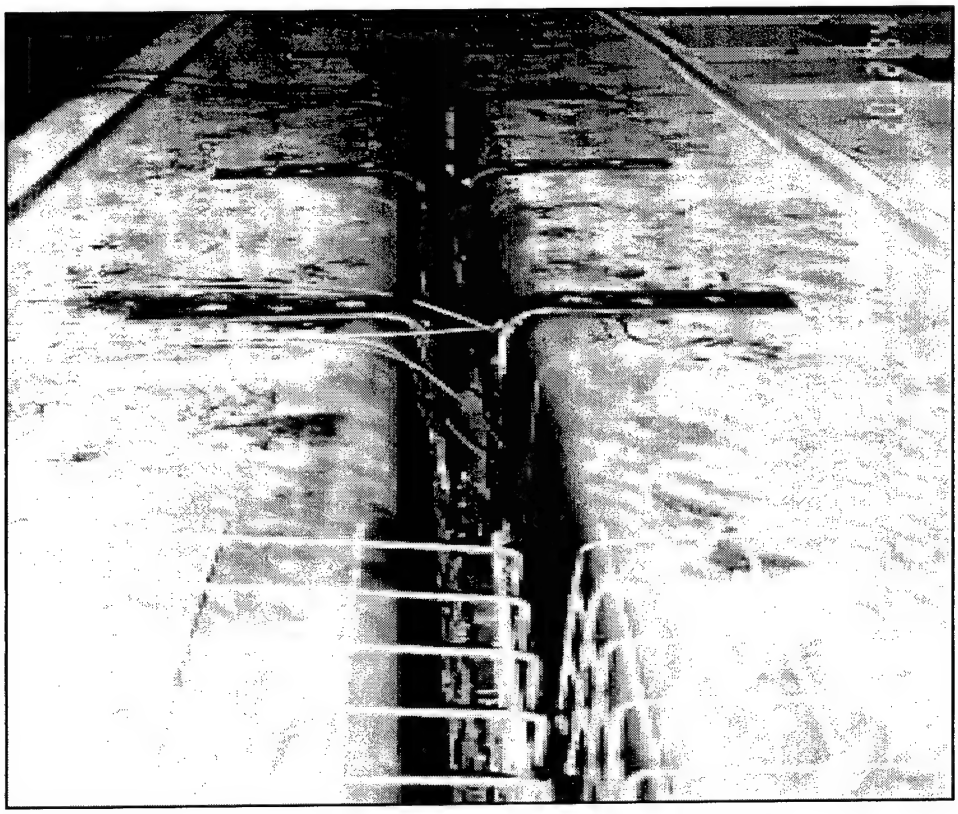

Figure 4.14. Placement of shear reinforcement in sample specimen.

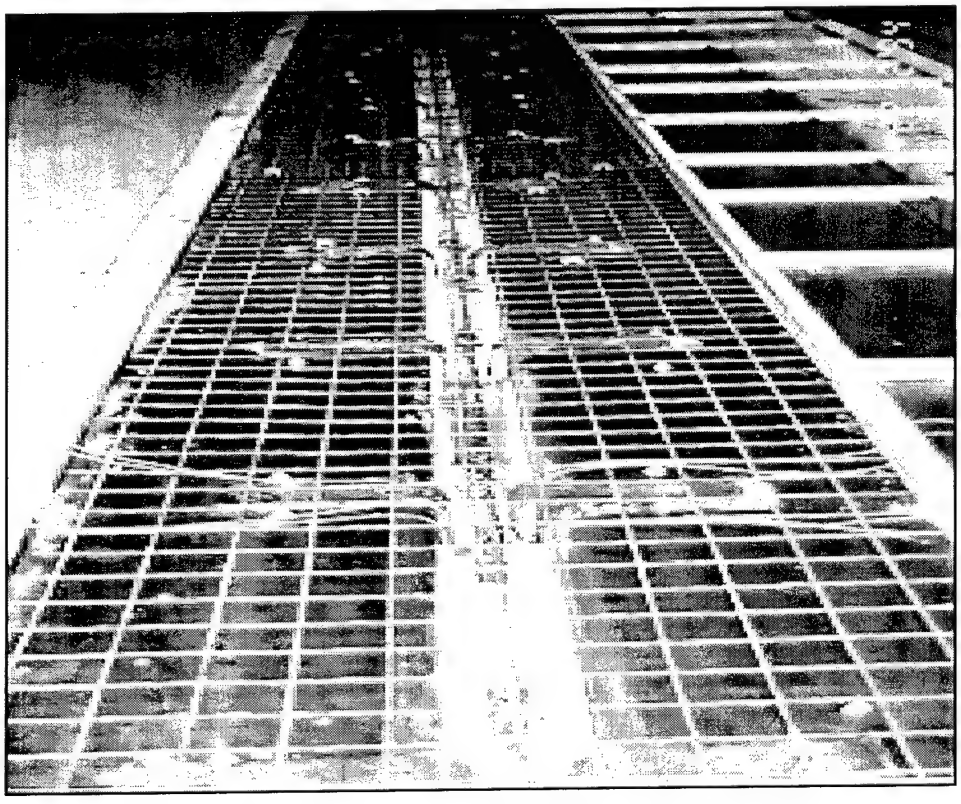

Figure 4.15. Placement of top flange reinforcement in sample specimen.

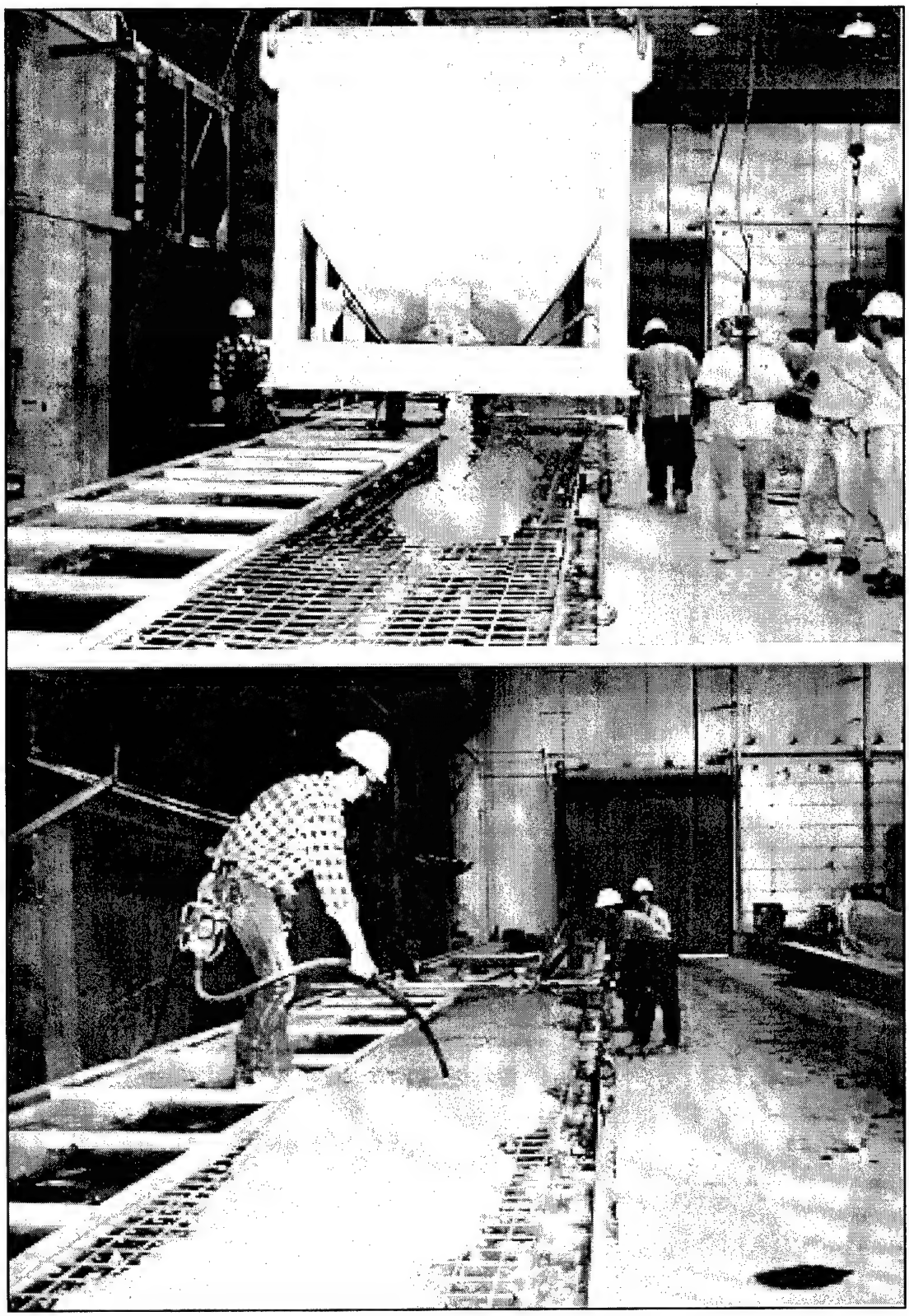

Figure 4.16. Casting the specimens.

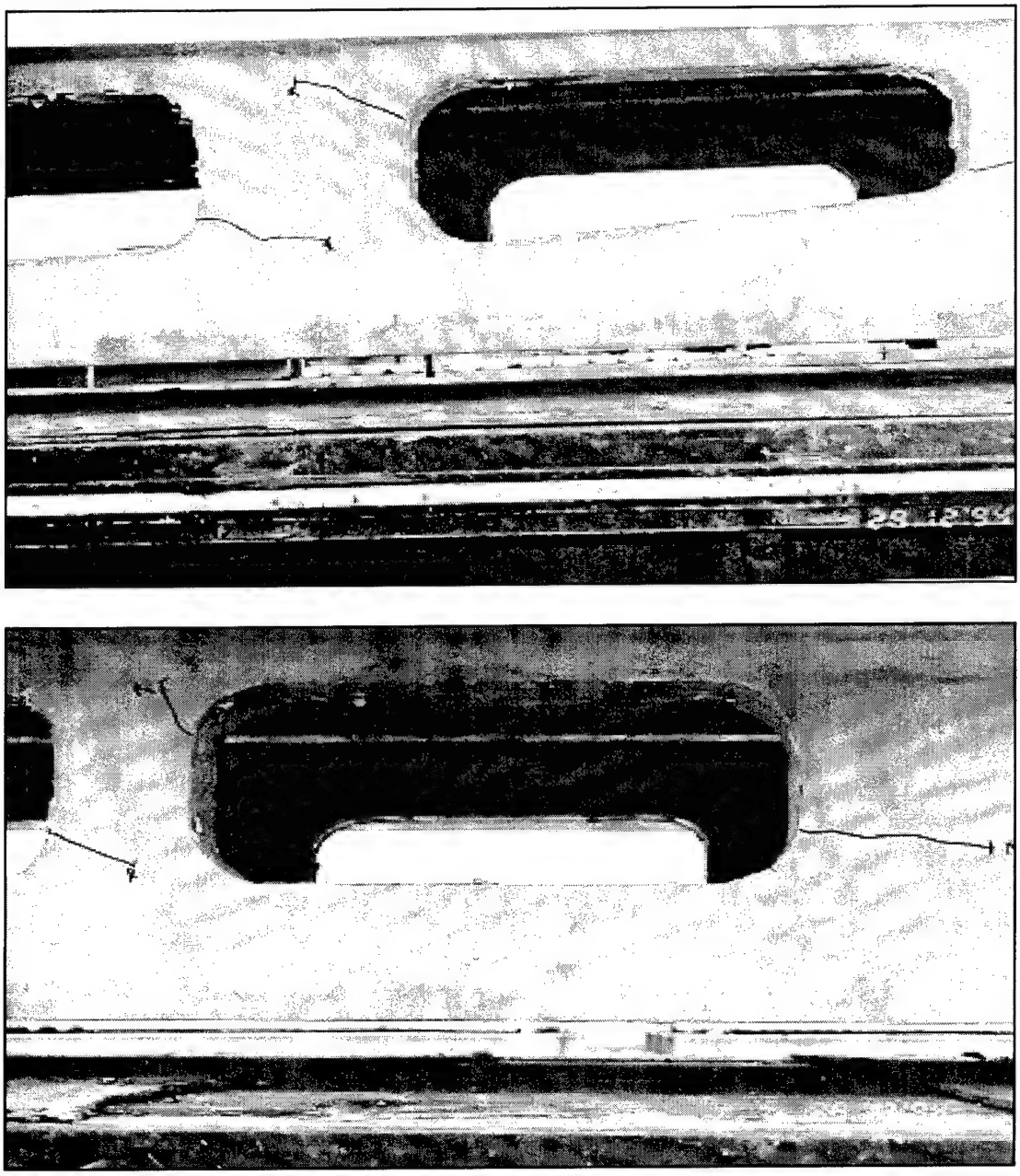

Figure 4.17. Specimen cracks at release of prestressing strands.

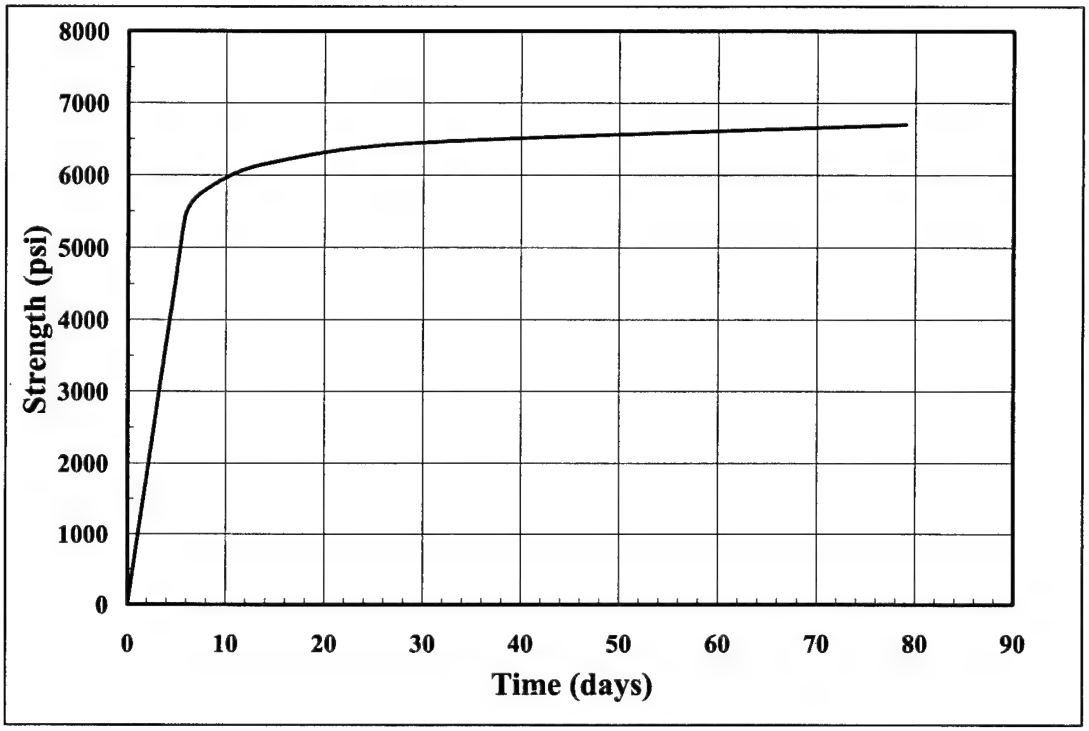

Figure 4.18. Test Series 1 concrete strength development versus time.

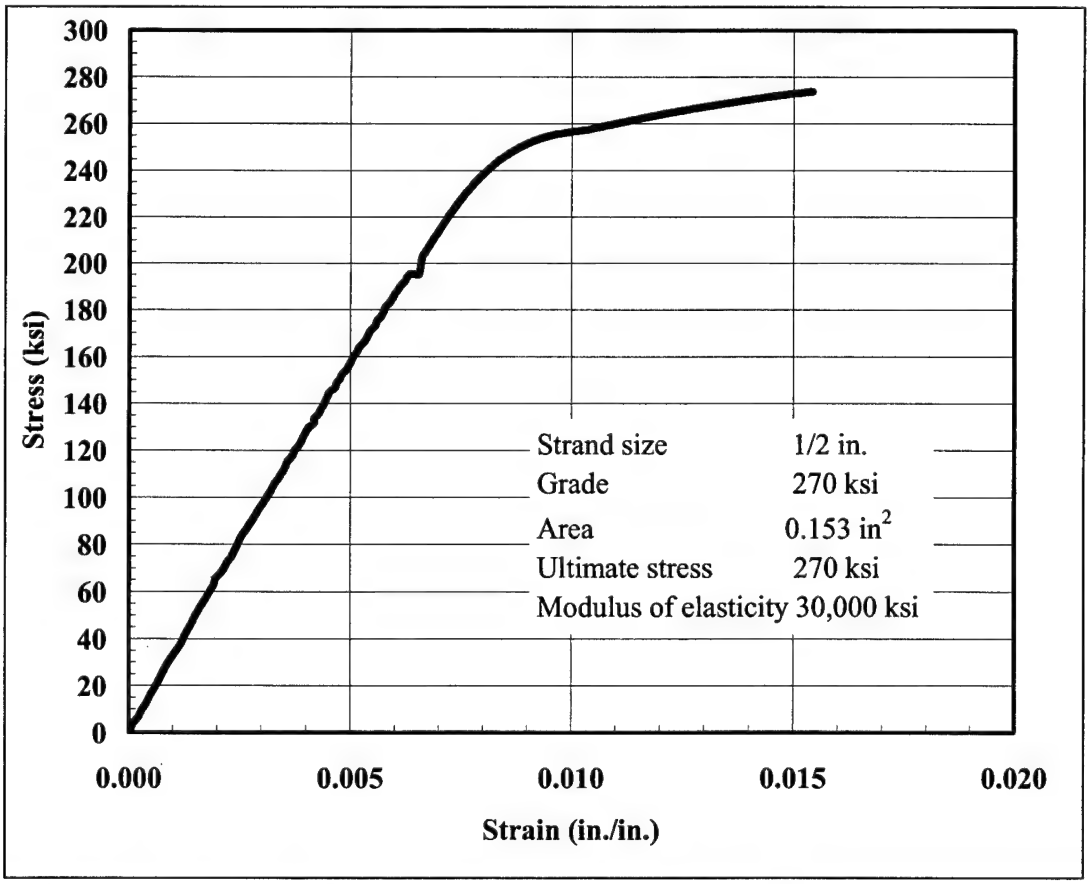

Figure 4.19. Test Series 1 concrete stress versus strain.

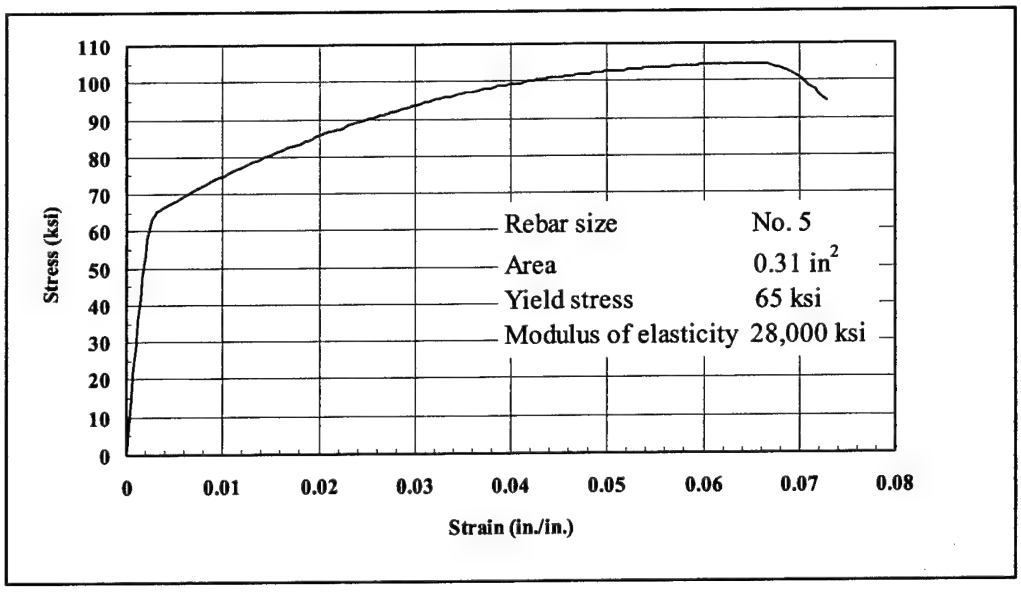

Figure 4.20. Grade 60 No. 5 reinforcing bars stress versus strain.

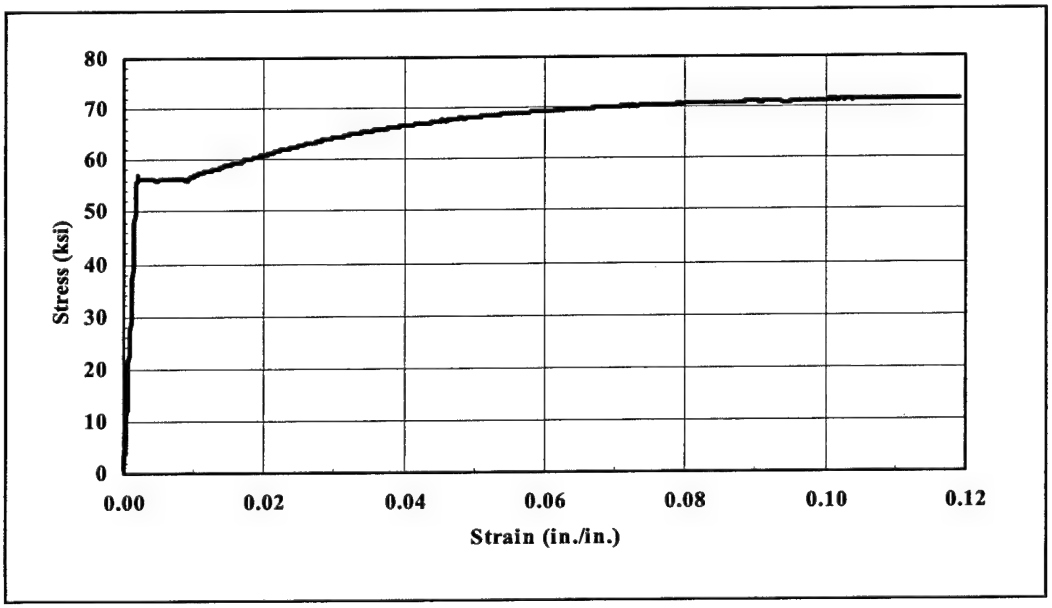

Figure 4.21. Grade 36 No. 2 spiral reinforcement stress versus strain.

5 Experimental Program

Introduction

The primary objective of this experimental investigation was to determine the optimal reinforcement configuration for double-tee joists with web openings to resist service and ultimate loads. Single tee specimens were tested at the Structures Laboratory of the University of Nebraska at Omaha. Details of the test setup and instrumentation, test program, data acquisition, and data processing are discussed.

Test Setup

Within the laboratory constraints, the test configuration was designed to simulate loading and support conditions of a typical double-tee joist in a floor or roof structure. A single tee specimen was used based upon the symmetry of the prototype double-tee joist. Each specimen had a clear span of 44 ft and was mounted on rollers at one end and in a saddle at the other end to simulate simple supports. For all specimens of Test Series 1, loads were applied manually by hydraulic jacks. A total of two 100 kilopound (kip) capacity hydraulic jacks were used. The test setup at the Structures Laboratory on the Omaha campus of the University of Nebraska is shown in Figure 5.1.

Test Series 2 was conducted in the new test bed facility at Wilson Concrete, Omaha, NE. The specimens were supported as in the first test series, with a roller and saddle. The joists were loaded at six points by three hydraulic jacks (Figures 5.2 and 5.3). The loads were applied through three 100 kips capacity hydraulic jacks using an electrical pump. Increments of 1.0 kips were used in applying the load. Joists were tested to failure.

Test Programs

The objective of incremental load testing of the joists was to determine corresponding strain and deflection readings at critical locations on the joist.

Additionally, visual identification of crack development and determination of failure mode were of interest. Table 5.1 provides a summary of all tests.

In the test program the jacks were operated under load control. Load was applied in 1.0 kip increments. Two 10,000 psi load pressure cells were used with the jacks to measure the hydraulic pressure and monitor applied loads. After each load step, the hydraulic pump was stopped, load was kept constant, and new cracks were marked. In Test Series 2, load increments of 1.0 kip were applied. During each increment the loads were kept constant while new cracks were marked. Joists were tested to failure in all cases.

Instrumentation and Data Recording

Test specimens were fully instrumented with displacement potentiometers and strain gages. All recorded displacements were absolute, measured with respect to the laboratory floor. Tables 5.2 through 5.5 summarize the instrumentation plans for Test Series 1 specimens D10R, D10W, S10W, and S11P, respectively. Tables 5.6 and 5.7 show the instrumentation for specimens D8R1 and D8R2.

Electrical resistance strain gages were installed on several locations on the steel reinforcing bars embedded in the concrete. These were Measurements Group Model EA-06-125BT-120 electrical resistance strain gages with constant grids and complete polyamide encapsulation. The sensing grid was 0.125 in. long by 0.062 in. wide. Also, electrical resistance strain gages were installed at several locations on the concrete surface. These strain gages were Model PL-60-11 with nominal resistance $120 \pm 0.3\Omega$ (ohms), made by Texas Measurements, Inc. (College Station, TX 77841). The gage length was 2.362 in. (60 mm) long by 0.039 in. (1 mm) wide. These gages were placed at the first and middle piers and located at two levels—the top of the web and bottom of the web. Figures 5.4 to 5.6 show the details and location of these strain gages for the four specimens of Test Series 1. Figs 5.7 and 5.8 show the details and location of these strain gages for Specimens D8R1 and D8R2 of Test Series 2.

Deflections were measured from the bottom of the joist at the first point load, midspan, and second point load by position transducers. Position Transducer Model P-10A variable resistance displacement transducers were used (MagneTek, Simi Valley, CA 93065). These units employ a spring-loaded precision rotary potentiometer with a flexible steel cable wrapped around the potentiometer shaft. The other end of the cable is attached to the point where the displacement is to be measured. When displacement occurs, the cable

motion rotates the shaft of the potentiometer causing a change in resistance. These transducers were mounted on the floor but independent of the test beam.

All transducers and the strain gauges were connected to a microcomputer for continuous data acquisition during specimen loading and unloading. The data acquisition system was Megadac Series 3000 (Data Acquisition and Control Systems, Germantown, MD 20874). Figure 5.9 is a functional block diagram of the instrumentation, data acquisition and test control systems. All of the transducer output signals were connected to the Megadac Series 3000 data logging system. The system was controlled by microcomputer through an instrument controller interface bus. The record channels were scanned at a predetermined sampling rate, and the data were recorded and then transformed to ASCII* text files on the personal computer.

The loading system consisted of two Enerpac Model RRH-6010 double-acting hollow-plunger hydraulic cylinders (Applied Power, Inc., Butler, WI 53007). The cylinders include transducers that measure the applied pressure. The pressure measurements are transformed to applied load through the data acquisition system. The pressure transducers used here were Omega PX-602 Model. The load was applied manually in Test Series 1 using Hydraulic Hand Pump Model P-84; in Test Series 2, electrical Dump Pump 30,000 Series (1.5 horsepower, 10,000 psi) was used.

Table 5.1. Test dates.

Specimen	Loading	Test Date
D10R	2 hydraulic jacks w/manual pump	4/5/95
D10W	2 hydraulic jacks w/manual pump	4/4/95
S10W	2 hydraulic jacks w/manual pump	4/5/95
S11P	2 hydraulic jacks w/manual pump	4/4/95
D8R1	3 hydraulic jacks w/ electric pump	8/20/96
D8R2	3 hydraulic jacks w/ electric pump	8/21/96

ASCII: American Standard Code for Information Interchange.

Table 5.2. Instrumentation plan for D10R.

Instrument	CIR Name	Location (X - Dir.) (in.)	Location (Y - Dir.) (in.)
POT_W	N / A	135.000	N / A
POT_Mid	N / A	270.000	N / A
POT_E	N / A	378.000	N / A
Int_1	s1	82.000	20.000
Int_2	s2	82.000	8.000
Int_3	s3	90.000	8.000
Int_4	s4	90.000	20.000
Int_5	s5	174.000	20.000
Int_6	s6	174.000	8.000
Int_7	s7	182.000	20.000
Int_8	s8	182.000	8.000
Ext_13C	13C	86.000	21.000
Ext_14C	14C	86.000	2.000
Ext_15C	15C	270.000	21.000
Ext_16C	16C	270.000	2.000

Table 5.3. Instrumentation plan for D10W.

Instrument	CIR Name	Location (X - Dir.) (in.)	Location (Y - Dir.) (in.)
POT_W	N / A	145.000	N / A
POT_Mid	N / A	270.000	N / A
POT_E	N / A	378.000	N / A
Int_9	s9	82.000	20.000
Int_10	s10	82.000	8.000
Int_11	s11	90.000	20.000
Int_12	s12	90.000	8.000
Int_13	s13	174.000	20.000
Int_14	s14	174.000	8.000
Int_15	s15	182.000	20.000
Int_16	s16	182.000	8.000
Ext_5C	5C	86.000	21.000
Ext_6C	6C	86.000	2.000
Ext_7C	7C	270.000	21.000
Ext_8C	8C	270.000	2.000

Table 5.4. Instrumentation plan for S10W.

Instrument	CIR Name	Location (X - Dir.) (in.)	Location (Y - Dir.) (in.)
POT_W	N / A	135.000	N / A
POT_Mid	N / A	270.000	N / A
POT_E	N / A	378.000	N / A
Int_17	s17	82.000	20.000
Int_18	s18	82.000	8.000
Int_19	s19	90.000	8.000
Int_20	s20	90.000	20.000
Int_21	s21	174.000	20.000
Int_22	s22	174.000	8.000
Int_23	s23	182.000	20.000
Int_24	s24	182.000	8.000
Ext_9C	9C	86.000	21.000
Ext_10C	10C	86.000	2.000
Ext_11C	11C	270.000	21.000
Ext_12C	12C	270.000	2.000

Table 5.5. Instrumentation plan for S11P.

Instrument	CIR Name	Location (X - Dir.) (in.)	Location (Y - Dir.) (in.)
POT_W	N / A	145.000	N / A
POT_Mid	N / A	270.000	N / A
POT_E	N / A	378.000	N / A
Int_25	s25	82.000	20.000
Int_26	s26	82.000	20.000
Int_27	s27	86.000	8.000
Int_28	s28	86.000	8.000
Int_29	s29	86.000	20.000
Int_30	s30	86.000	20.000
Int_31	s31	82.000	8.000
Int_32	s32	82.000	8.000
Int_33	s33	164.000	20.000
Int_34	s34	164.000	20.000
Int_35	s35	168.000	8.000
Int_36	s36	168.000	8.000
Int_37	s37	168.000	20.000
Int_38	s38	168.000	20.000
Int_39	s39	164.000	8.000

Int_40	s40	164.000	8.000
Ext_1C	1C	84.000	21.000
Ext_2C	2C	84.000	2.000
Ext_3C	3C	252.000	21.000
Ext_4C	4C	252.000	2.000

Table 5.6. Instrumentation plan for D8R1.

Instrument	CIR Name	Location (X - Dir.) (in.)	Location (Y - Dir.) (in.)
POT_W	N / A	132.000	N / A
POT_Mid	N / A	270.000	N / A
POT_E	N / A	408.000	N / A
Int_1	s1	128.000	8.000
Int_2	s2	128.000	20.000
Int_3	s3	136.000	8.000
Int_4	s4	136.000	20.000
Int_5	s5	174.000	8.000
Int_6	s6	174.000	20.000
Int_13	s13	46.000	5.000
Int_14	s14	109.000	4.000
Int_15	s15	270.000	4.000
Int_16	s16	270.000	22.000
Ext_1C	1C	270.000	23.000
Ext_2C	2C	270.000	21.000
Ext_3C	3C	270.000	2.000
Ext_4C	4C	132.000	23.000
Ext_5C	5C	132.000	21.000
Ext_6C	6C	132.000	2.000
Ext_7C	7C	89.000	23.000
Ext_8C	8C	89.000	21.000
Ext_9C	9C	89.000	2.000

Table 5.7. Instrumentation plan for D8R2.

Instrument	CIR Name	Location (X - Dir.) (in.)	Location (Y - Dir.) (in.)
POT_W	N / A	132.000	N / A
POT_Mid	N / A	270.000	N / A
POT_E	N / A	408.000	N / A
Int_7	s7	128.000	8.000
Int_8	s8	128.000	20.000
Int_9	s9	136.000	8.000
Int_10	s10	136.000	20.000
Int_11	s11	174.000	8.000
Int_12	s12	174.000	20.000
Int_17	s17	46.000	5.000
Int_18	s18	270.000	4.000
Int_19	s19	270.000	22.000
Ext_10C	10C	270.000	23.000
Ext_11C	11C	270.000	21.000
Ext_12C	12C	270.000	2.000
Ext_13C	13C	132.000	23.000
Ext_14C	14C	132.000	21.000
Ext_15C	15C	132.000	2.000
Ext_16C	16C	89.000	23.000
Ext_17C	17C	89.000	21.000
Ext_18C	18C	89.000	2.000

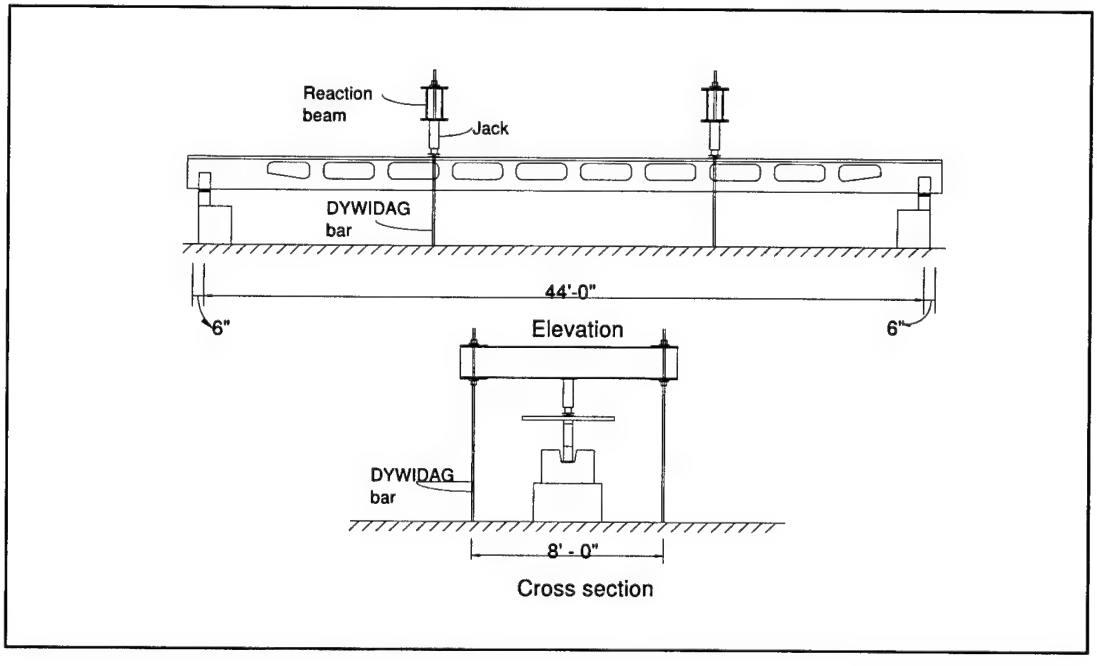

Figure 5.1. Test set-up for Series 1 single-tee beams with web openings.

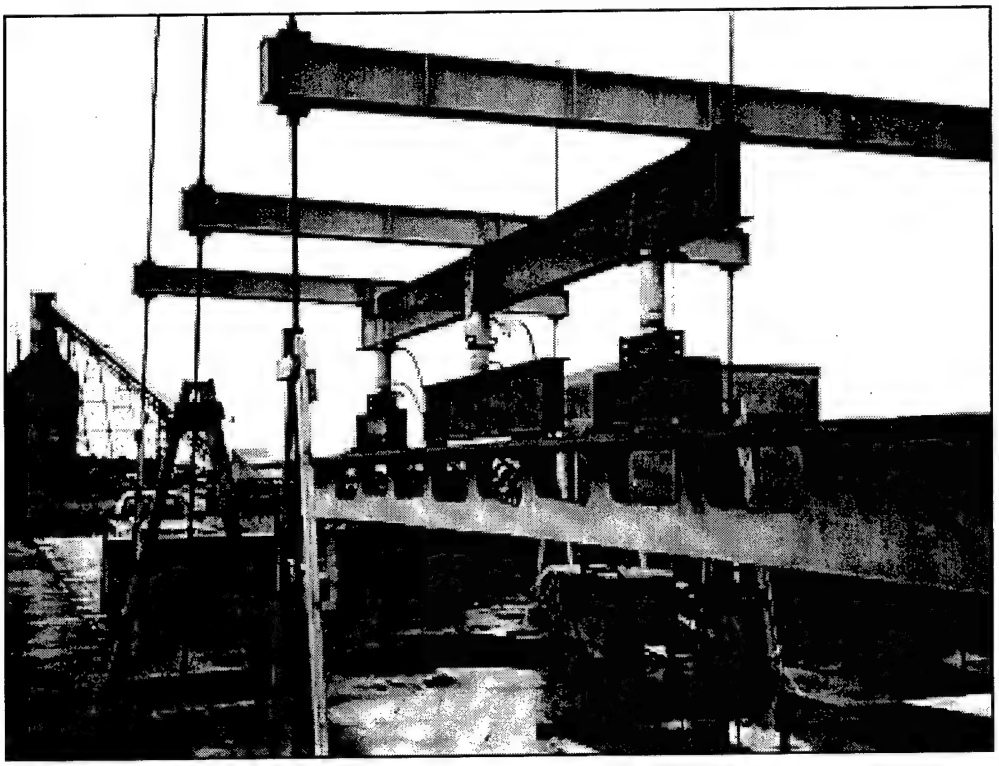

Figure 5.2. Test set-up of Series 2 single-tee beams with web openings.

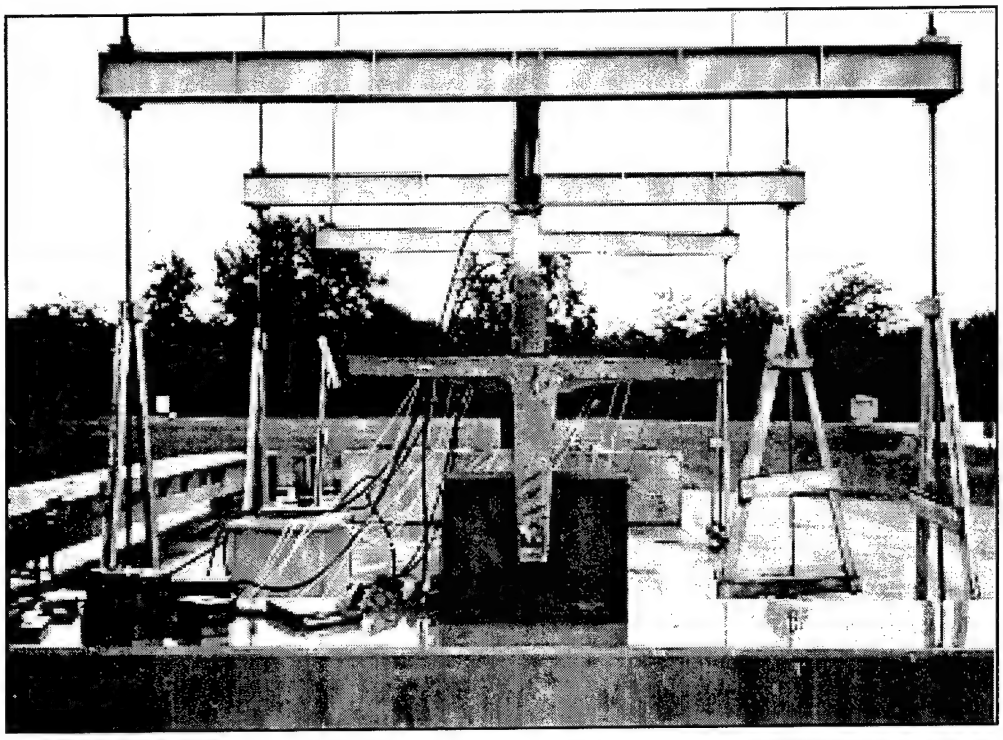

Figure 5.3. Test set-up of Series 2 single-tee beams with web openings.

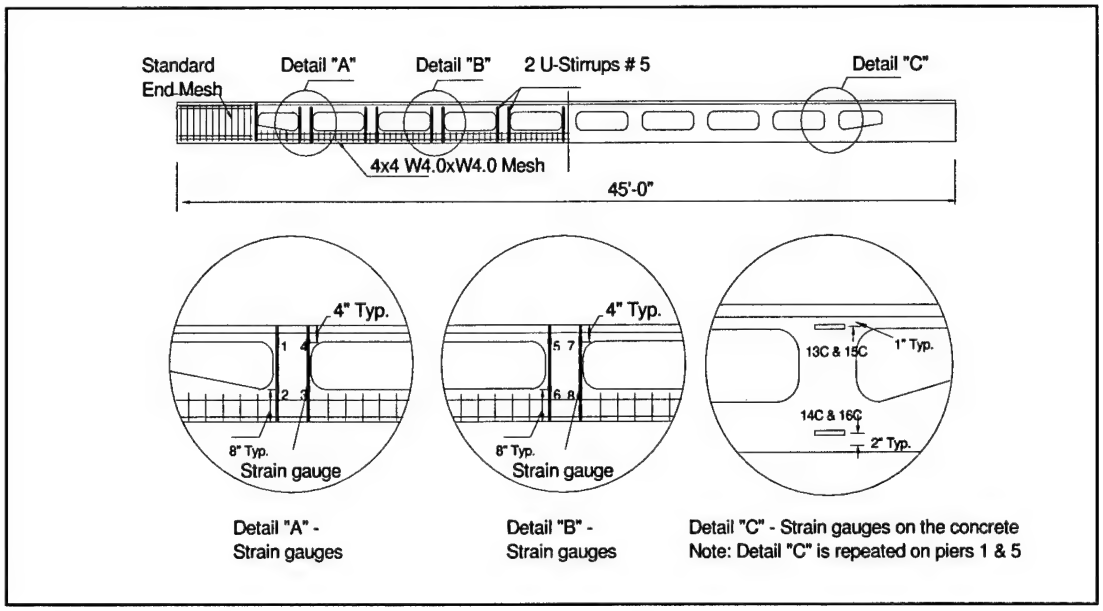

Figure 5.4. Instrumentation details for Series 1 Specimen D10R.

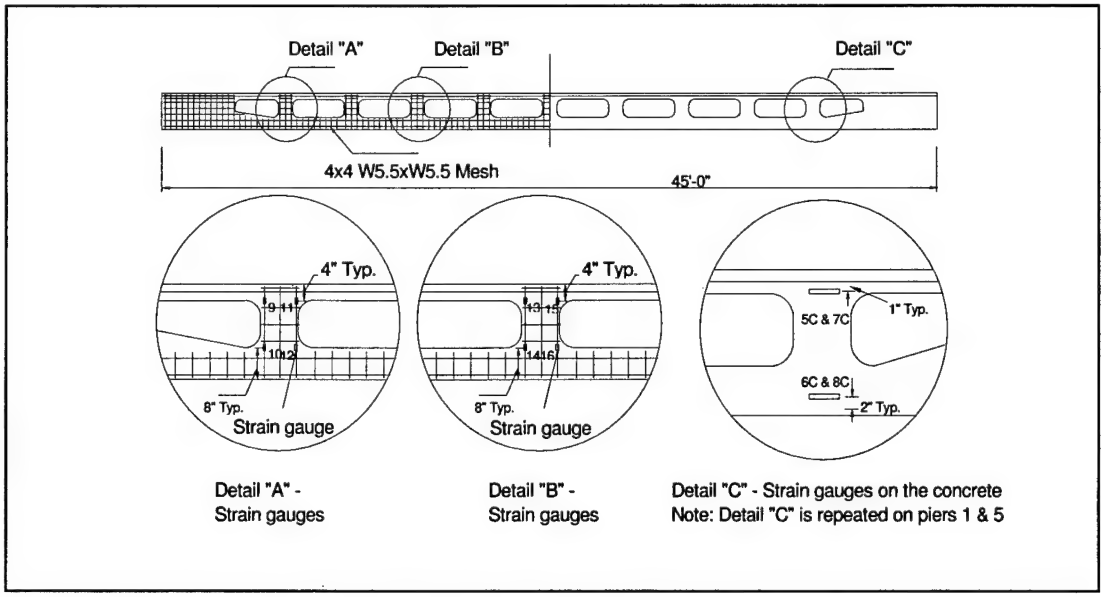

Figure 5.5. Instrumentation details for Series 1 Specimen D10W.

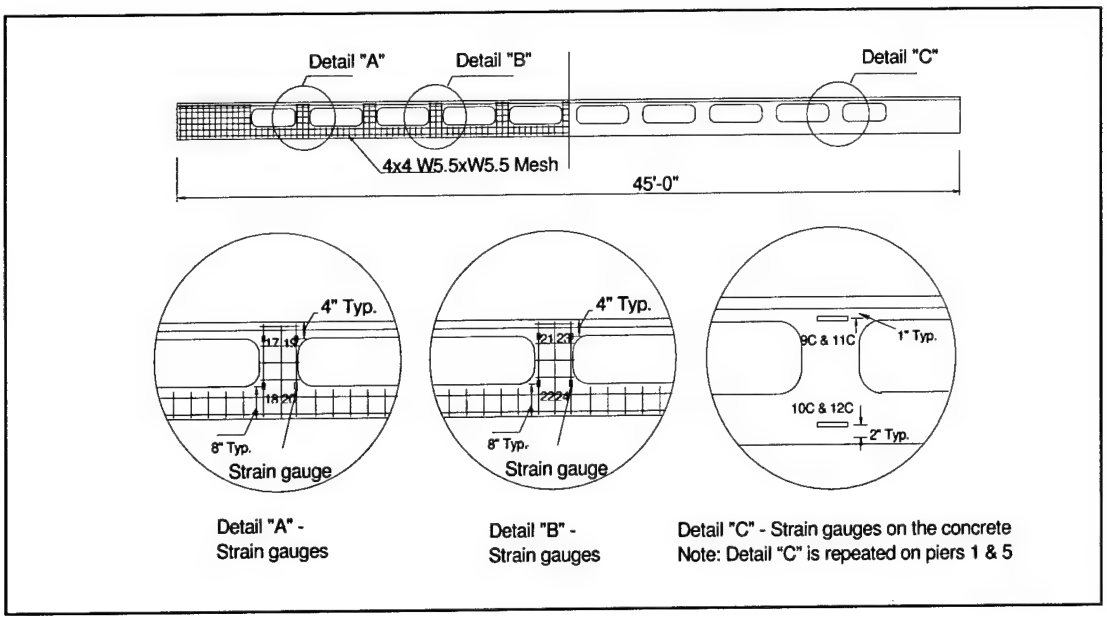

Figure 5.6. Instrumentation details for Series 1 Specimen S10W.

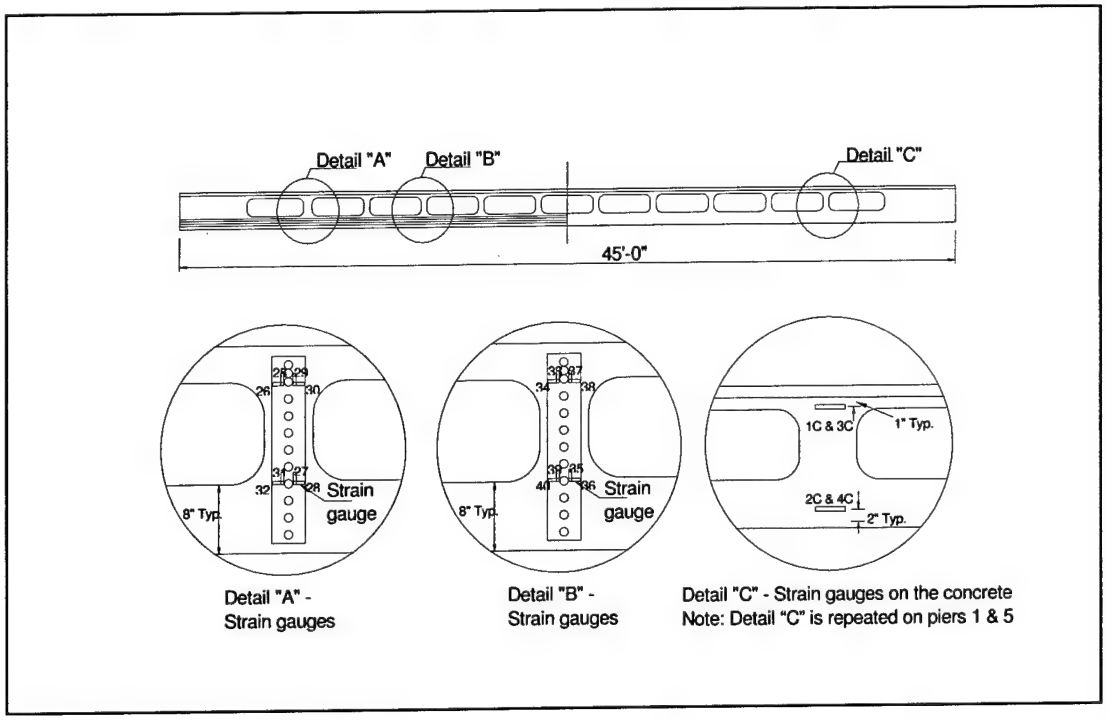

Figure 5.7. Instrumentation details for Series 1 Specimen S11P.

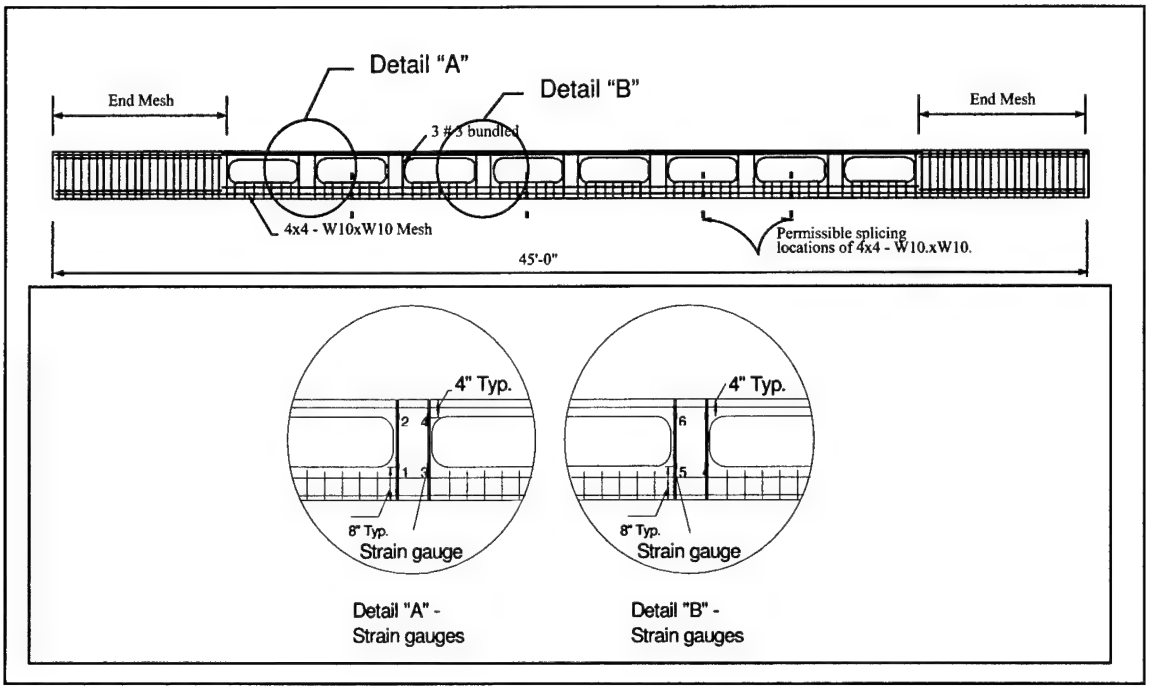

Figure 5.8. Instrumentation details for Series 2 Specimen D8R1.

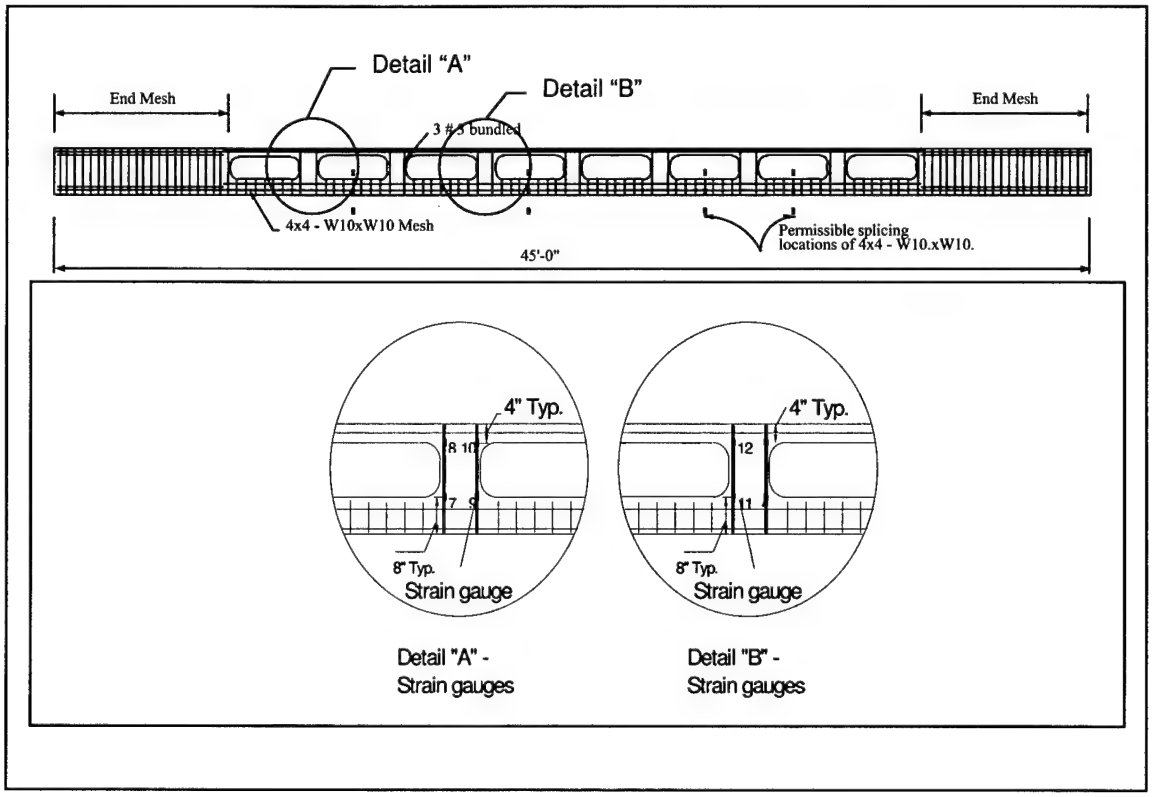

Figure 5.9. Instrumentation details for Series 2 Specimen D8R2.

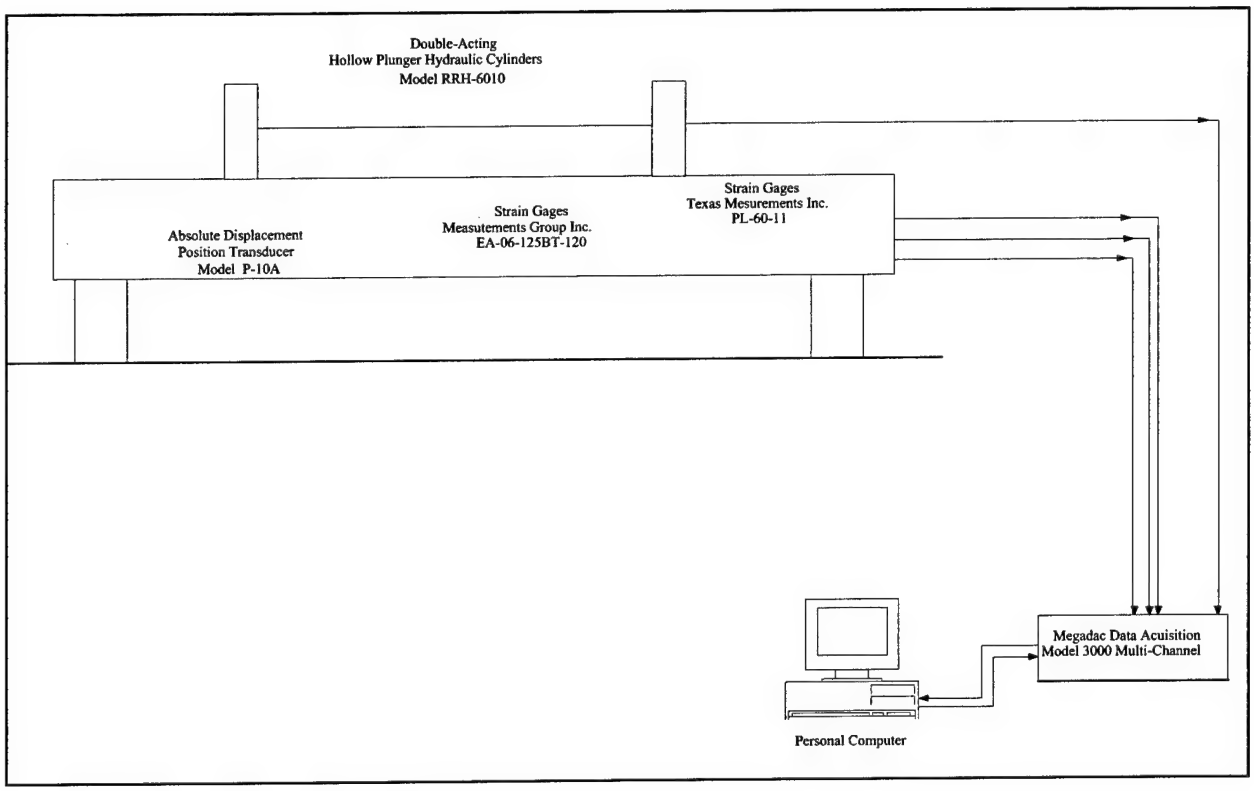

Figure 5.10. Data acquisition system.

6 Experimental Results

Introduction

This chapter presents the experimental results from the four double-tee specimens of Test Series 1 performed at the University of Nebraska (Omaha) Structures Laboratory and from the two beams of Test Series 2 performed at the Wilson Concrete Company testing facility. Load and deflection, concrete and prestressing steel strains, and specimen failure modes are discussed in detail.

Results of Test Series 1

Load and Deflection

Table 6.1 summarizes principal test results, including the location of the first cracking, failure load, equivalent uniform load (in psf) at failure, ratio between the equivalent uniform load at failure for the specimen with web openings to that for a solid joist, and the type of failure for each specimen of Test Series 1. Applied failure load represents the sum of the two hydraulic jack loads, and the total failure load includes the weight of the distribution beams and the applied loads. The applied failure loads for all specimens are less than those for the solid joist, as tested by Savage (1993). However, the total failure load for D10R is greater than that of the solid beam. D10R failed at a total load of 25.0 kips. This represents approximately 131 percent of the superimposed ultimate capacity, which was computed at 19.1 kips. The superimposed service load was computed as 11.7 kips, and D10R failed at 214 percent of this value. The other three joists failed at less than the superimposed ultimate load. D10W and S10 failed at 16.4 and 13.0 kips, respectively. Specimen D10W failed at approximately 86 percent of the superimposed ultimate load, or 140 percent of the superimposed service load. Specimen S10W failed at approximately 68 percent of the superimposed ultimate load, or 117 percent of the superimposed service load. S11P failed at 16.0 kips. This value is approximately 84 percent of the superimposed ultimate load, or 137 percent of the superimposed service load.

Applied load versus deflection curves for the tested specimens are shown in Figure 6.1. These are compared with experimental results of a solid single tee. The slope of the curves in the service load region is very similar for all Test Series 1 specimens with that for the solid joist. After this limit, the behavior of the specimens with web openings diverges from that of the solid joist, and the slope of their curves after the service load limit is shallower. Specimen D10R has behavior most similar to the solid joist although its applied failure load is also lower than that of the solid joist. The other three joists did not approach the failure load and deflection relationship of the solid joist.

Based on the experimentally measured deflections at specific load increments, the moment of inertia was computed for each specimen. Figure 6.2 shows the relationship of this computed moment of inertia to load. The moment of inertia decreases with increased loading due to increased cracking of the section. This figure also indicates that specimen D10R performed the best of all those tested. Table 6.2 shows the measured values for camber at release, deflection at a load comparable to the live load (LL), deflection at a load comparable to the superimposed dead load (SIDL) plus LL, and the maximum deflection achieved for each specimen. Figures 6.3 to 6.6 show the deflection along the span length for each specimens at different loading stages. Measured deflections due to loads comparable to the live load and superimposed dead load plus live load were well below the allowable limitations of the ACI L/360 (1.47 in.) and L/240 (2.20 in.), respectively.

Strains

For all four specimens of Test Series 1, the strain distribution at the midspan section was approximated at various load stages. Gages located on the concrete surface just below the beam flange and gages on the prestressing strands were used to define the curves. Figures 6.7 to 6.10 show these strain values for D10R, D10W, S10W, and S11P, respectively. The neutral axis in specimens D10R, D10W, and S10W is located above the openings for all load increments, but in S11P the neutral axis is located at approximately the midheight of the openings at low load levels and remains within the opening height through the maximum sustained load level. At a load level of 16 kips, specimens D10R and D10W had similar levels of strain in the prestressing strands; however, beyond this load level the prestressing strand strain of D10R increased significantly and D10R was able to achieve a much greater ultimate strain level. Both draped strand specimens developed greater prestressing strains than the straight strand specimens. The prestressing strands were strained the least in specimen S11P.

Cracking and Failure Mechanism

Cracks were marked at selected load increments throughout the testing. The crack patterns provide insight into the behavior of the specimen at various loading stages. All specimens experienced some initial cracks at transfer of the prestress forces to the joist. During testing, D10R developed uniformly spaced flexural cracks across the bottom chord of the middle part of the specimen; the other specimens did not. Prior to failure, all four specimens developed concentrated cracks in the top outside corner of the first web opening from each end. This location coincided with the point of load application. A shear failure ultimately occurred in all specimens due to the concentrated loading configuration.

Figure 6.11 shows the failure location of specimen D10R—the first opening where the shear reinforcement pulled through the top flange. The crack pattern of Specimen D10W indicated some Vierendeel truss behavior around the openings. Figure 6.12 shows the specimen failure location. The mode of failure was shear, which occurred by crushing of the concrete cover around the wire mesh shear reinforcement at the first opening.

During testing, specimen S10W developed some horizontal cracks at the first opening at both ends of the beam extending toward the support and parallel to the bottom strand profile. Cracking — and ultimately failure — in this region occurred due to a lack of concrete bond around the strand at the opening edge. Figure 6.13 shows the point of failure of specimen S10W. The failure mode was shear at the edge of the first opening. Figure 6.14 shows the mode of failure of specimen S11P. Failure occurred at the first pier where the shear reinforcement strap plate was pulled from the concrete in the top flange. There was insufficient confinement and cover around the plate, as noted under "Construction" in Chapter 4.

Discussion of Experimental Results

Both of the draped strand specimens, D10R and D10W, had greater ultimate strength than the straight strand specimens, as indicated by their ultimate load and the strain distribution in the prestressing strands. A draping point of 0.16 L from the end of the specimens performed well.

Specimens with straight prestressing strands were vulnerable to a problem identified by Barney et al. (1977). The capacity of specimens with openings in high shear regions was limited by an unrestrained shear crack extending from

the lower side of the opening toward the support. These cracks normally propagated along the prestressing strands.

As evidenced by damage and failure of all specimens, pier reinforcement must extend to and be anchored in the top flange of the joist. Figures 6.11 through 6.14 clearly show the failure resulting from a lack of bond between the shear reinforcement and the concrete of the top flange. The problem was particularly severe for the bent plate pier reinforcement, which cannot be anchored appropriately in the thin flange.

The concentrated loads negatively affected the performance of all specimens, ultimately forcing a shear failure in all beams. A more distributed method of applying the loads would aid in evaluating the performance of beams with web openings.

Draped strands and U-shaped shear reinforcement in the web opening piers, as used in specimen D10R, provided the best performance. Flexural cracking was evident in the early load stages to indicate that a flexural mode of failure may occur when loads are more uniformly applied. This reinforcement combination is recommended. While the pier reinforcement in specimen D10R was the easiest to place, an optimum solution would simplify the reinforcement details around the openings and the reinforcement anchorage in the top flange. The difficulties experienced in casting these specimens and the resulting misplaced openings (see "Construction," Chapter 4) negatively affected their performance.

Construction simplification was sought in the development of two additional joist specimens for Test Series 2. A second objective of the follow-on experimental work was to verify the overall performance of the joist design.

Results of Test Series 2

Load and Deflection

Table 6.3 shows the principal test results for the specimens of Test Series 2. Figure 6.15 compares unfactored (11.7 kips) and factored (19.1 kips) load demand due to combined dead and live load with the load capacities of all tested joists. The load capacities of the final two specimens, D8R1 and D8R2, were superior to those of the first series and well above the load demand. The total failure loads, including the weight of the distribution beams and the applied loads, were 38.0 and 32.0 kips for D8R1 and D8R2, respectively. For specimen

D8R1, this represents 199 percent of the superimposed ultimate load or 325 percent of the superimposed service load. D8R2 failed at approximately 168 percent of the superimposed ultimate load, or 274 percent of the superimposed service load.

The load versus deflection curves of specimens D8R1 and D8R2 are compared with that of D10R in Figure 6.16. In the service load range their behavior is similar. The curve of D8R2 generally follows the shape of that for D10R, but D8R2 achieves a higher failure load and deflection at failure. D8R1 is stiffer with less deflection through its loading history than the other joists. Table 6.4 shows the camber and the deflections of the specimens of Test Series 2, as was done for Test Series 1. Figures 6.17 and 6.18 show the deflection along the span at different load stages for D8R1 and D8R2, respectively. The deflected shapes are as would be expected for a solid beam. Total dead load and live load deflections were well below the allowable limits of the ACI code.

Strains

Measured strains taken from the gages mounted on the concrete surface at the top of the web and on the bottom prestressing strands were plotted for selected load increments at the specimens' midspan sections. A curve approximating the strain distribution in each specimen is shown in Figures 6.19 and 6.20. The neutral axis of D8R1 remained at essentially the same location through the loading history, appearing to be just below the joist flange. It appears that in D8R2 the neutral axis stabilizes at a height above the web openings.

Cracking and Failure Mechanism

Crack patterns were monitored throughout Test Series 2. Both specimens had initial hairline cracks upon prestress release at the corners of the first openings. Figures 6.21 and 6.22 show the crack patterns for D8R1 and D8R2 midway through the loading program. Uniformly spaced flexural cracks appeared across the bottom chord of the middle part of both specimens. Prior to failure, cracking in the area of the construction weaknesses was evident in both specimens. There was also concentrated cracking beneath the areas of load application.

Figure 6.23 shows the failure of D8R1 at the first web opening. The shear reinforcement in the pier pulled through the concrete at the top flange. Exposed reinforcement at the top of the first opening had been patched prior to testing. The failure mode in this case was shear. In D8R2 the lack of well bonded cover caused the specimen to fail at the location of the patch in the bottom chord.

Figure 6.24 shows the failure of this specimen. A concentration of shear stress at the first pier adjacent to the defect is evident from the large diagonal crack.

Discussion of Experimental Results

Specimens D8R1 and D8R2 (Test Series 2) performed much better than the specimens of Test Series 1. The failure loads for these two specimens were greater than for either D10R of Test Series 1 or the solid beam tested by Savage. D8R1 resisted a greater load than D8R2. The minimum experimental failure load for these two specimens—32.0 kips—represents a factor of 2.7 times the unfactored load demand and 1.7 times the factored load demand.

Problems in joist construction resulted in a large void in the bottom chord of D8R2. While the hole was patched before testing, it is believed that this weakness contributed to an early failure in the joist. D8R1 also had slightly misplaced openings, which caused a lack of adequate concrete cover above some openings. Failure in this specimen occurred above an opening.

The development of the crack patterns in both beams and the deflections and strains in the prestressing strands give evidence that uniform loading of this tee design would produce a flexural failure mode had there been no construction weaknesses.

Table 6.1. Principal results of Test Series 1.

Specimen	First crack location	Applied failure load (kips)	Total failure load* (kips)	Equivalent uniform load** (psf)	Ratio***	Type of failure
D10R		24.0	25.0	210	1.32	shear
D10W	corner of	15.4	16.4	130	0.82	shear
S10W	first opening	12.0	13.0	105	0.66	shear
S11P		15.0	16.0	127	0.80	shear

* Load includes weight of distribution beams and applied loads.

** Based on total failure load.

*** Equivalent uniform load of specimen relative to equivalent uniform load of solid joist.

Table 6.2. Cambers and deflections of Test Series 1 specimens.

Specimen	Camber at release (in.)	LL deflection (in.)	SIDL + LL deflection (in.)	Maximum deflection (in.)
D10R	1.31	0.40	.60	3.80
D10W	1.31	0.45	.67	1.74
S10W	1.25	0.65	.85	1.31
S11P	1.19	0.55	.80	2.38

Table 6.3. Principal results of Test Series 2.

Specimen	Location of first cracking	Applied failure load (kips)	Total failure load* (kips)	Equivalent uniform load** (psf)	Ratio***	Type of failure
D8R1	first openings	35.5	38.0	319	2.01	shear
D8R2		29.5	32.0	269	1.69	shear

* Load includes weight of distribution beams and applied loads.

** Based on total failure load.

*** Equivalent uniform load of specimen relative to equivalent load of solid joist.

Table 6.4. Cambers and deflections of Test Series 2 specimens.

Specimen	Camber at release (in.)	LL deflection (in.)	SIDL + LL deflection (in.)	Maximum deflection (in.)
D8R1	1.33	0.45	.65	4.00
D8R2	1.25	0.65	.78	3.20

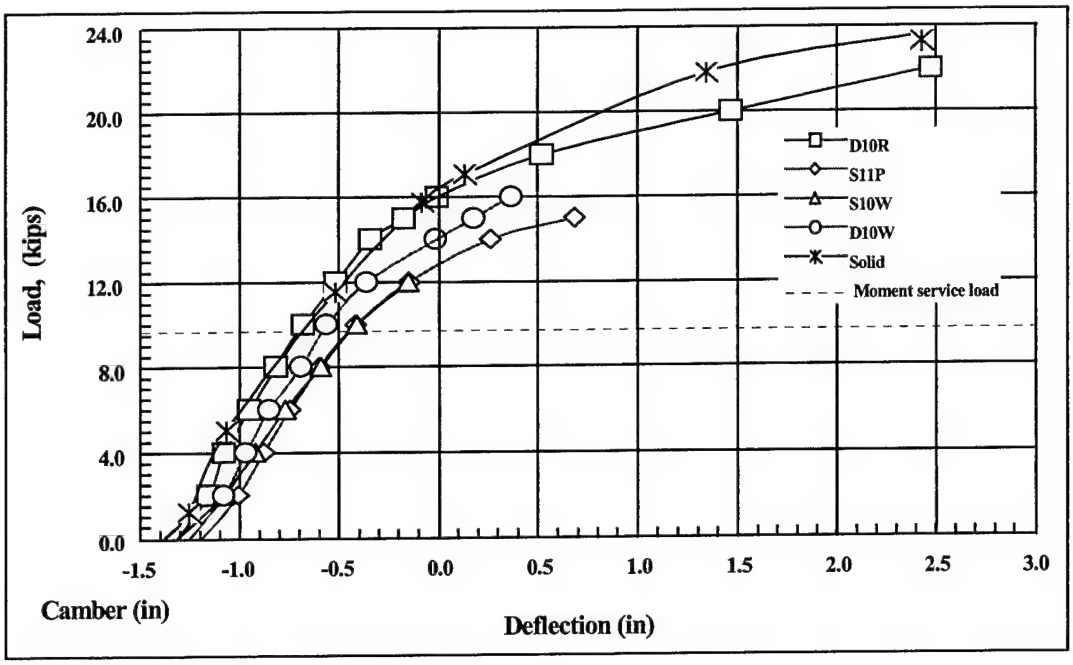

Figure 6.1. Test Series 1 specimen load versus deflection.

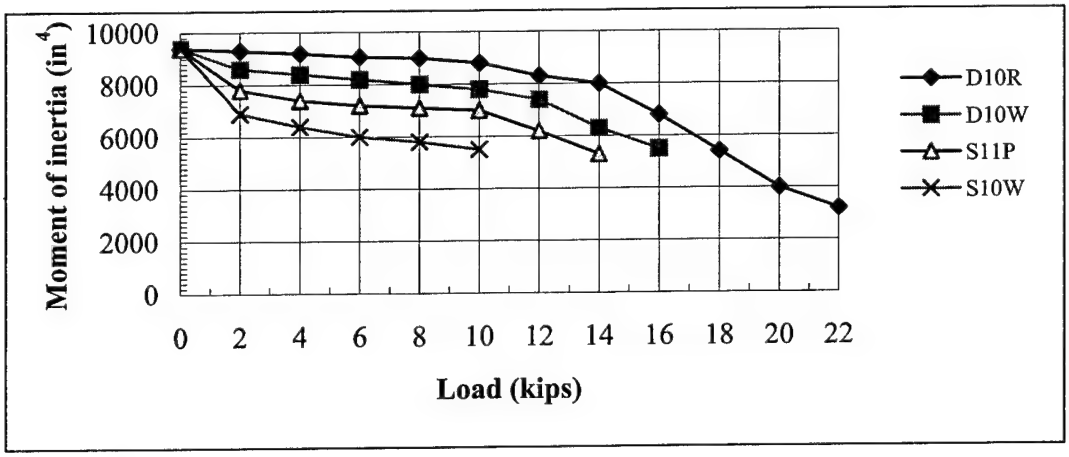

Figure 6.2. Test Series 1 specimen computed moment of inertia.

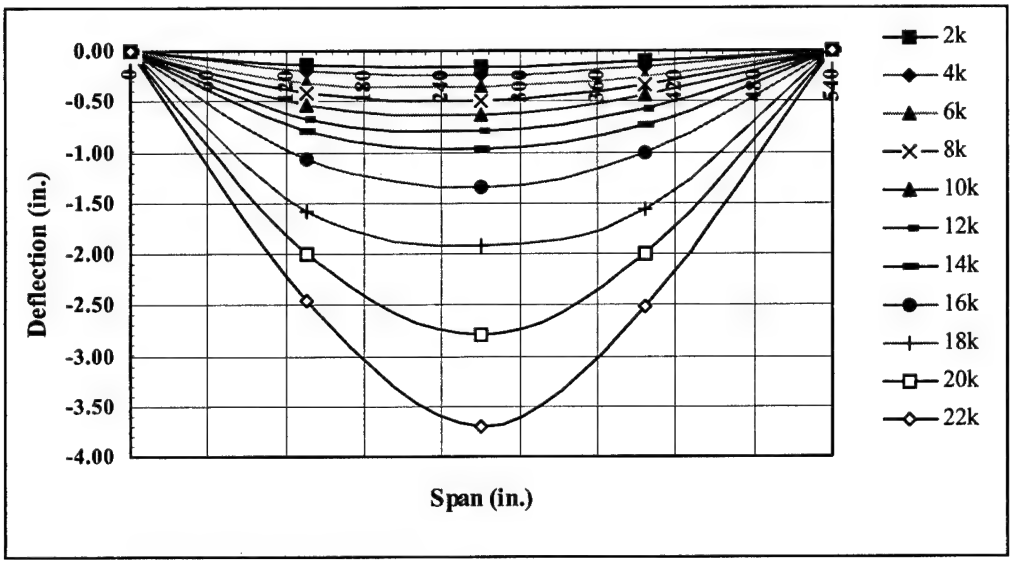

Figure 6.3. Specimen D10R deflected shape.

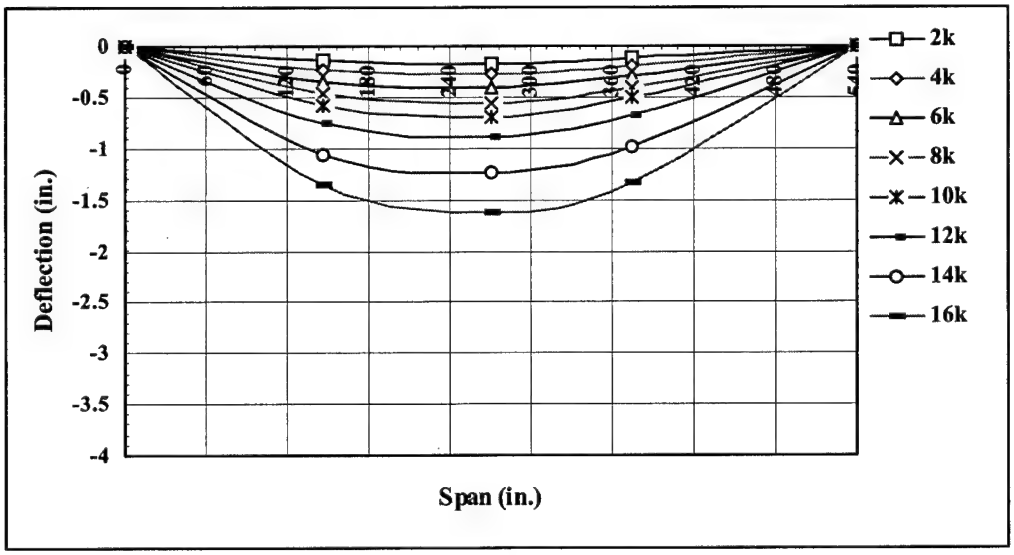

Figure 6.4. Specimen D10W deflected shape.

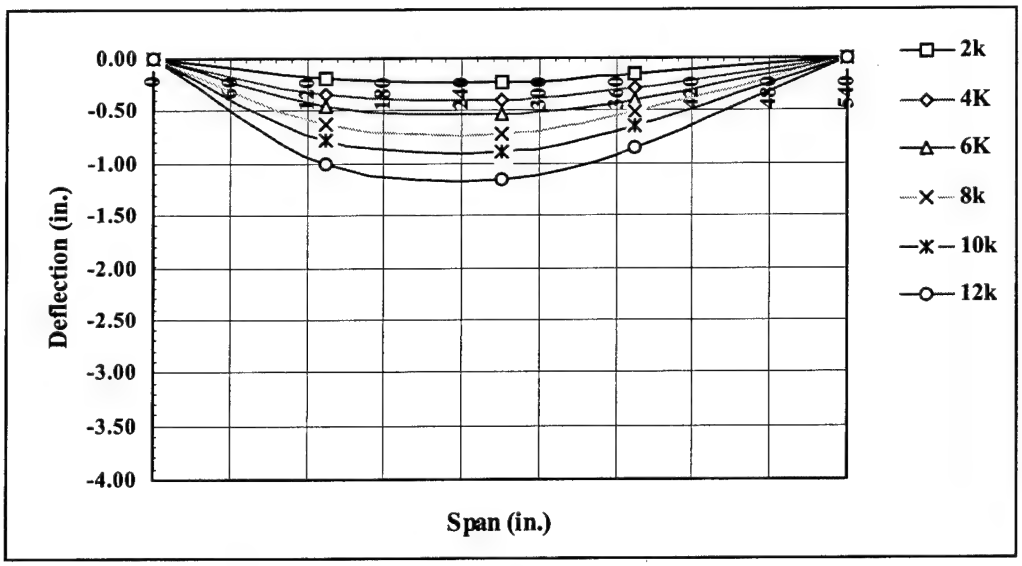

Figure 6.5. Specimen S10W deflected shape.

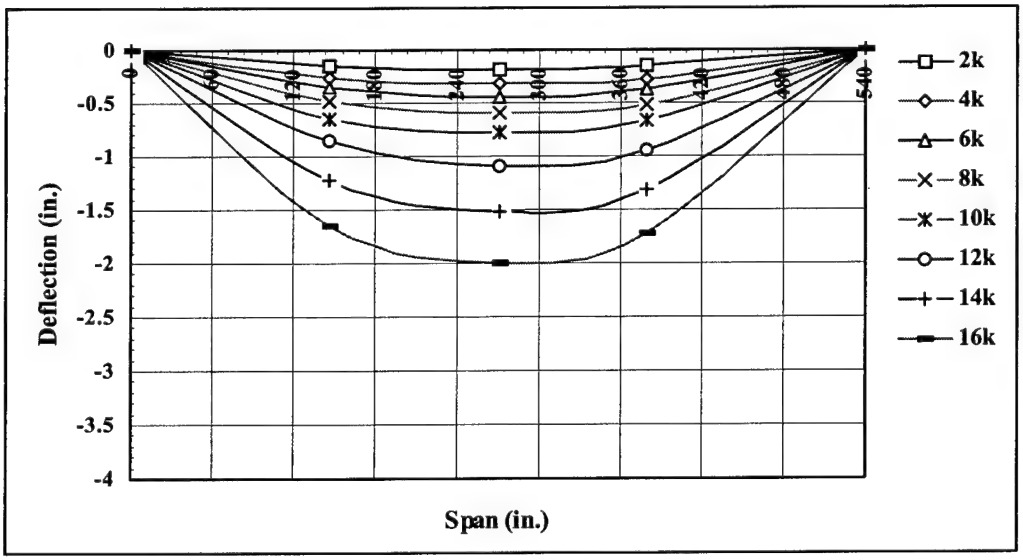

Figure 6.6. Specimen S11P deflected shape.

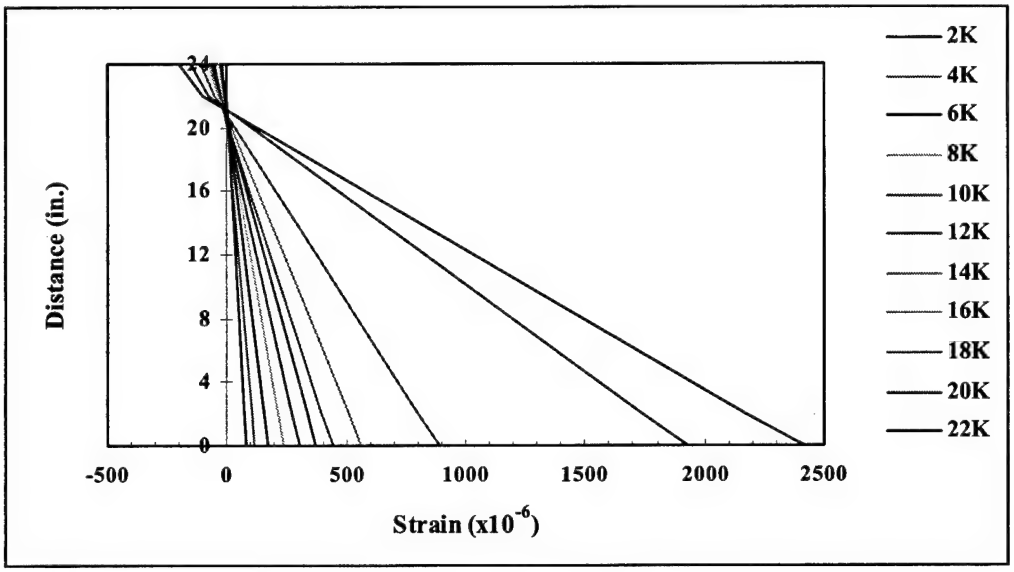

Figure 6.7. Specimen D10R strain distribution at midspan.

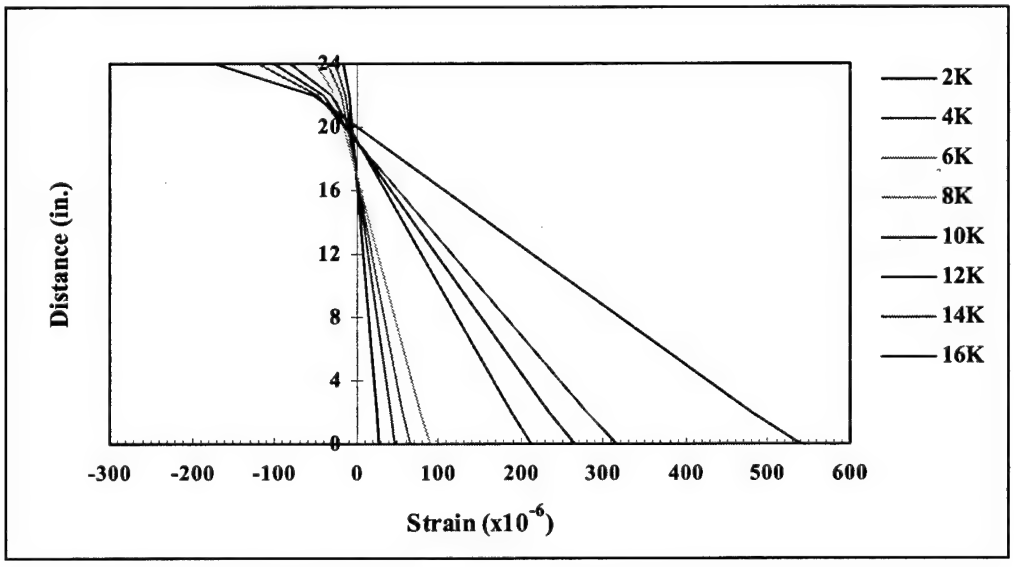

Figure 6.8. Specimen D10W strain distribution at midspan.

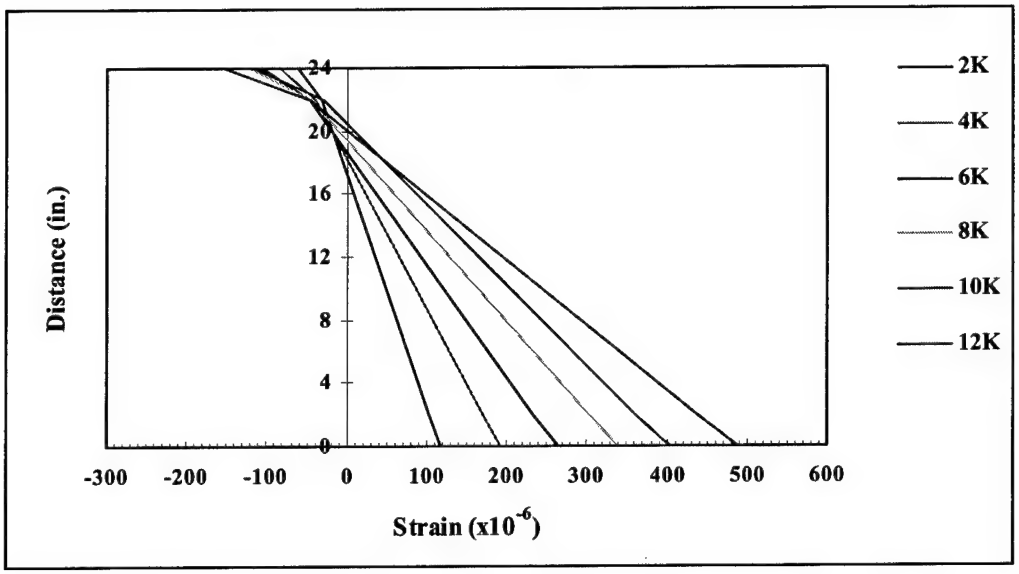

Figure 6.9. Specimen S10W strain distribution at midspan.

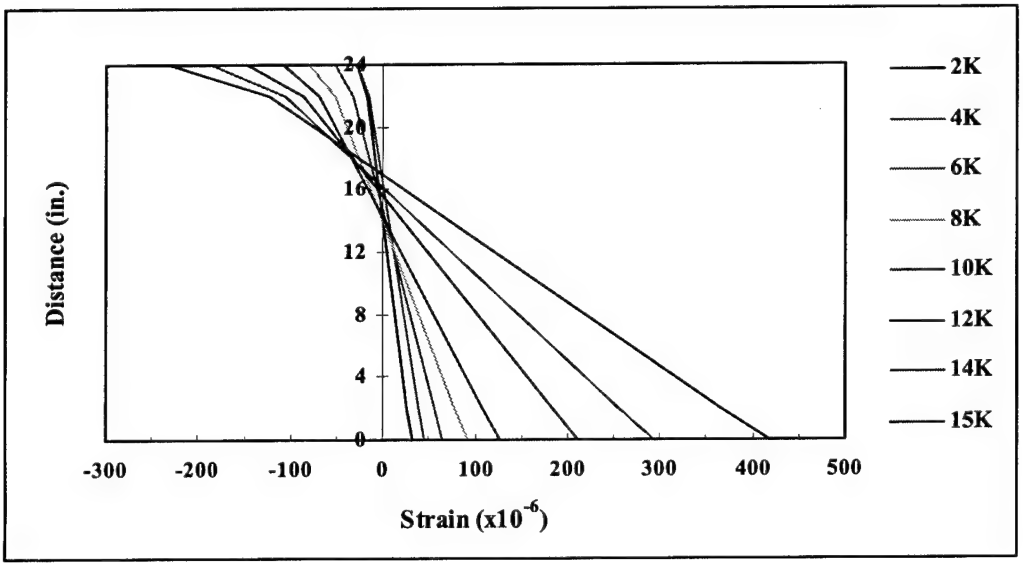

Figure 6.10. Specimen S11P strain distribution at midspan.

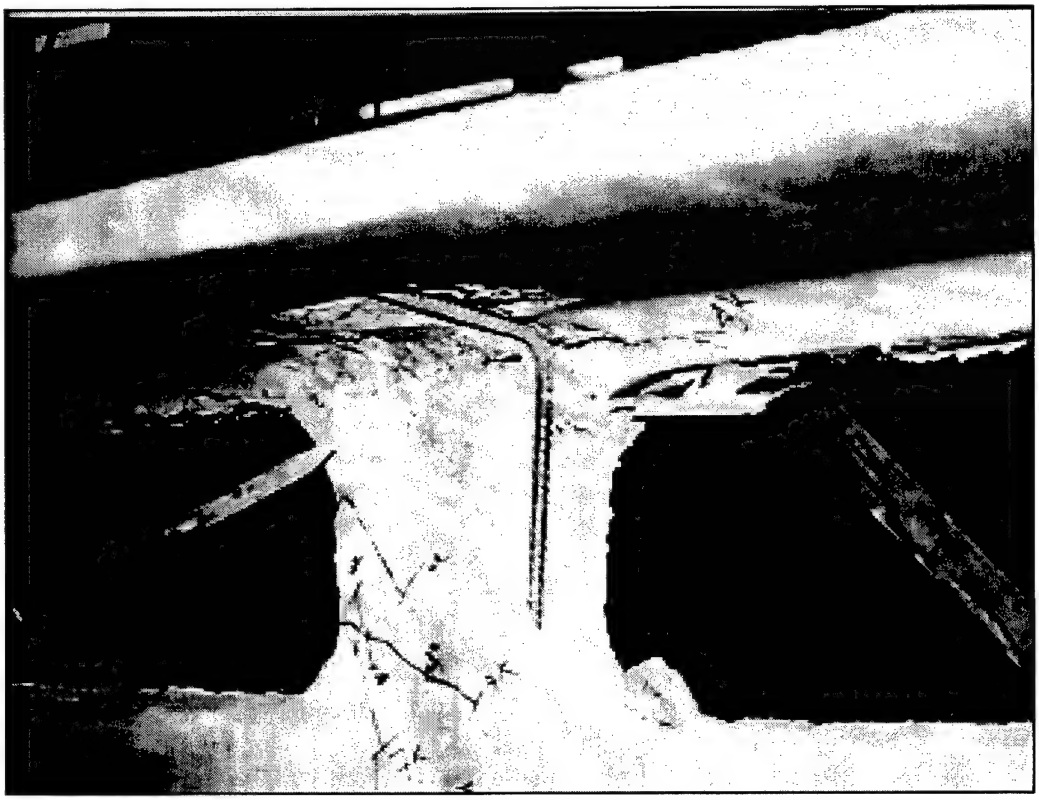

Figure 6.11. Specimen D10R failure.

Figure 6.12. Specimen D10W failure.

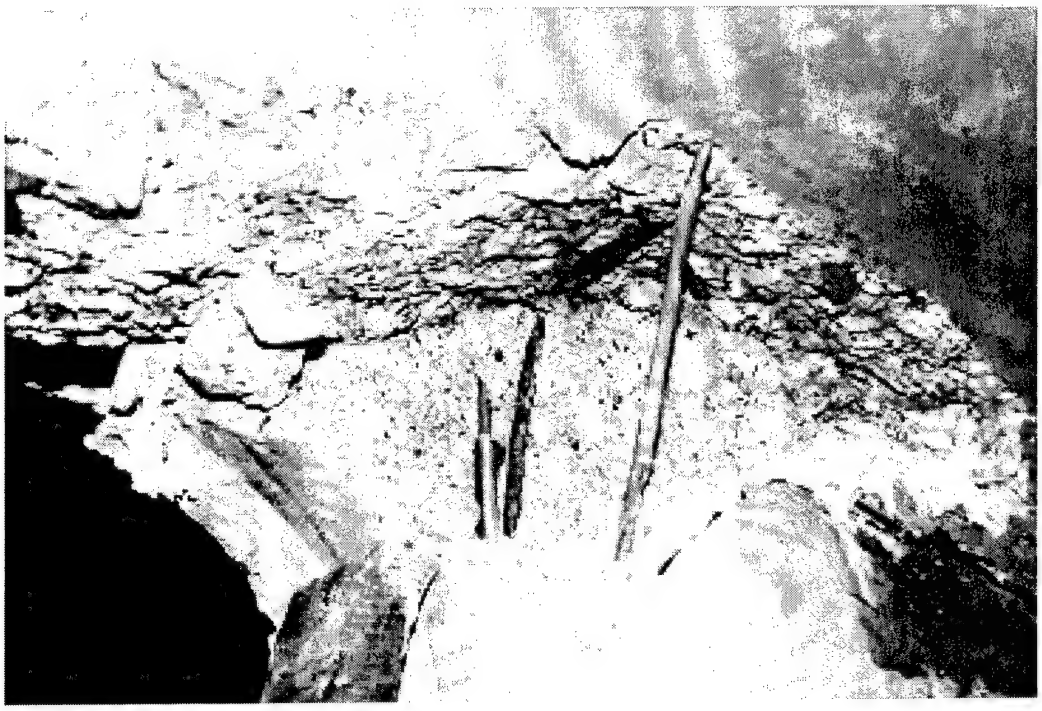

Figure 6.13. Specimen S10W failure.

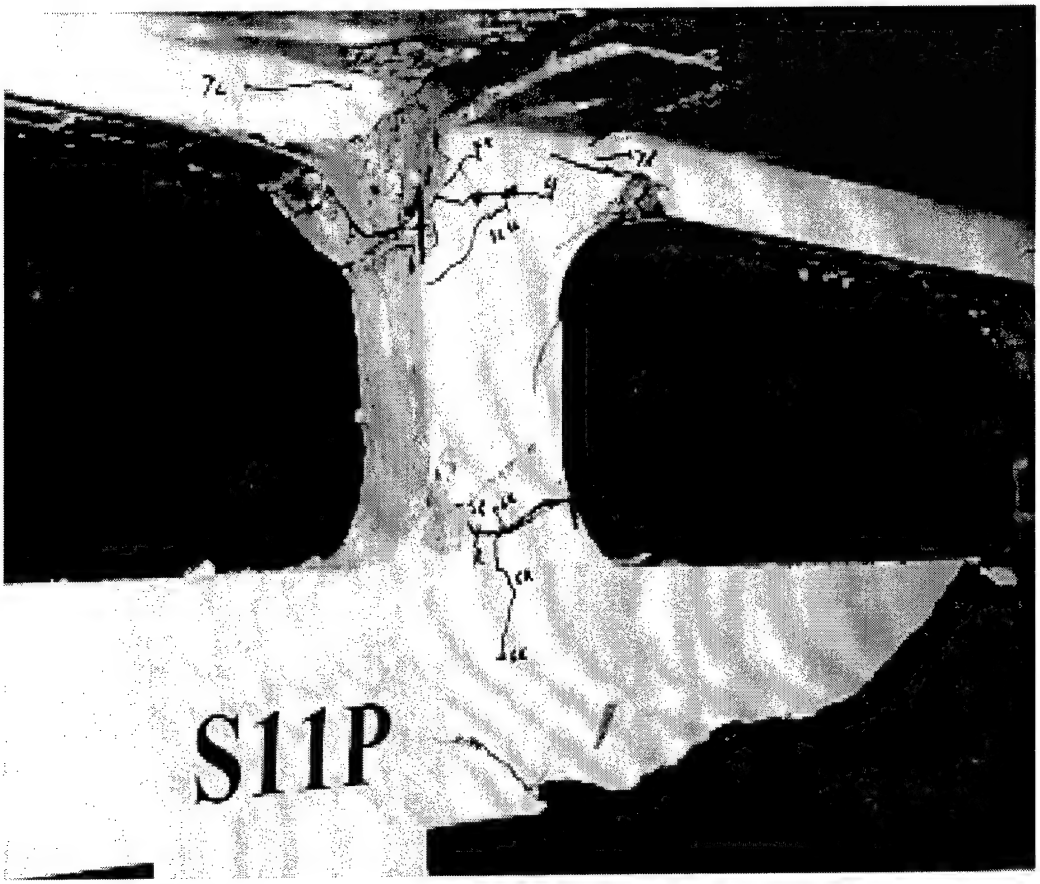

Figure 6.14. Specimen S11P failure.

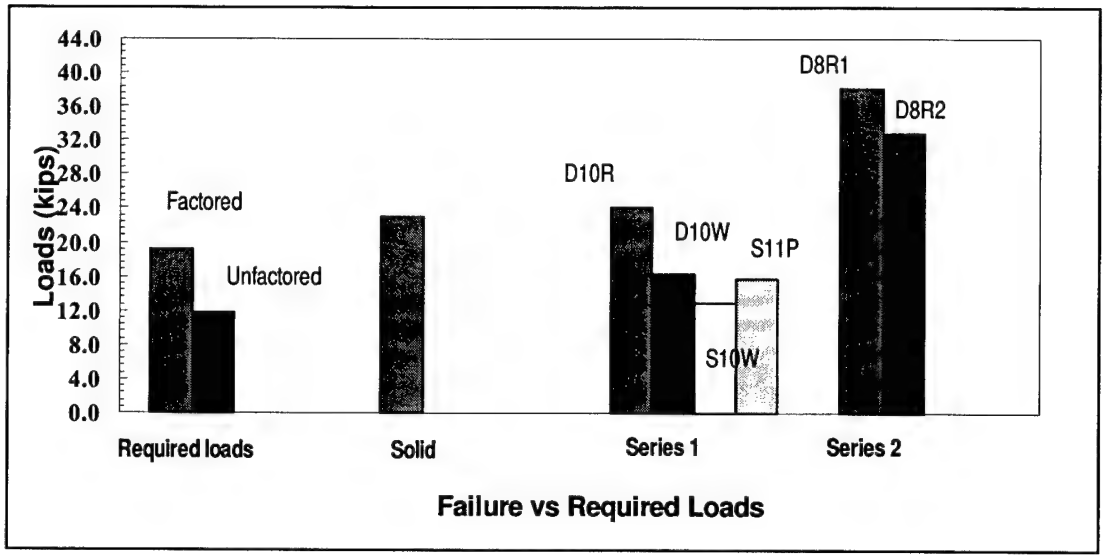

Figure 6.15. Test Series 2 specimen load capacity.

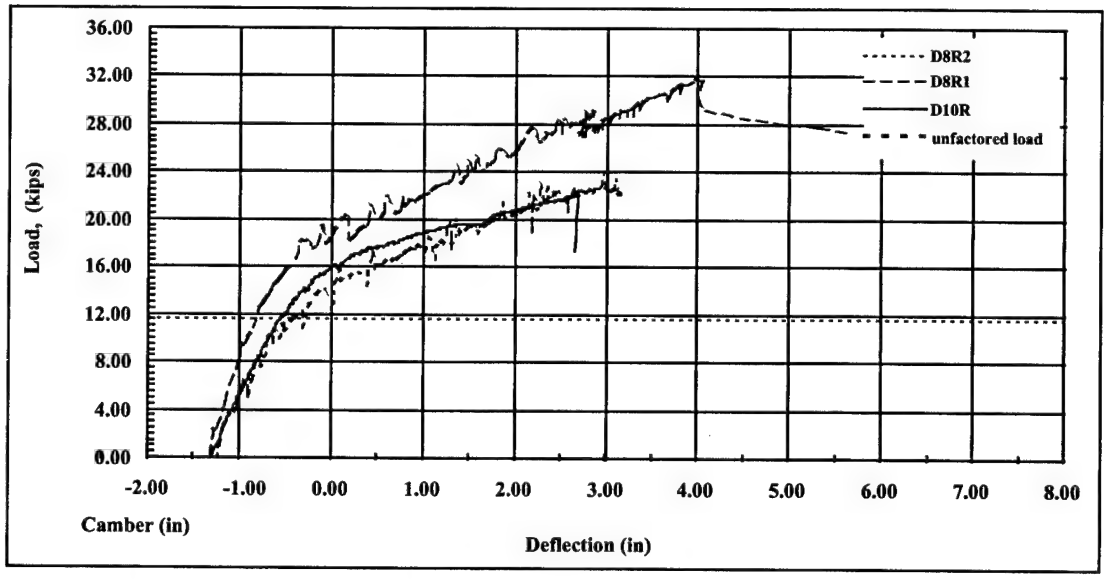

Figure 6.16. Test Series 2 specimen load versus deflection.

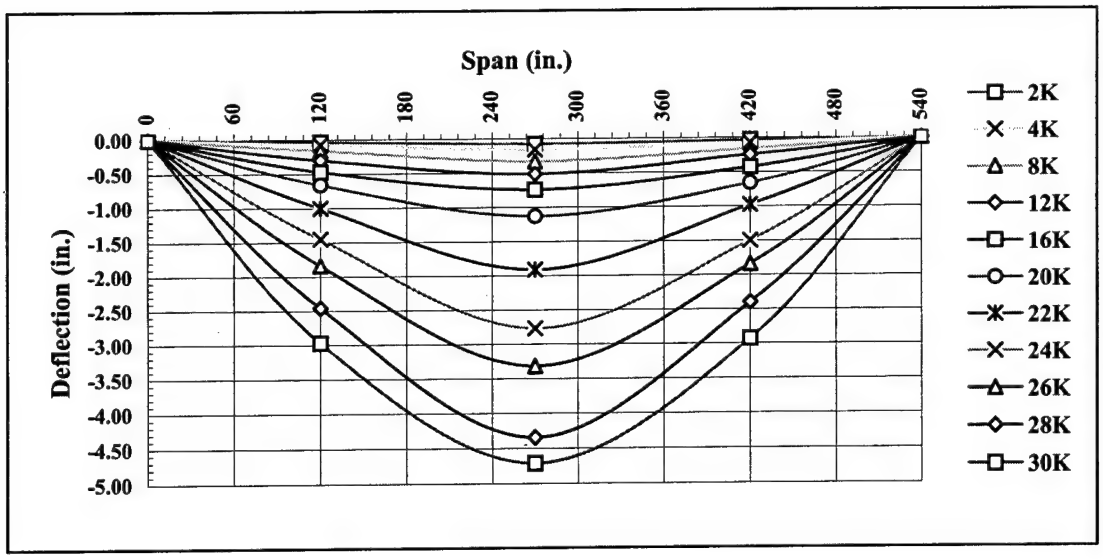

Figure 6.17. Test Series 2 specimen D8R1 deflected shape.

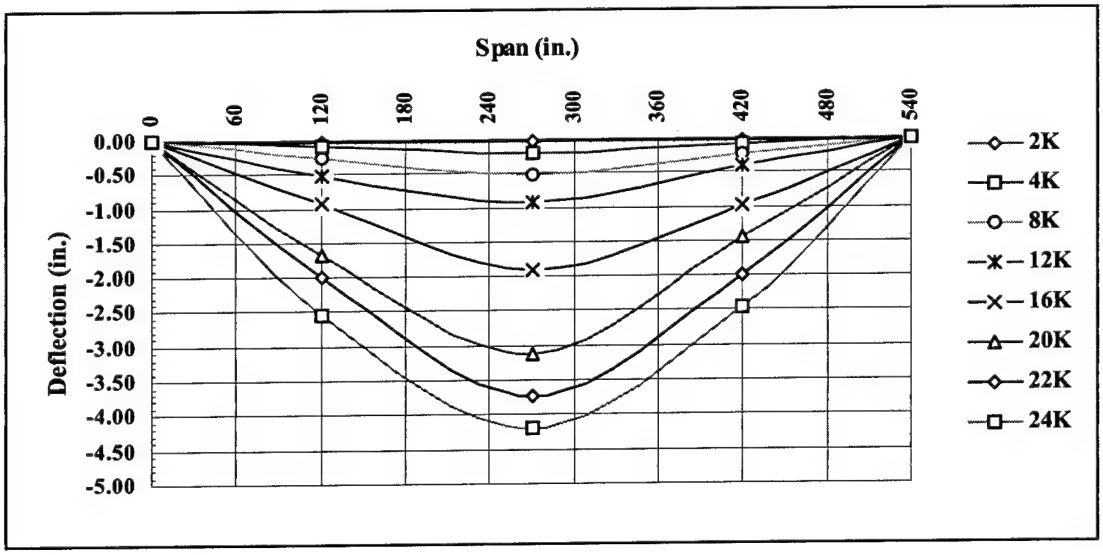

Figure 6.18. Test Series 2 specimen D8R2 deflected shape.

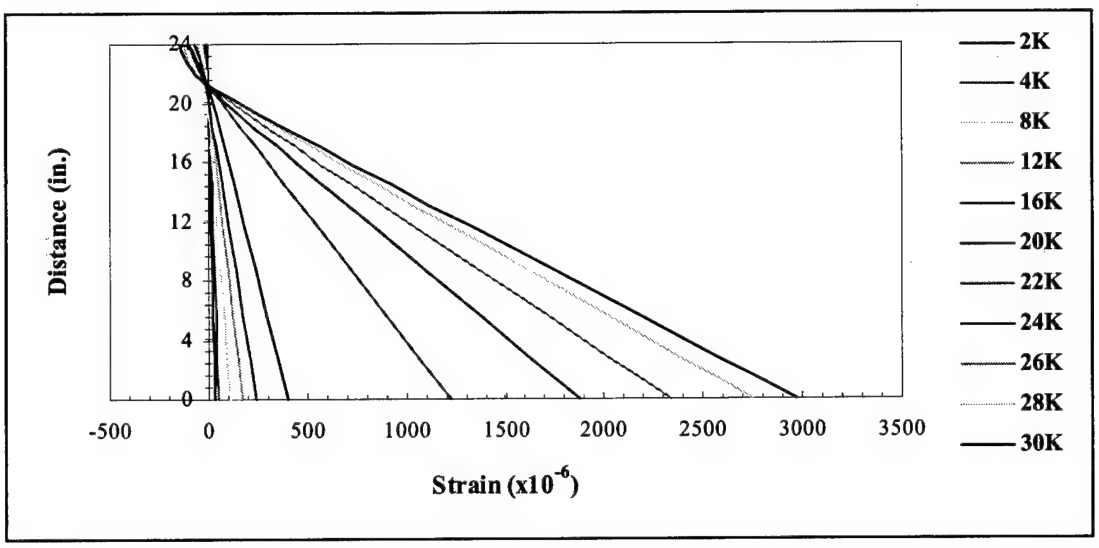

Figure 6.19. Specimen D8R1 strain distribution at midspan.

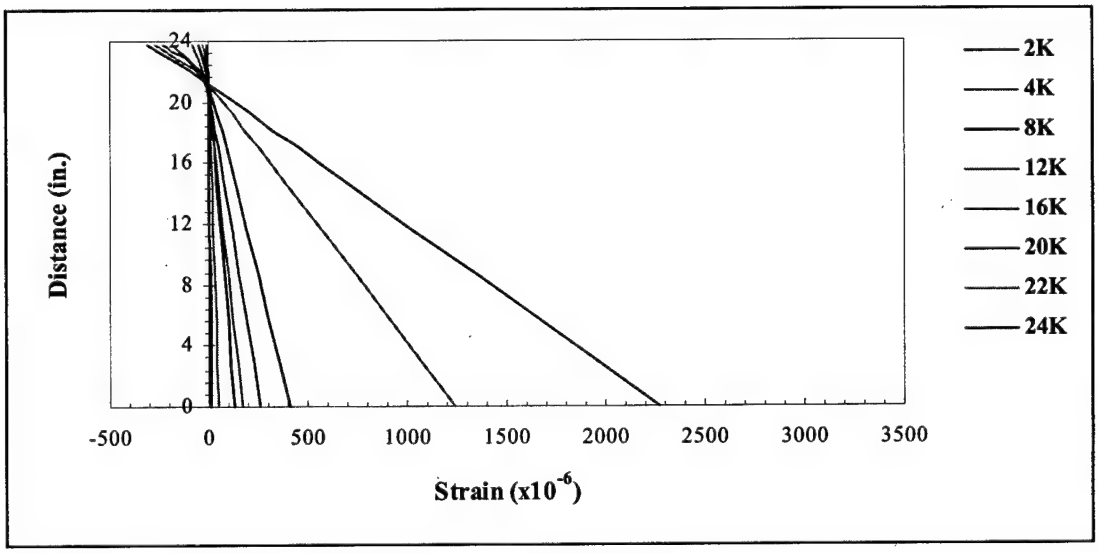

Figure 6.20. Specimen D8R2 strain distribution at midspan.

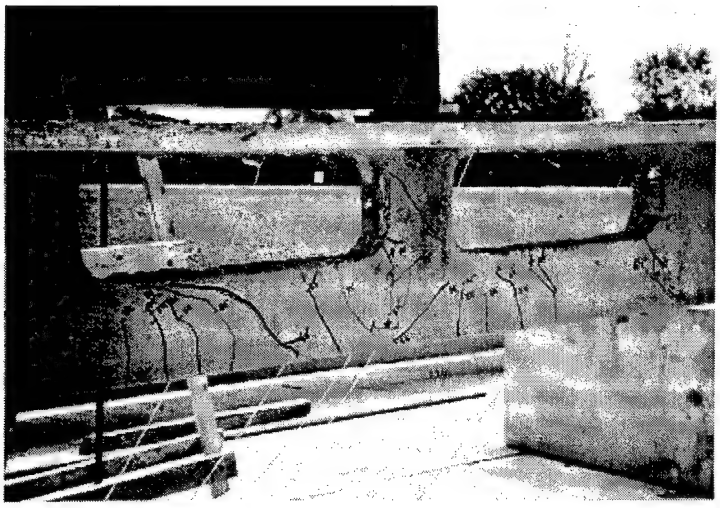

Figure 6.21. Specimen D8R1 cracking at midpoint of loading program.

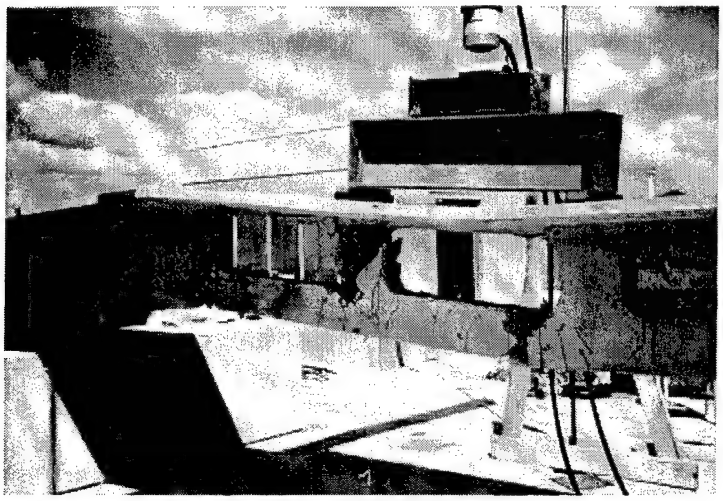

Figure 6.22. Specimen D8R2 cracking at midpoint of loading program.

Figure 6.23. Specimen D8R1 failure.

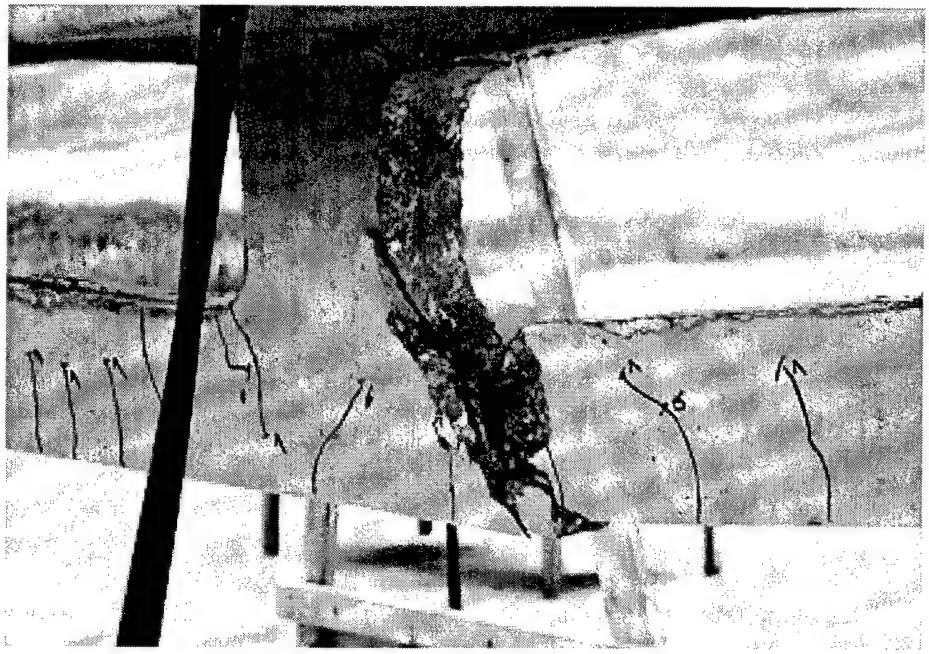

a. Failure location

b. Detail of failure

Figure 6.24. Specimen D8R2 failure.

7 Design Procedure and Cost Analysis

Introduction

Based on theoretical analyses, experimental tests, and the work done by Savage (1993) and Kennedy and Abdalla (1992), a simple procedure was developed to design a prestressed double tee with web openings. The design procedure presented below is a step-by-step process wherein load demands are assessed, a member cross-section is selected, prestressing and shear reinforcement are designed, and stresses and deflections are checked. A cost analysis of several representative prestressed concrete joist cross sections is provided to show the effectiveness of double-tee joists with web openings.

A design aid and design example are presented in the Appendix to facilitate understanding of the design procedure and application of double-tee sections with web openings.

Design Criteria and Assumptions

Criteria are based on *Building Code Requirements for Structural Concrete and Commentary* (ACI 318-95). Load and strength reduction factors specified by the code are used. Flexural strength is calculated using strain compatibility. The critical moment is assumed to be at midspan. End stresses are calculated 50 strand diameters from the end of the section, the theoretical point of full transfer. The flange flexural and shear strengths and the service load stresses are not considered as limiting criteria. The section is not allowed to crack under service loads. The estimated cambers and deflections shown are calculated using the multipliers given in the *PCI Design Handbook, Precast and Prestressed Concrete*, 4th ed. (PCI 1992).

The design of the double tee is in accordance with PCI (1992). The double tee is assumed to be uniformly loaded with a simple span and roller supports. Either a straight or draped strand profile is selected. If draped, the depression points are at either development length of the strands or one-sixth of the span at both ends, whichever is larger.

Material properties for concrete and steel are assumed as ≥ 7000 psi for concrete compressive strength, f'_c, at 28 days and ≥ 3500 psi at release. The concrete weight is 150 pcf. All strands are 0.5 in. diameter with an ultimate strength of 270 ksi and have low relaxation properties. Strands have an initial jacking tension of 75 percent of the ultimate strand strength.

The ratio of width to height of web openings is 3:1, with a minimum height of 8 in. The minimum filled diameter of the opening corners is 4 in. and the minimum pier width is 10 in. The openings are placed horizontally at least 2 in. below the bottom of the flange. For draped strand profiles the openings are longitudinally placed between draping points. Openings are placed interior of the development length required of straight strands.

Design Procedure

Define Loading

As stated above, uniform loading of the beam is assumed. Service loading is defined as the unfactored load. This will generally be a combination of the beam self-weight, superimposed dead load, and live load. Ultimate load is typically defined by the expression shown in Equation 1:

$$\text{Ultimate Load} = 1.4\,DL + 1.7\,LL \qquad \text{Eq. 1}$$

where: DL is the sum of the self-weight and superimposed dead load and
LL is the live load

Caution should be used in designing double-tee beams with web openings when concentrated loads are expected.

Select Configuration

Using a specific section depth, determine a preliminary number of prestressing strands using the load tables for double-tee beams in PCI (1992). Strands may be either straight or draped. Drape points should be at the distance of the strand development length or one-sixth of the span length from each beam end, whichever is greater. Place the bottom strands so their centroid coincides with the centroid of the bottom chord. One additional strand should be placed in the web above the opening at the same level as the bottom of the flange. Place the strands at both ends of the tee as close to the bottom of the tee as possible to

minimize the required depression force. Locate and center the openings over the cross-section and span.

Check Stresses

Flexural, shear, and axial stresses should be checked for selected loading stages. At transfer of prestressing, critical sections are located at the transfer length, the depression point for draped strand and the midspan. The section properties for solid section should be used for these calculations at the transfer length and depression point. At midspan, the section properties should incorporate the opening. In particular, compressive stresses in the bottom chord below the openings should be checked at the midspan section of the beam. Equations 2 and 3 may be used with appropriate member properties to calculate the stresses.

$$f_b = + \frac{P_{si}}{A} + \frac{P_{si}\ e}{S_b} - \frac{M_b}{S_b} \qquad \text{Eq. 2}$$

$$f_t = + \frac{P_{si}}{A} - \frac{P_{si}\ e}{S_t} + \frac{M_b}{S_t} \qquad \text{Eq. 3}$$

where f_t = concrete stress at top of beam
f_b = concrete stress at bottom of beam
P_{si} = prestress force at release after initial losses
e = eccentricity of the strand at the section under consideration
M_b = self weight moment of the beam.

At service load stage the critical sections are located at midspan, at the edge of the first opening, and at the depression point for sections with draped strands. Section properties should include the effect of the opening. Equations 4 and 5 may be used:

$$f_b = + \frac{P_{se}}{A} + \frac{P_{se}\ e}{S_b} - \frac{M_b + M_{SIDL} + M_{LL}}{S_b} \qquad \text{Eq. 4}$$

$$f_t = + \frac{P_{se}}{A} - \frac{P_{se}\ e}{S_t} + \frac{M_b + M_{SIDL} + M_{LL}}{S_t} \qquad \text{Eq. 5}$$

where P_{se} = prestress force at service after all losses
M_{SIDL} = superimposed dead load moment
M_{LL} = live load moment.

Flexural stresses in the bottom chord due to a distribution of the shear force at the opening should be included. The distribution of the shear force between the chords depends on whether the chords have cracked. A full-depth crack has not occurred if $T < 6A_{gt}\sqrt{f'_c}$, where A_{gt} is the gross area of tensile chord and f'_c is the concrete compressive strength. In this case the shear forces in the chords are given by Equation 6, which was developed by Barney et al. (1977) and confirmed by further work by Kennedy and Abdalla (1992):

$$V_b = V \frac{\sqrt{A_b I_b}}{\sqrt{A_b I_b} + \sqrt{A_t I_t}} \quad \text{Eq. 6}$$

where V_b = shear carried by the bottom chord
V = the ultimate shear force at the section under consideration (middle of the first opening)
A_b = area of the bottom chord
A_t = area of the top chord
I_b = moment of inertia of bottom chord
I_t = moment of inertia of top chord.

The moment of this force should be computed at the edge of the opening fillet. Therefore, additional stresses due to bending of the bottom chord are expressed as shown in Equation 7:

$$f_b = \frac{V_b \times (0.5 \text{ opening length} - \text{fillet dimension})}{S_b} \quad \text{Eq. 7}$$

This stress should be added to the stress due to applied load. If $T \geq 6A_{gt}\sqrt{f'_c}$, then a full-depth crack of the tension chord has probably occurred, and the shear forces in the chords are given by: $V_c = V$, $V_t = 0$.

At ultimate loading the critical section is at the midspan. The flexural strength of the tee should be checked using ACI code approximate equations or the strain compatibility method. The top strand should be ignored in the calculation of the ultimate strength capacity.

Permissible stresses in concrete are in accordance with the requirements of ACI 318-95, Section 18.4. These are summarized below:

- *Stresses in concrete immediately after prestress transfer*:

extreme fiber stress in compression = $0.6f'_{ci}$

extreme fiber stress in tension = $6\sqrt{f'_{ci}}$

extreme fiber stress in tension at the ends = $3\sqrt{f'_{ci}}$

where f'_{ci} = compressive strength of concrete at time of initial prestress

- *Stresses in concrete at service loads*:

  extreme fiber stress in compression due to prestress force plus sustained loads = $0.45f'_c$

  extreme fiber stress in compression due to prestress force plus total loads = $0.60\ f_c$

  extreme fiber stress in tension due = $6\sqrt{f'_c}$

Design Shear Reinforcement

For shear design, the critical section is at a distance h/2 from face of support where h is the total depth of the section. For the solid sections of the double tee, design shear reinforcement as if the beam had no web openings. To control cracks extending from the corners of openings and shear in the opening piers, use the total factored shear force at the center of the first opening to compute the area of additional stirrups to be placed adjacent to the opening. The required area of stirrups is given in Equation 8:

$$A_V = \frac{V_u}{f\ f_y d} \qquad \text{Eq. 8}$$

where A_v = required area of stirrups in., sq in.
V_u = ultimate shear at center of the first opening, kips
ϕ = strength reduction factor, 0.85
f_y = yield strength of stirrups steel, ksi.

Size shear reinforcement at openings assuming U-shaped stirrups and place the same reinforcement at both ends of all openings.

Design the shear reinforcement in the chords above and below the openings based on a conservative estimate of the compressive and tensile chord forces at ultimate load:

$$C = T = A_{ps} f_{se} \qquad \text{Eq. 9}$$

where A_{ps} = area of prestressed strands, sq in.
f_{se} = effective prestressing stress in the strands, ksi

$$V_c = 2\left[1 + \frac{C}{2000\ A_g}\right]\sqrt{f'_c}\ b_w\ d \qquad \text{Eq. 10}$$

where A_g = cross section area of the top chord
d = depth of the top chord.

Shear capacity should be greater than ultimate shear demand: $\phi V_c > V_u$.

A U-shaped welded wire fabric should be placed in the tension chord below the openings to prevent shear cracks under service loads. The minimum welded wire fabric should be 4x4-W4.0xW4.0 and the spacing of the vertical wires should be approximately half the depth of the tension chord.

Assume that the tension chord is cracked at ultimate load. The ultimate shear force, V_u, should be carried completely by the compression chord. Shear capacity of the compression chord, V_c, can be conservatively estimated by ACI Code equation (11-4) for nonprestressed members. The value of V_u should be less than or equal to ϕV_c where $\phi = 0.85$:

$$V_c = 2\left[1 + \frac{N_u}{2000\ A_g}\right]\sqrt{f'_c}\ b_w\ d < 6\sqrt{f'_c}\ b_w\ d \qquad \text{Eq. 11}$$

where b_w = width of compression chord, in.
d = depth of flange, in.
f'_c = concrete strength at 28 days, psi
A_g = cross-sectional area of compression chord, sq in.
N_u = axial compression force = C, lb.
V_c = nominal shear strength provided by concrete, lb.

Check Deflections

Deflections should be checked using standard methods of structural analysis for double tees without openings. Estimated cambers are based on elastic members. The estimated long-term deflection includes superimposed dead load but does not include live load.

Cost Analysis

The following cost analysis (Table 7.1) compares the material costs for double-tee joists with web openings and conventional double-tee joists without web openings. For comparison purposes, material cost figures also are included for the hybrid concrete joists developed in related CPAR work (Saleh et al. 1997). The assumptions used in the cost analysis of all systems are listed below.

Assumptions for cost analysis

Span ..... 50 ft
Live load ..... 50 psf
Partitions, floor covering & miscellaneous dead load ..... 15 psf
Double tee top flange ..... 4 in.
Cast-in-place slab for the hybrid joist ..... 4 in.
Double tee web spacing ..... 4 ft
Hybrid joist spacing ..... 6 ft
Double tee depth ..... 24 in.
Hybrid joist depth ..... 24 or 36 in.
28-day concrete strength ..... 7000 psi for double tee
10,000 psi for the hybrid joist
Strands ..... 1/2 inch diameter 270 ksi low relaxation

Table 7.1. Materials cost analysis.

Item		Unit Cost ($)	Material quantity / unit floor area							
			Solid double tee		Double tee with web openings		Hybrid joist, 24 in. depth		Hybrid joist, 36 in. depth	
			Quantity	Cost	Quantity	Cost	Quantity	Cost	Quantity	Cost
Strands, ft/ft²		0.50/ft	2.00	1.00	2.25	1.13	2.03	1.02	3.01	1.51
Reinforcing bars, lb/ft²		0.35/lb	---	---	0.50	0.18	0.21	0.07	0.29	0.10
Welded wire fabric, lb/ft²		0.50/lb	1.22	0.61	1.41	0.55	0.43	0.22	0.43	0.22
Hold-down devices		18.00/piece	0.01	0.18	0.01	0.18	0.01	0.18	0.01	0.18
Concrete	Precast, ft³/ft²	120/yd³	0.51	2.27	0.47	2.09	0.11	0.49	0.17	0.76
	CIP, ft³/ft²	60/yd³	---		---	---	0.17	0.38	0.17	0.38
Total/ ft²				4.06		4.13		2.36		3.15

This analysis shows that the materials required for producing double-tee joists with openings is slightly greater than the cost of materials for conventional solid double-tee joists. Production costs for the joists are anticipated to be comparable to those for standard solid double-tee joists.

The use of double-tee joists with web openings in construction would provide additional cost savings over standard double-tee construction because environmental systems could be passed through the webs of the joists. This would require less overall building height, saving in wall material costs and lowering the overall cost of the building by reducing its weight.

8 Conclusions, Recommendations, and Commercialization

Conclusions

Reinforced concrete double-tee joists can be designed and manufactured with many web openings without jeopardizing strength. Specimens with draped prestressing strands performed better than those with straight prestressing strands. The capacity of specimens with straight strands and openings in high shear regions was limited by an unrestrained crack beginning at the edge of the first opening and extending toward the support. The cracks propagated along the prestressing strands. In draped strand specimens a draping point of one-sixth the span length from the beam end performed well. This length was shorter than that used by Savage (1993).

The location of web openings along the span and the amount and type of web shear reinforcement were the variables with the greatest affect on beam strength and behavior. This result confirms observation made by Barney et al. (1977). In the final design, web openings were eliminated in the area 0.16 L from each beam end. The reinforcement in opening piers must extend to and be anchored in the joist top flange. Bundled U-shaped reinforcement at the pier openings performed the best and was the easiest to place.

Caution must be used in designing double tees with web openings when concentrated loads are expected. Concentrated loading greatly affected the resulting shear failure modes in the first four specimens (Test Series 1). Failure in shear of the final two specimens (Test Series 2) may be attributed primarily to weaknesses in their initial construction and to the type of loading used in testing (i.e., concentrated loading). The development of the crack patterns in both of the Test Series 2 beams, the deflections, and the strains in the prestressing strands give evidence that uniform loading of this double-tee design would produce a flexural failure mode had there been no construction weaknesses.

The overall benefits to the constructed project realized by using double-tee joists with web openings outweigh the slightly higher material costs as compared to a

conventional double-tee design. The openings allow pipes and ductwork for the building's environmental systems to pass through the joist webs, thereby reducing the building's height requirements. This reduction in height will translate into additional cost savings by reducing overall building weight and material requirements.

Recommendations

The final designs evaluated in this experimental and analytical research program are recommended for use by USACE and the construction industry to replace standard double-tee beams in precast prestressed reinforced concrete floor and roof construction where only uniform loading will occur. Double-tee joists with web openings are not recommended for applications where concentrated loads may be present.

The optimum design for a double-tee joist with web openings uses a draped strand profile. The draping point should not be less than 0.16 L from the end of the beam or the strand development length. Joist shear reinforcement, as shown in Figure 4.12 (Chapter 4), is recommended.

The use of expanded polystyrene foam to form the opening blockouts created difficulties in consolidating concrete around the openings (see "Construction," Chapter 4). For commercial production, it is recommended that blockouts be fabricated from steel plates or fiber reinforced plastic molds. The blockouts should be tapered for easy removal. Securing the blockouts, either by bolting them to the side form of the double tee or by vertical threaded bars inserted from the top and held by a cross frame above the form, are recommended. Note that the latter method may cause some inconvenience in finishing the top surface of the double tee.

This research confirmed the excellent performance of double-tee beam designs with web openings for uniform load applications. Further optimization may be possible by increasing the spacing between web openings. It is recommended that research be conducted to evaluate the performance of this design concept for concentrated loadings. Additional experimental evaluation of the beam design related to vibrations and fatigue loading also would be beneficial. Finally, the long-term effects of creep on the behavior of double-tee beams with web openings should be investigated.

Technology Transfer and Commercialization Plan

The Prestressed Concrete Institute (PCI) is the primary organization in the United States dedicated to the advancement of the design, manufacture, and use of prestressed and precast concrete. PCI disseminates information on the latest concepts, techniques, and design data to the architecture and engineering professions through regional and national programs and technical publications. This organization represents the essential vehicle for the production and marketing of the double-tee joist design to the engineering profession and precast concrete industry.

The design procedure for double-tee beams with web openings has been submitted to PCI for review and inclusion in its design handbooks. These handbooks provide guidance to engineers in designing and specifying precast concrete products in accordance with commonly accepted industry practice and codes. After PCI reviews and accepts the design procedure and design aids, the organization has agreed to publish the material in the next edition of the *PCI Design Handbook*. The review process is expected to take 6 months.

Based on this research, double-tee beams with web openings will be incorporated into the design of the new Information Science, Technology, and Engineering Building, to be constructed at the Omaha campus of the University of Nebraska. Beams 24 in. deep spanning 30 ft will be used as roof members in the building's Structural Laboratory. Construction is scheduled to be completed in the summer of 1999.

Technical presentations and papers published in refereed technical journals will also promote transfer of this double-tee technology. The contribution of the research has already been recognized for a paper authored by Savage, Tadros, et al., entitled "Behavior and Design of Double Tee with Web Openings," published in the Jan/Feb 1996 edition of *PCI Journal*. The paper received the PCI Martin P. Korn Award for best design/research paper appearing in the journal during 1996.

As design professionals increasingly specify double-tee beams for their construction projects, the precast concrete industry is likely to respond to the demand by offering new products. As a participant in the research that produced the double-tee designs, the Precast Concrete Association (PCA) of Nebraska supports the commercialization of this product. At this time Concrete Industries, Inc., of Lincoln, NE, a member of the PCA of Nebraska, is prepared to produce open web double-tee beams upon request of the owner or designer. The PCI can also

encourage commercialization of the double tee as a standard product of the precast concrete industry on a national scale.

As the primary design and construction agent for the U.S. military services, the Army Corps of Engineers should disseminate design and application guidance on this technology through the appropriate Corps publication series. Information on the double-tee design has been published in *Structural Engineering For Military Programs* (HQUSACE, October 1996).

Applicable Corps guide specifications, CWGS 03425, *"Precast Prestressed Concrete,"* and CEGS* 03550, *"Precast Prestressed Concrete Floor and Roof Units,"* currently specify that designs conform to ACI and PCI standards. Neither guide specification prohibits the use of double-tee beams with openings, and both acknowledge that members may be cast with holes, or openings. CWGS 03425 states that shop drawings are to show all openings equal to or greater than 12 in. wide cast into members. CEGS 03550 states that "Structural analysis shall include evaluation of the effects of... holes.... Units shall be designed for... additional loads imposed by openings...." Inclusion of the design of double-tee joists with web openings in the PCI handbooks will further facilitate Corps application of these joists.

CWGS: Civil Works Guide Specification.
CEGS: Corps of Engineers Guide Specification.

References

Abdalla, H.A., "Static and Dynamic Response of Prestressed Concrete Beams with Openings" (Ph.D. Dissertation, University of Windsor, 1993).

Abdalla, H,. and J.B. Kennedy, "Design of Prestressed Concrete Beams with Openings," *American Society of Civil Engineering [ASCE] Journal of Structural Engineering*, vol 121, no. 5 (May 1995).

American Concrete Institute [ACI] Committee 318, Building Code Requirements for Structural Concrete and Commentary (ACI, 1995).

ACI Committee 544, Guide of Specifying, Proportioning, Mixing, Placing and Finishing Steel Fiber Reinforced Concrete (ACI,1993).

Barney, G.B., "Design of Prestressed Concrete Beams with Large Web Openings" (Ph.D. Dissertation, Northwestern University, June 1975).

Barney, G.B., W.G. Corley, J.M. Hanson, and R.D. Parmelee, "Behavior and Design of Prestressed Concrete Beams," *PCI Journal*, vol 22, no. 6 (PCI, 1977).

Carrasquillp, R.L., A.H. Nilson, and F.O. Slate, "Properties of High Strength Concrete Subject to Short-Term Loads," *ACI Structural Journal*, vol 78, no. 3 (May-June 1981).

Dinakaran, V., and M.K.L.N. Sastry, "Behavior of Post-Tensioned Prestressed Concrete I-Beams with Large Web Openings," *Indian Concrete Journal* (February 1984).

Ghali, A., and A.G. Razaqpur, "Design of Transverse Reinforcement in Flanges of T-Beams," *ACI Structural Journal*, vol 83, no. 4 (July/August 1986).

Grossfield, B., and C. Birnstiel, "Test of T-Beams with Precast Webs and Cast-in-place Flanges," *ACI Structural Journal*, vol 59, no. 6 (May-June 1962).

Hamoudi, A.A., M.K.S Phang, and R.A Bierweiler, "Diagonal Shear in Prestressed Concrete Dapped-Beams," *ACI Structural Journal*, vol 72, no. 7 (July 1975).

Haque, M., "Stress Distribution in Deep Beams with Web Openings," *ASCE Journal of Structural Engineering*, vol 113, no. 5 (May 1986).

Kennedy, J., S. Chami, and N.F. Grace, "Dynamic and Fatigue Response of Prestressed concrete Girders with Openings," *Canadian Journal of Civil Engineering*, vol 17 (1990).

Kennedy, J.B., S. Chami, and N.F. Grace, "Cracking at Openings in Prestressed Beams at Transfer," *Proceedings of the Structural Division*, vol 108, no. ST6 (ASCE, June 1982).

Kennedy, J.B., and H. Abdalla, "Static Response of Prestressed Girders with Openings," *ASCE Journal of Structural Engineering*, vol 118, no. 2 (February 1992).

Levy, M.P., and T. Yoshizawa, "Interstitial Precast Prestressed Concrete Trusses for Ciba-Geigy Life Science Building," *PCI Journal*, vol 37, no. 6 (November/December 1992).

Loov, R.E., and A.K. Pantnaik, "Horizontal Shear Strength of Composite Concrete Beams with a Rough Interface," *PCI Journal*, vol 39, no. 1 (January/February 1994).

Mansur, M.A., K.H. Tan, and S.L. See, "Design Method for Reinforced Concrete Beams with Large Openings," *ACI Structural Journal* (July/August 1985).

Mattocak, A.H., and T.C. Chan,., "Design and Behavior of Dapped-End Beams," *PCI Journal*, vol 24, no. 6 (November/December 1979).

Mattock, A.H., and T.S. Theryo, "Strength of Members with Dapped Ends," Research Project No. 6 (PCI, 1986).

Mattock, A.H., and T.S. Theryo, "Strength of Precast Prestressed Concrete Members with Dapped Ends,' *PCI Journal*, vol 31, no. 5 (September/ October 1986).

Nasser, K.W., et. al., "Behavior and Design of Large Openings in Reinforced Concrete Beams," *ACI Journal*, vol 64 (January 1967).

Noritake, K., Shima, H. and Kumagai, S., "A Study of Structures with Prestressed Concrete Slabs and Truss Members, Using High-Strength Concrete," *Proceedings of the Federation International Prestressed (FIP) Symposium* (Oct. 17-20, 1993) pp 319-326.

Noritake, K., H. Shima,. and S. Kumagai, "Study on a New Construction Method for Concrete Structures Using Suspended Concrete Slabs," *Proceedings of the FIP Symposium* (Oct. 17-20, 1993) pp 425-432.

PCI Design Handbook—Precast and Prestressed Concrete, Fourth Edition (PCI, 1992).

Pool, R.B., and R. Lopes, "Cyclically Loaded Concrete Beams with Web Openings," *ACI Structural Journal*, vol 83, no. 5 (September/October 1986).

Ragan, H.S., and J. Warwaruk, "Tee Members with Large Web Openings," *PCI Journal*, vol 12, no. 4 (August 1967).

Salam, S.A., and J. Harrop, "Prestressed Concrete Beams with Transverse Circular Holes," *Proceedings of the Structural Division*, vol 105, no. ST3 (ASCE, March 1979).

Saleh, M.A., "Optimization of Prefabricated Joists" (Ph.D. Dissertation, University of Nebraska, December 1996).

Saleh, Mohsen A., P.A. Brady, A. Einea, and M.K. Tadros, *Design and Performance Testing of Prestressed Precast Reinforced Concrete Hybrid Joists*, Technical Report 98/04 (USACERL, December 1997).

Sargious, M., and W. Dilger, "Prestressed Concrete Deep Beams with Openings," *PCI Journal*, vol 22, no. 3 (May/June 1977).

Savage, J.M., "Optimized Prefabricated Concrete Joist Systems" (Master's Thesis, University of Nebraska, December 1993).

Savage, J.K., M.K. Tadros, P. Arumugasaamy, and L.G. Fischer, "Behavior and Design of Double Tee with Web Openings," *PCI Journal*, vol 41, no. 1 (Jan/Feb 1996).

Sopko, S., "Investigation of a Failed Concrete Joist System," *Proceedings of the Structures Congress* (ASCE, 19-21 April 1993) pp 550-555.

"Steel Joists and Joist Girders," marketing publication (Vulcraft [a division of NUCOR Corp.], 1991 and 1995).

Structural Engineering For Military Programs (HQUSACE, October 1996).

Wafa, F.F., and A.D. Akhtaruzzaman, "Prestressed Concrete Beams with Openings under Torsion and Bending," *ASCE Journal of Structural Engineering*, vol 115, no. 11 (September 1989).

Wechsler, M.B., "Precast Concrete Trusses," *ACI Concrete International Design and Construction*, vol 8, no. 11 (November 1986).

Werner, M.P., and W.H. Dilger, "Shear Design of Prestressed Concrete Stepped Beams," *PCI Journal*, vol 18, no. 4 (July/August 1973).

Yoshimi, M., T. Saito, T. Ohishi, Y. Yonekura, and Y. Kakayama, "A Study on Composite Light-Weight Prestressed Concrete for Long Spans," *Proceedings of the FIP Symposium* (17-20 October 1993) pp 457-462.

Appendix A: Design Aids and Examples

This appendix presents three double-tee design aids and two design examples. The sections chosen represent double-tee joists with openings and 8 ft wide flanges. Joist web depths are 20 in., 24 in., and 32 in. Double tees with and without topping slabs are presented. Information is provided for spans between 24 ft and 110 ft. The spans used in these tables are the effective span length between the center lines of supports.

Tables A.1, A.2, and A.3* provide section property details for sections with webs both solid and with openings. The joists are designated DT-08-20, DT-08-24, and DT-08-32 respectively. Figures A.1, A.2, and A.3 show the configuration for each section with details of the opening dimensions.

Design Assumptions

Concrete strength of these sections is assumed as 7000 psi for compressive strength, f'_c, at 28 days and 5500 psi at the time of prestressing strand release. The composite topping slab is assumed to have a concrete strength at 28 days of 4000 psi. All concrete is assumed to be normal weight, 150 pcf. Prestressing strands are ½ in. diameter with an ultimate strength of 270 ksi and have low relaxation properties. Epoxy coated strands are recommended for protection from corrosion and fire in this application based on the assumption that service loads will produce cracking in the member. The initial prestress value is assumed to be 0.75 f_{pu}. Stresses at transfer of prestress are assumed to be 90 percent of the initial stresses. Effective prestress is assumed 80 percent of initial.

The tee is subjected to uniformly distributed load and is not allowed to crack under service loads. Caution must be exercised in designing double tees with web openings when concentrated loads are expected. The strand profiles are either straight or draped. The draped points are at either development length of

* Tables and figures for this appendix are presented at the end of the text.

the strands or one-sixth of the span from both ends, whichever is larger. Typical opening dimensions are 3:1 width to height with minimum height of 8 in. The minimum filled diameter of the opening corners is 4 in. and the minimum pier width is 10 in. The openings should be placed horizontally with at least 2 in. below the bottom of the flange. The openings should be placed between the draping points. Additional stirrups should be placed at 1 in. from the opening edges to control the cracks. These stirrups should be anchored to the flange of the double tee as shown in Figure A.4.

The required reinforcement around the openings should be used with recommended reinforcement details.

Load Table Description

The load tables show the allowable uniform superimposed service load, estimated camber at the time of erection, the estimated long-term deflection, required vertical shear reinforcement, required reinforcement at the openings, and instantaneous deflection coefficient. At the bottom of each load table, the number of openings and draping point are shown. For each double tee section two tables are provided. One table shows parameters for the section without topping, and the other for the section with 2 in. concrete topping acting compositely with the precast section. These table values assume the section to be unshored at the time the topping is placed.

The allowable uniform superimposed service load includes dead load of 10 psf for untopped members, typical for roofs, and 15 psf for topped members, typical for floors. The capacity shown is in addition to the weight of the topping.

The values for safe superimposed uniform service load are based on the capacity of the section as governed ultimate flexural strength, service load flexural stresses, or shear strength. A portion of the safe load shown is assumed to be dead load for the purpose of applying load factors and determining cambers and deflections.

The criteria used to determine the safe superimposed load and strand placement are based on *Building Code Requirements for Reinforced Concrete*, ACI 318-95. The Code provisions used in the development of these load tables are as follows:

1. Capacity governed by design flexural strength:
   Load factors: 1.4 DL + 1.7 LL

Strength reduction factor, $\Phi = 0.90$

Calculation of design moments assumes spans with simple supports. If the strands are fully developed, the critical moment is assumed to be at midspan. Flexural strength is calculated using strain compatibility.

2. Capacity governed by design shear strength:
Load factors: 1.4 DL + 1.7 LL
Strength reduction factor, $\Phi = 0.85$

3. End stresses are calculated 50 strand diameters from the end of the section, the theoretical point of full transfer.

4. The flange flexural and shear strengths and the service load stresses are not considered as limiting criteria.

5. The estimated cambers and deflections shown are calculated using the multipliers given in the PCI Handbook.

Estimated cambers are based on the elastic members. The estimated long-term deflection includes superimposed dead load but does not include live load. An instantaneous deflection coefficient (C) was developed to account for the openings and their effects on the stiffness of the member. The coefficient C was developed based on the assumption that the middle part of the beam has a moment of inertia (I_o) which represents the web opening part and the edges have a moment of inertia (I_s) which represents the solid part (Figure A.5).

$$\Delta = \frac{w}{2\,E}\left\{\frac{1}{I_s}\left(\frac{L\,L_1^3}{3} - \frac{L_1^4}{4}\right) + \frac{1}{I_o}\left[\frac{5\,L^4}{192} - \frac{L\,L_1^3}{3} + \frac{L_1^4}{4}\right]\right\}$$

where w= uniformly distributed superimposed load, kip/in.

E= modules of elasticity at the time of application of the load, ksi

I_s= moment of inertia of the solid section, in^4

I_o= moment of inertia at an opening, in^4

The estimated long-time deflection was calculated using PCI Handbook multipliers and before the application of superimposed live loads.

Quantity, size, and profile of strands are shown in the load tables under the column headed Strand Pattern (88-D2, for example). The first digit indicates the total number of strands in the unit (2 legs), the second digit is the diameter of the strand (in sixteenths of an inch), D indicates that the strands are draped, and the last digit indicates two depression points. The eccentricities of the strands at the ends and midspan are shown in the load tables. The value (e_e) in the load tables represents the distance between the c.g. of the strand and the c.g. of the cross section at the end of the beam. The value (e_c) in the load tables represents the distance between the c.g. of the strand and the c.g. of the cross section between the depression points.

Load tables A.4 through A.15 show the load-carrying capabilities of the double-tee sections with web openings for depths of 20 in., 24 in., and 32 in. Tables A.4 through A.9 are for untopped sections and Tables A.10 through A.15 are for topped sections.

Design Example No. 1 (Untopped Section)

Design Conditions and Joist Configuration

Design a double-tee beam with web openings for 54 ft span length. Assume a double tee joist configuration without a topping slab and with a web depth of 24 in. and flange width of 8 ft. Figure A.6 shows typical section dimensions. Nine openings are located in the middle portion of the beams (Figure A.7). Opening dimensions are shown in Figure A.8. The first opening at each end is located 10 ft-2 in. from the end. The spacing between the openings is 10 in. Draped prestressing strands are assumed with draping points at 9 ft from each beam end (Figure A.7). Strand spacing is as shown in Figure A.9.

Design the Beams

Strand profile is as shown in Figure A.9. Design the beam to carry 10 psf superimposed dead load and 50 psf live load in addition to its self weight.

Material properties are as defined below:

DT-08-24 web concrete strength at release f'_{ci} = 5500 psi

concrete strength at 28-days $f_c^{'}$ = 7000 psi

modulus of elasticity at release E=4496 ksi

at 28-days E=5072 ksi

Prestressing strand: ultimate strength $f_s^{'}$ = 270 ksi

yield strength f_y^{*} = 0.9 $f_S^{'}$ = 243 ksi

initial prestressing f_{si} = 0.75 $f_S^{'}$ = 202.5 ksi

modulus of elasticity E_s = 28,000 ksi

Reinforcing bars: yield strength f_{sy} = 60,000 psi

Table A.16 shows the section properties for a single-tee section of DT-08-24 with and without web openings.

Define Loading

Loads

Self weight $= (214 * (10.17 * 2 + 8 * \frac{10}{12}) + 146 * 9 * 3)\frac{1}{54} = 180$ plf

Superimposed dead load = 10 psf = 10 x 4 = 40 plf

Live load = 50 psf = 50 x 4 = 200 plf

Service loads = 180 + 40 + 200 = 420 plf

Ultimate loads = (180 + 40) * 1.4 + 200 * 1.7 = 648 plf

Check Stresses

For a simple beam under a uniformly distributed load (W), the bending moment at any distance (x) from the support is given by:

$$M_x = \frac{WL^2}{2}\left[\left(\frac{x}{L}\right) - \left(\frac{x}{L}\right)^2\right]$$

At release of the strands, only the prestressing force and self weight are acting on the beam.

At transfer length, x = 50 diameter of the strand = 50 x 0.5 = 25 inches = 2.08 ft:

M = 9.72 ft-kips (due to self weight only)

M = 22.68 ft-kips (due to service loads)

At draping points, x = 9 ft:

M = 36.45 ft-kips (due to self weight only)

M = 85.05 ft-kips (due to service load)

M_u = 131.22 ft-kips (due to ultimate loads)

At midspan section, x = 27 ft:

M = 153.09 ft-kips (due to service loads)

M_u = 236.20 ft-kips (due to ultimate loads)

Check ultimate flexural capacity. Using the design tables, the suggested number of strands for this span is four per chord with end span eccentricity (y_{be}) = 14.40 in. and midspan eccentricity (y_{bc}) = 9.15 in. The top strand is located 2 in. from the joist web top with a straight profile. Ignore the top strand in the calculating the ultimate strength capacity:

d_{ps} = 21.25 in.

b = 48 in.

A_{ps} = 4 x 0.153 = 0.612 in^2

for f'_c = 7000 psi, β_1 = 0.70

γ_p = 0.28 for low relaxation strand

$$\rho_p = \frac{0.612}{48 \times 20.5} = 0.000622$$

$$f_{ps} = 270\left[1 - \frac{0.28}{0.70} \times 0.000622 \times \frac{270}{7}\right] = 267 \text{ ksi}$$

$$a = \frac{0.612 \times 267}{0.85 \times 7 \times 48} = 0.57 \text{ in.} < \text{thickness of the flange} = 2 \text{ in.}$$

$$\phi M_n = 0.90 \times 0.612 \times 267 \left(21.25 - \frac{0.57}{2}\right)\frac{1}{12}$$

= 257 ft-kips > M_u = 236.20 ft-kips (at midspan)

Allowable working stresses are:

1. Stresses in concrete immediately after prestress transfer:

   extreme fiber stress in compression 0.6 f'_{ci} = 3300 psi

   extreme fiber stress in tension $6\sqrt{f'_{ci}}$ = 445 psi

   extreme fiber stress in tension at the ends $3\sqrt{f'_{ci}}$ = 222 psi

2. Stresses in concrete at service loads:

   extreme fiber stress in compression due to prestress force plus sustained loads

   0.45 f'_c = 3150 psi

   extreme fiber stress in compression due to prestress force plus total loads

   0.60 f'_c = 4200 psi

   extreme fiber stress in tension due $6\sqrt{f'_c}$ = 502 psi

Assume losses at 10% f_{se} = 0.75 x 270 x 0.90 = 182 ksi

3. Check working stresses:

Force in the strands

top strand P_{ti} = 0.153 x 1 x 182 = 28 kips

bottom strand P_{bi} = 0.153 x 4 x 182 = 111 kips

4. Check the stresses at release:

At transfer length, x = 2.08 ft, eccentricity of the bottom strands is 10.32 in. and of top strands is 4.85 in.

M = 9.72 ft-kips (due to self weight only)

$$f_b = -\frac{111+28}{201} - \frac{111 \times 10.32}{612} + \frac{28 \times 4.85}{612} + \frac{9.72 \times 12}{612}$$

$$= -0.692 - 1.872 + 0.222 + 0.191 = -2.151 \text{ ksi} < -3.300 \text{ ksi (comp.)}$$

$$f_t = -\frac{111+28}{201} + \frac{111 \times 10.32}{1532} - \frac{28 \times 4.85}{1532} - \frac{9.72 \times 12}{1532}$$

$$= -0.692 + 0.748 - 0.089 - 0.076 = -0.109 \text{ ksi} < +0.222 \text{ ksi (ten.)}$$

At draping point, eccentricity of the bottom strands is 14.40 in. and of top strands is 4.85 in.

M = 36.45 ft-kips (due to self weight only)

$$f_b = -\frac{111+28}{201} - \frac{111 \times 14.40}{612} + \frac{28 \times 4.85}{612} + \frac{36.45 \times 12}{612}$$

$$= -0.692 - 2.612 + 0.222 + 0.715 = -2.367 \text{ ksi} < -3.300 \text{ ksi (comp.)}$$

$$f_t = -\frac{111+28}{201} + \frac{111 \times 14.40}{1532} - \frac{28 \times 4.85}{1532} - \frac{36.45 \times 12}{1532}$$

$$= -0.692 + 1.043 - 0.089 - 0.286 = -0.024 \text{ ksi} < +0.445 \text{ ksi (ten.)}$$

4. Check the stresses at service stresses:

Assume losses at 20% f_{se} = 0.75 x 270 x 0.80 = 162 ksi

Force in the strands

top strand P_{te} = 0.153 x 1 x 162 = 25 kips

bottom strand P_{be} = 0.153 x 4 x 162 = 99 kips

At transfer length,x=2.08 ft, eccentricity of the bottom strands is 10.32 in. and of the top strands is 4.85 in.

M = 22.68 ft-kips (due to service loads)

$$f_b = -\frac{99+25}{201} - \frac{99 \times 10.32}{612} + \frac{25 \times 4.85}{612} + \frac{22.68 \times 12}{612}$$

= - 0.617 - 1.669 + 0.198 + 0.445 = - 1.643 ksi < + 0.502 ksi (ten.)

$$f_t = -\frac{99+25}{201} + \frac{99 \times 10.32}{1532} - \frac{25 \times 4.85}{1532} - \frac{22.68 \times 12}{1532}$$

= - 0.617 + 0.667 - 0.079 - 0.178 = - 0.207 ksi < - 4.200 ksi (comp.)

At the draping point, eccentricity of the bottom strands is 14.40 in. and of the top strands is 4.85 in.

M = 85.05 ft-kips (due to service load)

$$f_b = -\frac{99+25}{201} - \frac{99 \times 14.40}{612} + \frac{25 \times 4.85}{612} + \frac{85.05 \times 12}{612}$$

= - 0.617 - 2.329 + 0.198 + 1.668 = - 1.080 ksi < + 0.502 ksi (ten.)

$$f_t = -\frac{99+25}{201} + \frac{99 \times 14.40}{1532} - \frac{25 \times 4.85}{1532} - \frac{85.05 \times 12}{1532}$$

= - 0.617 + 0.931 - 0.079 - 0.666 = - 0.431 ksi < - 4.200 ksi (comp.)

At midspan, eccentricity of the bottom strands is 14.40 in., and of the top strands is 4.85 in.

$$M = 153.09 \text{ ft-kips}$$

$$f_b = -\frac{99 + 25}{201} - \frac{99 \times 14.40}{612} + \frac{25 \times 4.85}{612} + \frac{153.09 \times 12}{612}$$

$$= -0.617 - 2.329 + 0.198 + 3.002 = +0.254 \text{ ksi} < +0.502 \text{ ksi (ten.)}$$

$$f_t = -\frac{99 + 25}{201} + \frac{99 \times 14.40}{1532} - \frac{25 \times 4.85}{1532} - \frac{153.09 \times 12}{1532}$$

$$= -0.617 + 0.931 - 0.079 - 1.199 = -0.964 \text{ ksi} < -4.200 \text{ ksi (comp.)}$$

5. Check cracking of bottom chord:

At the midspan section, the bottom chord should be checked using the opening section properties. Eccentricity of the bottom strands is 15.66 in. and of the top strands is 3.59 in.

$$f_b = -\frac{99 + 25}{140} - \frac{99 \times 15.66}{491} + \frac{25 \times 3.59}{491} + \frac{153.09 \times 12}{491}$$

$$= -0.886 - 3.158 + 0.183 + 3.742 = -0.119 \text{ ksi} < +0.502 \text{ ksi (ten.)}$$

At end of the fillet of the first opening, x = 10.5 ft, the bottom chord should be checked using the opening section properties. Eccentricity of the bottom strands is 15.66 in., and of the top strands is 3.59 in.

$$M_{Service} = 95.92 \text{ ft-kips}$$

$$f_b = -\frac{99 + 25}{140} - \frac{99 \times 15.66}{491} + \frac{25 \times 3.59}{491} + \frac{95.92 \times 12}{491}$$

$$= -0.886 - 3.158 + 0.183 + 2.344 = -1.517 \text{ ksi} < +0.502 \text{ ksi (ten.)}$$

To assess the additional stresses due to bending of the bottom chord use Abdalla (1993) equation to distribute the shear forces between the top and bottom chords at service loads.

$$V_b = V \frac{\sqrt{A_b I_b}}{\sqrt{A_b I_b} + \sqrt{A_t I_t}}$$

where

V_b = shear carried by the bottom chord

V = the ultimate shear force at the section under consideration (mid of the first opening) = 6.44 kips

A_b = area of the bottom chord = 38 in^2

A_t = area of the top chord = 105 in^2

I_b = moment of inertia of bottom chord = 175.52 in^4

I_t = moment of inertia of top chord = 76.91 in^4

$$V_b = 6.44 \frac{\sqrt{38 \times 175.52}}{\sqrt{38 \times 175.52} + \sqrt{105 \times 76.91}} = 3.07 \text{ kips}$$

Take the moment of this force at the edge of the fillet of the openings.

$$f_b = -1.517 + \frac{3.07 \times (\frac{36}{2} - 4)}{491} = -1.429 \text{ ksi} < +0.502 \text{ ksi (ten.)}$$

Design Shear Reinforcement

The ultimate load is 648 plf. Height of the section, h, is 24 in., effective section depth, d, is 21.25 in.

At the critical section (h/2),

Ultimate shear, V_u = 16.85 kips

Ultimate moment occurring simultaneously with ultimate shear, M_u = 17.17 ft-kips

Section width, b_w, is 4.75 in. Assume tie spacing, S, of 12 in.

$$\text{Calculated } \frac{V_u d}{M_u} = \frac{16.85 \times 21..25}{17.17 \times 12} = 1.7$$

This value should be equal or less than 1.0. Therefore, $\frac{V_u\ d}{M_u} = 1.0$

The shear strength provided by the concrete, (ACI Section 11.4)

$$V_c = \left(0.6\sqrt{f_c'} + 700\frac{V_u\ d}{M_u} \right) b_w\ d$$

$$V_c = \left(0.6 \text{ x } \sqrt{7000} + 700 \text{ x } 1.0\right)\frac{4.75 \text{ x } 21.25}{1000} = 75.72 \text{ kips}$$

But minimum $V_c = 2\sqrt{f_c'}\ b_w\ d = 16.89$ kips, and

maximum $V_c = 5\sqrt{f_c'}\ b_w\ d = 42.23$ kips

Therefore, $V_c = 42.23$ kips

$\phi\ V_c = 42.23 / 0.85 = 35.89$ kips

$V_u < V_c/2$

Use minimum shear reinforcement:

$$A_{s-min} = \frac{50\ b_w\ s}{f_y} = \frac{50 \text{ x } 4.75 \text{ x } 12}{60000} = 0.05 \text{ in}^2/\text{ft}$$

Design shear reinforcement at opening edges. At the first opening, x = 10.17 ft:

V_u=10.91 kips

Assuming the vertical shear at this section is completely carried by reinforcement the required steel area is:

$$A_v = \frac{10.91 \text{ x } 12}{0.85 \text{ x } 60 \text{ x } 21.25} = 0.12 \text{ in}^2/\text{ft}$$

The reinforcement required for the critical section should be a single-welded wire fabric provided in the region before the first openings. The reinforcement at the edge of first opening should be provided at the edges of all openings using the same recommended details in the experimental part.

Check shear capacity of compression chord.

At ultimate loads, the tension chord will be cracked and all the shear force will be carried by the compression chord. Use the ACI 318-95 equation to calculate the capacity of non-prestressed members. The critical section for this case is at the middle of the first opening.

$$C = T = A_{ps} \times f_{ps} = (4 \times 0.153) \times 267 = 163 \text{ kips}$$

$$V_c = 2\left[1 + \frac{C}{2000\, A_g}\right]\sqrt{f_c'}\, b_w\, d$$

$$= 2\left[1 + \frac{163 \times 1000}{2000 \times 2 \times 48}\right]\sqrt{7000} \times \frac{48 \times 2}{1000}$$

$$= 29.70 \text{ kips}$$

$$\phi V_c = 0.85 \times 29.70 = 25.25 \text{ kips} > V_u = 10.91 \text{ kips}$$

Check Deflections

Estimated cambers are based on the elastic and solid members. Three deflection equations were developed to account for the openings and their effect on the stiffness of the member. These equations were developed based on the assumption that the middle part of the beam has a moment of inertia (I_o) that represents the web with openings, and the edges have a moment of inertia (I_s) that represents the solid part.

Deflection due to the prestressing force in straight strand pattern (top strand):

$$\Delta = \frac{P_t\, e\, L_1^2}{2\, E_{ci}\, I_s} + \frac{2\, P_t\, e}{E_{ci}\, I_o}\left(\frac{L}{2} - L_1\right)\left(\frac{L_1}{4} + \frac{L}{8}\right)$$

where P_t = prestressing force in the top strand = 28 kips

e = eccentricity of the top strand = 4.85 in.

L = span length = 648 in.

L_1 = length to the edge of the first openings = 122 in.

E_{ci} = modulus of elasticity at release = 4496 ksi

I_s = moment of inertia of the solid part = 10,492 in^4

I_o = moment of inertia of the opening part = 9032 in^4

Then, due to the force in the prestressed top strands, Δ = 0.17 in. (deflection)

Deflection due to the prestressing force in draped strand pattern (bottom strands):

$$\Delta = \frac{P_b\, e_c\, L_1^2}{2E_{ci}\, I_s} + \frac{2\, P_b\, e_c}{E_{ci}\, I_o}\left(\frac{L^2}{16} - \frac{L_1^2}{4}\right) - \frac{P_b\,(e_c - e_e)\, L_d^2}{6\, E_{ci}\, I_s}$$

where P_b = prestressing force in the strands = 111 kips

e_c = eccentricity of the strand at midspan = 14.40 in.

e_e = eccentricity of the strands at end span = 9.15 in.

L_d = length from the end of the span to the draping point = 108 in.

Then, due to the force in the prestressed bottom strands, Δ = 2.01 in. (camber)

Deflection due to uniformly distributed load:

$$\Delta = \frac{w}{2\, E}\left\{\frac{1}{I_s}\left(\frac{L\, L_1^3}{3} - \frac{L_1^4}{4}\right) + \frac{1}{I_o}\left[\frac{5\, L^4}{192} - \frac{L\, L_1^3}{3} + \frac{L_1^4}{4}\right]\right\}$$

where w = uniformly distributed superimposed load, kip/in.

E_c = modulus of elasticity at the time of load application = 5072 ksi

due to the self weight of the beam = 0.180 k/ft Δ = 0.83 inches (deflection)

due to superimposed dead load = 0.040 k/ft Δ = 0.17 in. (deflection)

due to live load = 0.200 k/ft Δ = 0.83 in. (deflection)

Total initial camber = 2.01 - 0.17 - 0.83 Δ = 1.01 in. (camber)

The long-term deflections (in inches) are shown below.

Load case	At release	Multiplier	Erection	Multiplier	Final
prestressing	- 1.84	1.80	- 3.31	2.45	- 4.51
self weight	+ 0.83	1.85	+ 1.54	2.70	+ 2.24
SIDL			+ 0.17	3.00	+ 0.51
LL					+ 0.83

Allowable deflection due to live load

$$= \frac{L}{360} = \frac{648}{360} = 1.80 \text{ in.} > \text{deflection due to LL} = 0.83 \text{ in.}$$

Total deflection at final = 0.51 + 0.83 = 1.34 in.

Allowable total deflection due to sustained loads and LL

$$= \frac{L}{240} = \frac{648}{240} = 2.70 \text{ in.} > \text{total deflection} = 1.34 \text{ in.}$$

Design Example No. 2 (Topped Section)

Design Conditions

Design a double-tee beam with web openings for 46 ft span length. The beams are double tee with a topping slab, web depth of 20 in. and flange width of 8 ft. Figure A.10 shows the dimensions of the double tee section. Eleven openings are placed in the middle portion of the beam (Figure A.11). The first openings are located at 7 ft-10 in. from each beam end and the spacing between openings is 10 in. The opening dimensions are shown in Figure A.12. Strands are draped with draping points at 7.7 ft from each end of the beam. Design the beams to carry 15 psf superimposed dead load and 50 psf live load in addition to self weight.

Material properties are as defined below:

DT-08-24 web concrete strength at release f'_{ci} = 5500 psi

concrete strength at 28-days f'_c = 7000 psi

Topping thickness t = 2 in.

concrete strength at 28-days $f_c^{'}$ = 5000 psi

Modulus of elasticity

at release E=4496 ksi

at 28-days E=5072 ksi

Prestressing strand: 1/2″ diameter, low relaxation

ultimate strength $f_s^{'}$ = 270 ksi

yield strength f_y^{*} = 0.9 $f_S^{'}$ = 243 ksi

initial prestressing f_{si} = 0.75 $f_S^{'}$ = 202.5 ksi

modulus of elasticity E_s = 28,000 ksi

Reinforcing bars: yield strength f_{sy} = 60,000 psi

Table A.17 shows properties for a single tee of the same configuration.

Define Loading

Self weight $= (189 * (7.83 * 2 + 10 * \frac{10}{12}) + 147 * 11 * 2)\frac{1}{46} = 169$ plf

Topping dead load $= \frac{2}{12}$ x 150 x 4 = 100 plf

Superimposed dead load = 15 psf = 15 x 4 = 60 plf

Live load = 50 psf = 50 x 4 = 200 plf

Service loads = 169 + 100 + 60 + 200 = 529 plf

Ultimate loads = (169 + 100 + 40) * 1.4 + 200 * 1.7 = 801 plf

Check Stresses

Bending moment for a simple beam is as defined in Design Example No. 1. At release of the strands, only the prestressing force and self weight are acting on the beam. Table A.18 shows bending moments for different loadings.

Check ultimate flexural capacity:

Using the design tables, the suggested number of strands for this span is 4 in each chord with end eccentricity (y_{be}) = 6.59 in. and midspan eccentricity (y_{bc}) = 11.84 in. The top strand is located 2 in. from the web top with a straight profile. Ignore the top strand in the calculating the ultimate strength capacity.

d_{ps} = 19.25 in.

b = 48 in.

A_{ps} = 4 x 0.153 = 0.612 in^2

for f_c' = 7000 psi, β_1 = 0.70

γ_p = 0.28 for low relaxation strand

$$\rho_p = \frac{0.612}{48 \times 19.25} = 0.000662$$

$$f_{ps} = 270\left[1 - \frac{0.28}{0.70} \times 0.000662 \times \frac{270}{7}\right] = 267 \text{ ksi}$$

$$a = \frac{0.612 \times 267}{0.85 \times 7 \times 48} = 0.57 \text{ in.} < \text{thickness of the flange} = 2 \text{ in.}$$

$$\phi M_n = 0.90 \times 0.612 \times 267 \left(19.25 - \frac{0.57}{2}\right)\frac{1}{12}$$

$$= 232 \text{ ft-kips} > M_u = 212 \text{ ft-kips (at midspan)}$$

Allowable stresses are as defined in Design Example No. 1.

Check working stresses:

At release:

At transfer length, 2.08 ft, eccentricity of the bottom strands is 8.01 in. and of the top strands is 3.41 in.

M = 7.72 ft-kips (due to self weight only)

$$f_b = -\frac{111+28}{182} - \frac{111 \times 8.01}{430} + \frac{28 \times 3.41}{430} + \frac{7.72 \times 12}{430}$$

$$= -0.764 - 2.078 + 0.222 + 0.215 = -2.405 \text{ ksi} < -3.300 \text{ ksi (comp.)}$$

$$f_t = -\frac{111+28}{182} + \frac{111 \times 8.01}{1160} - \frac{28 \times 3.41}{1160} - \frac{7.72 \times 12}{1160}$$

$$= -0.764 + 0.766 - 0.082 - 0.080 = -0.160 \text{ ksi} < +0.222 \text{ ksi (ten.)}$$

At draping point, eccentricity of the bottom strands is 11.84 in. and of the top strands is 3.41 in.

M = 24.92 ft-kips (due to self weight only)

$$f_b = -\frac{111+28}{182} - \frac{111 \times 8.01}{430} + \frac{28 \times 3.41}{430} + \frac{24.92 \times 12}{430}$$

$$= -0.764 - 2.078 + 0.222 + 0.695 = -1.925 \text{ ksi} < -3.300 \text{ ksi (comp.)}$$

$$f_t = -\frac{111+28}{182} + \frac{111 \times 8.01}{1160} - \frac{28 \times 3.41}{1160} - \frac{24.92 \times 12}{1160}$$

$$= -0.764 + 0.766 - 0.082 - 0.258 = -0.338 \text{ ksi} < +0.222 \text{ ksi (ten.)}$$

Check the stresses at service load. Assume losses at 20%, $f_{se} = 0.75 \times 270 \times 0.80 = 162$ ksi.

Force in the strands

top strand $P_{te} = 0.153 \times 1 \times 162 = 25$ kips

bottom strand $P_{be} = 0.153 \times 4 \times 162 = 99$ kips

At transfer length, 2.08 ft, eccentricity of the bottom strands is 8.01 in. and of the top strands is 3.41 in.

$$f_b = -\frac{99+25}{182} - \frac{99 \times 8.01}{430} + \frac{25 \times 3.41}{430} + \frac{(7.72+4.57) \times 12}{430} + \frac{(2.74+9.14) \times 12}{529}$$

$$= -0.681 - 1.844 + 0.198 + 0.342 + 0.269 = -1.716 \text{ ksi} < +0.502 \text{ ksi (ten.)}$$

$$f_t = -\frac{99+25}{182} + \frac{99 \times 8.01}{1160} - \frac{25 \times 3.41}{1160} - \frac{(7.72+4.57) \times 12}{1160} - \frac{(2.74+9.14) \times 12}{1712}$$

$$= -0.681 + 0.684 - 0.073 - 0.127 - 0.083 = -0.280 \text{ ksi} < -4.200 \text{ ksi (comp.)}$$

At draping point, eccentricity of the bottom strands is 11.84 in. and of the top strands is 3.41 in.

$$f_b = -\frac{99+25}{182} - \frac{99 \times 11.84}{430} + \frac{25 \times 3.41}{430} + \frac{(24.92+14.75) \times 12}{430} + \frac{(8.85+29.49) \times 12}{529}$$

$$= -0.681 - 2.726 + 0.198 + 1.107 + 0.870 = -1.232 \text{ ksi} < +0.502 \text{ ksi (ten.)}$$

$$f_t = -\frac{99+25}{182} + \frac{99 \times 11.841}{1160} - \frac{25 \times 3.41}{1160} - \frac{(24.92+14.75) \times 12}{1160} - \frac{(8.85+29.49) \times 12}{1712}$$

$$= -0.681 + 1.010 - 0.073 - 0.410 - 0.269 = -0.423 \text{ ksi} < -4.200 \text{ ksi (comp.)}$$

At midspan, eccentricity of the bottom strands is 11.84 in. and of the top strands is 3.41 in.

$$f_b = -\frac{99+25}{182} - \frac{99 \times 11.84}{430} + \frac{25 \times 3.41}{430} + \frac{(44.70+26.45) \times 12}{430} + \frac{(15.87+52.90) \times 12}{529}$$

$$= -0.681 - 2.726 + 0.198 + 1.986 + 1.560 = +0.337 \text{ ksi} < +0.502 \text{ ksi (ten.)}$$

$$f_t = -\frac{99+25}{182} + \frac{99 \times 11.841}{1160} - \frac{25 \times 3.41}{1160} - \frac{(44.70+26.45) \times 12}{1160} - \frac{(15.87+52.90) \times 12}{1712}$$

$$= -0.681 + 1.010 - 0.073 - 0.736 - 0.482 = -0.962 \text{ ksi} < -4.200 \text{ ksi (comp.)}$$

Check cracking of bottom chord:

At midspan section the bottom chord should be checked using the opening section properties. Eccentricity of the bottom strands is 12.55 in. and of the top strands is 2.70 in.

$$f_b = -\frac{99+25}{141} - \frac{99 \times 12.55}{375} + \frac{25 \times 2.70}{375} + \frac{(44.70+26.45) \times 12}{375} + \frac{(15.87+52.90) \times 12}{433}$$

$$= -0.879 - 3.313 + 0.180 + 2.277 + 1.906 = +0.171 \text{ ksi} < +0.502 \text{ ksi (ten.)}$$

At first opening fillet end, (x = 7.83 ft), the bottom chord should be checked using the opening section properties. Eccentricity of the bottom strands is 12.55 in. and of the top strands is 2.70 in.

$$f_b = -\frac{99+25}{141} - \frac{99 \times 12.55}{375} + \frac{25 \times 2.70}{375} + \frac{(25.26+14.95) \times 12}{375} + \frac{(8.97+29.90) \times 12}{433}$$

$$= -0.879 - 3.313 + 0.180 + 1.287 + 1.077 = -1.648 \text{ ksi} < +0.502 \text{ ksi (ten.)}$$

To check the additional stresses due to bending of the bottom chord, use Abdalla's equation (Abdalla 1993) to distribute the shear forces between the top and bottom chords at service loads.

$$V_b = V \frac{\sqrt{A_b I_b}}{\sqrt{A_b I_b} + \sqrt{A_t I_t}}$$

where V_b = shear carried by the bottom chord

V = the service shear force at the section under consideration (mid of the first opening) = 8.02 kips

A_b = area of the bottom chord = 34 in^2

A_t = area of the top chord = 203 in^2

I_b = moment of inertia of bottom chord = 179 in^4

I_t = moment of inertia of top chord = 356 in^4

$$V_b = 8.02 \frac{\sqrt{34 \times 179}}{\sqrt{34 \times 179} + \sqrt{203 \times 356}} = 1.80 \text{ kips}$$

Take the moment of this force at the opening fillet edge. Therefore:

$$f_b = -1.648 + \frac{1.80 \times (\frac{24}{2} - 4)}{433} = -1.615 \text{ ksi} < +0.502 \text{ ksi (ten.)}$$

Design Shear Reinforcement

Shear reinforcement at the critical section (h/2):

Ultimate load = 648 plf (pounds per linear foot)

Height of the section, h = 22 in.

Depth of the section, d = 19.25 in.

At the critical section (h/2), ultimate shear, V_u = 17.69 kips

Ultimate moment occurred simultaneously with ultimate shear, M_u = 18.74 ft-kips

Width of the section, b_w = 4.75 in.

Assume spacing of the ties, S = 12 in.

$$\text{Calculated } \frac{V_u d}{M_u} = \frac{17.69 \times 19..25}{18.74 \times 12} = 1.51$$

This value should be equal or less than 1.0. So, $\frac{V_u d}{M_u} = 1.0$

The shear strength provided by the concrete (ACI Section 11.4)

$$V_c = \left(0.6\sqrt{f_c'} + 700 \frac{V_u\, d}{M_u} \right) b_w\, d$$

$$V_c = \left(0.6 \text{ x } \sqrt{7000} + 700 \text{ x } 1.0\right) \frac{4.75 \text{ x } 19.25}{1000} = 68.60 \text{ kips}$$

But minimum $V_c = 2\sqrt{f_c'}\, b_w\, d = 15.30$ kips, and

maximum $V_c = 5\sqrt{f_c'}\, b_w\, d = 38.25$ kips

Therefore, $V_c = 38.25$ kips

$\phi V_c = 38.25 / 0.85 = 32.51$ kips

$V_u < V_c/2$

Use minimum shear reinforcement

$$A_{s-min} = \frac{50\, b_w\, s}{f_y} = \frac{50 \text{ x } 4.75 \text{ x } 12}{60000} = 0.05 \text{ in}^2/\text{ft}$$

Shear reinforcement at the opening edges:

At edge of first opening (x = 7.83 ft), $V_u = 12.15$ kips

Assuming the vertical shear at this section is completely resisted by reinforcement the required area of the vertical steel is:

At the first opening edge

$$A_v = \frac{12.15 \text{ x } 12}{0.85 \text{ x } 60 \text{ x } 19.25} = 0.15 \text{ in}^2/\text{ft}$$

The reinforcement required for the critical section should be a single welded wire fabric provided in the region before the first openings. The reinforcement for the edge should be provided at the edges of all openings using the same recommended details in the experimental part.

Check shear capacity of compression chord. At ultimate loads, the tension chord will be cracked, and all the shear force will be carried by the compression chord.

Use the ACI 318-95 equation to calculate the capacity of non-prestressed members. The critical section for this case is at the middle of the first opening.

$$C = T = A_{ps} \times f_{ps} = (4 \times 0.153) \times 267 = 163 \text{ kips}$$

$$V_c = 2\left[1 + \frac{C}{2000\, A_g}\right]\sqrt{f_c'}\, b_w\, d$$

$$= 2\left[1 + \frac{163 \times 1000}{2000 \times 2 \times 48}\right]\sqrt{7000} \times \frac{48 \times 2}{1000}$$

$$= 29.70 \text{ kips}$$

$$\phi V_c = 0.85 \times 29.70 = 25.25 \text{ kips} > V_u = 17.69 \text{ kips}$$

Check Deflections

Estimated cambers are based on the elastic and solid members. Three deflection equations were developed to account for the openings and their effect on the stiffness of the member. These equations were developed based on the assumption that the middle part of the beam has moment of inertia (I_o) that represents the web with openings, and the edges have moment of inertia (I_s)that represents the solid part.

Deflection due to the prestressing force in straight strand pattern (top strand):

$$\Delta = \frac{P_t\, e\, L_1^2}{2\, E_{ci}\, I_s} + \frac{2\, P_t\, e}{E_{ci}\, I_o}\left(\frac{L}{2} - L_1\right)\left(\frac{L_1}{4} + \frac{L}{8}\right)$$

where P_t = prestressing force in the top strand = 28 kips

e = eccentricity of the top strand = 3.41 in.

L = span length = 552 in.

L_1 = length to the edge of the first openings = 111 in.

E_{ci} = modulus of elasticity at release = 4496 ksi

I_s = moment of inertia of the solid part without topping = 6276 in^4

I_o = moment of inertia of the opening part without topping = 5740 in^4

Then, due to the force in the prestressed top strands, Δ = 0.14 in. (deflection)

Deflection due to the prestressing force in draped strand pattern (bottom strands):

$$\Delta = \frac{P_b\, e_c\, L_1^2}{2 E_{ci}\, I_s} + \frac{2\, P_b\, e_c}{E_{ci}\, I_o}\left(\frac{L^2}{16} - \frac{L_1^2}{4}\right) - \frac{P_b\,(e_c - e_e)\, L_d^2}{6\, E_{ci}\, I_s}$$

where P_b = prestressing force in the strands = 111 kips

e_c = eccentricity of the strand at midspan = 11.84 in.

e_e = eccentricity of the strands at end span = 6.59 in.

L_d = length from the end of the span to the draping point = 92 in.

Then, due to the force in the prestressed bottom strands, Δ = 1.89 in. (camber)

Deflection due to uniformly distributed load:

$$\Delta = \frac{w}{2\, E}\left\{\frac{1}{I_s}\left(\frac{L\, L_1^3}{3} - \frac{L_1^4}{4}\right) + \frac{1}{I_o}\left[\frac{5\, L^4}{192} - \frac{L\, L_1^3}{3} + \frac{L_1^4}{4}\right]\right\}$$

where w = uniformly distributed superimposed load, kip/in.

E_c = modulus of elasticity at the time of application of the load = 5072 ksi

I_s = moment of inertia of the solid part with topping = 8890 in^4

I_o = moment of inertia of the opening part with topping = 7626 in^4

due to the self weight of the beam = 0.169 k/ft Δ = 0.66 in. (deflection)

due to topping dead load = 0.100 k/ft Δ = 0.39 in. (deflection)

due to superimposed dead load = 0.060 k/ft Δ = 0.15 in. (deflection)

due to live load = 0.200 k/ft Δ = 0.51 in. (deflection)

Total initial camber = 1.89 - 0.14 - 0.66 Δ = 1.09 inches (camber)

The long-term deflections (in inches) are shown below.

Load case	At release	Multiplier	Erection	Multiplier	Final
prestressing	+ 1.75	1.80	+ 3.15	2.45	+ 4.29
self weight	- 0.66	1.85	- 1.22	2.70	- 1.79
SIDL			- 0.15	3.00	- 0.46
LL					- 0.51

Allowable deflection due to live load = $\frac{L}{360} = \frac{552}{360}$ = 1.53 in. > deflection due to LL = 0.51 in.

Total deflection at final = 0.46 + 0.51 = 0.97 in.

Allowable total deflection due to sustained loads and LL = $\frac{L}{240} = \frac{552}{240}$ = 2.30 in. > total deflection = 0.97 in.

Table A.1. Section properties of DT-8'-20" double tee.

Concrete strength	
double tee, psi	7000
topping, psi	4000

n	0.76

Section ID	DT-08'-20"

		without openings			with openings	
		untopped	topped		untopped	topped
depth, in.		20	22		20	22
width, ft.		8	8		8	8
bottom web width, in.		3.75			3.75	
top web width, in.		5.75			5.75	
opening height, in.					8	
bottom chord height, in.					8	
cross section area, in^2	A_s	363	508	A_o	282	427
depth of c.g. from bot., in.	Y_{bs}	14.59	16.42	Y_{bo}	15.30	17.24
depth of c.g. from top, in.	Y_{ts}	5.41	5.58	Y_{to}	4.70	4.76
moment of inertia, in^4	I_s	12551	16879	I_o	11479	14655
bottom modulus of section, in^3	Z_{bs}	860	1028	Z_{bo}	750	850
top modulus of section, in^3	Z_{ts}	2319	3024	Z_{to}	2442	3078
Wt, plf	W_s	378	529	W_o	293	445
Wt, psf	W_s	47	66	W_o	37	56
V/S		1.35			1.19	

Table A.2. Section properties DT-8'-24" double tee.

Concrete strength	
double tee, psi	7000
topping, psi	4000

n	0.76

Section ID	DT-08'-24"

		without openings			with openings	
		untopped	topped		untopped	topped
depth, in.		24	26		24	26
spacing, ft.		8			8	
bottom web width, in.		3.75			3.75	
top web width, in.		5.75			5.75	
opening height, in.					12	
bottom chord height, in.					8	
cross section area, in^2	A_s	401	546	A_o	280	426
depth of c.g. from bottom, in.	Y_{bs}	17.15	19.23	Y_{bo}	18.41	20.66
depth of c.g. from top, in.	Y_{ts}	6.85	6.77	Y_{to}	5.59	5.34
moment of inertia, in^4	I_s	20985	27619	I_o	18064	22284
bottom modulus of section, in^3	Z_{bs}	1224	1436	Z_{bo}	981	1079
top modulus of section, in^3	Z_{ts}	3063	4082	Z_{to}	3230	4170
Wt, plf	W_s	418	569	W_o	292	443
Wt, psf	W_s	52	71	W_o	37	55
V/S		1.41			1.19	

Table A.3. Section properties of DT-8'-32" double tee.

Concrete strength

double tee, psi	7000
topping, psi	4000

n	0.76

Section ID	DT-08'-32"

		without openings			with openings	
		untopped	topped		untopped	topped
depth, in.		32	34		32	34
spacing, ft.		8	8		8	8
bottom web width, in.		4.75			4.75	
top web width, inc.		7.75			7.75	
opening height, in.					17	
bottom chord height, in.					10	
cross section area, in^2	A_c	567	712	A_o	343	488
depth of c.g. from bottom, in.	Y_{bc}	21.21	23.61	Y_{bo}	22.75	25.80
depth of c.g. from top, in.	Y_{tc}	10.79	10.39	Y_{to}	9.25	8.20
moment of inertia, in^4	I_c	55464	71586	I_o	48044	58822
bottom modulus of section, in^3	Z_{bc}	2615	3031	Z_{bo}	2112	2280
top modulus of section, in^3	Z_{tc}	5141	6893	Z_{to}	5193	7173
Wt, plf	W_c	591	742	W_o	357	508
Wt, psf	W_c	74	93	W_o	45	64
V/S		1.79			1.38	

Table A.4. Section DT-08'-20" without topping, strand patterns 48-S, 68-S, and 68-D2.

Strand Pattern	e_s / e_c	Span, ft																						
		24	26	28	30	32	34	36	38	40	42	44	46	48	50	52	54	56	58	60	62	64	66	68
48-S		178	147	122	102	86	73	61	52	44	36	30												
	11.59	0.16	0.18	0.20	0.22	0.23	0.24	0.24	0.24	0.23	0.21	0.18												
		0.20	0.23	0.26	0.30	0.34	0.38	0.41	0.46	0.50	0.53	0.58												
		0.05	0.05	0.05	0.05	0.05	0.05	0.05	0.05	0.05	0.05	0.05												
		0.08	0.09	0.08	0.09	0.10	0.10	0.09	0.09	0.09	0.09	0.09												
	11.59	1.06	1.07	1.07	1.07	1.08	1.08	1.08	1.08	1.09	1.08	1.09												
68-S			187	157	132	113	96	82	70	60	52	44	37	32										
	8.59		0.22	0.24	0.26	0.28	0.30	0.30	0.31	0.31	0.29	0.28	0.24	0.21										
			0.29	0.33	0.37	0.42	0.47	0.52	0.58	0.63	0.68	0.74	0.78	0.84										
			0.05	0.05	0.05	0.05	0.05	0.05	0.05	0.05	0.05	0.05	0.05	0.05										
			0.14	0.12	0.13	0.14	0.14	0.13	0.13	0.14	0.12	0.13	0.12	0.12										
	8.59		1.07	1.07	1.07	1.08	1.08	1.08	1.08	1.09	1.08	1.09	1.09	1.09										
68-DS					175	150	129	112	97	84	73	64	56	49	42	37	31							
	8.59				0.43	0.47	0.52	0.55	0.59	0.62	0.64	0.66	0.66	0.66	0.63	0.61	0.56							
					0.48	0.54	0.61	0.67	0.74	0.82	0.89	0.97	1.04	1.12	1.19	1.27	1.33							
					0.05	0.05	0.05	0.05	0.05	0.05	0.05	0.05	0.05	0.05	0.05	0.05	0.05							
					0.13	0.14	0.15	0.13	0.13	0.14	0.12	0.13	0.12	0.12	0.11	0.11	0.10							
	12.09				1.07	1.08	1.08	1.08	1.08	1.09	1.08	1.09	1.09	1.09	1.09	1.09	1.09							
No. of openings		3	4	4	5	6	7	7	8	9	9	10	10	11	11	12	12	13	13	14	14	15	15	16
Draped point, ft		7.0	7.0	7.0	7.0	7.0	7.0	7.0	7.0	7.0	7.0	7.3	7.7	8.0	8.3	8.7	9.0	9.3	9.7	10.0	10.3	10.7	11.0	11.3

The span is the effective span length between the bearings centerline to centerline

Strand pattern designation:108-D2: 10 = number of strands, 8 = diameter of strand in 16ths, D depressed (S = straight), and 2 = number of depression points

Key:
- 82 Allowable superimposed service load, psf
- 0.3 Estimated camber at erection, in.
- 0.52 Estimated long-term deflection (due to self weight and superimposed dead load only), in.
- 0.05 Required area of steel for shear, in^2
- 0.13 Required area of steel at each edge of all opening, in^2
- 1.08 Instantaneous deflection coefficient.

Table A.5. Section DT-08'-20" without topping,, strand patterns 88-D2, 108-D2, and 128-D2.

Strand Pattern	e_s / e_c	Span, ft																						
		34	36	38	40	42	44	46	48	50	52	54	56	58	60	62	64	66	68	70	72	74	76	78
88-D2		179	156	137	120	109	94	83	73	65	58	51	45	40	35	31								
	6.59	0.75	0.81	0.88	0.95	1.00	1.05	1.09	1.13	1.15	1.17	1.16	1.16	1.12	1.09	1.01								
		0.81	0.90	1.00	1.10	1.20	1.31	1.41	1.52	1.62	1.74	1.84	1.97	2.07	2.19	2.29								
		0.05	0.05	0.05	0.05	0.05	0.05	0.05	0.05	0.05	0.05	0.05	0.05	0.05	0.05	0.05								
		0.19	0.17	0.18	0.18	0.16	0.17	0.15	0.15	0.14	0.14	0.13	0.13	0.13	0.13	0.12								
	11.84	1.08	1.08	1.08	1.09	1.08	1.09	1.09	1.09	1.09	1.09	1.09	1.09	1.09	1.09	1.09								
108-D2										87	78	70	63	56	50	45	40	36	32					
	4.59									1.63	1.69	1.73	1.77	1.77	1.79	1.76	1.74	1.67	1.60					
										2.04	2.19	2.34	2.49	2.64	2.79	2.93	3.10	3.24	3.39					
										0.05	0.05	0.05	0.05	0.05	0.05	0.05	0.05	0.05	0.05					
										0.18	0.18	0.16	0.17	0.16	0.16	0.15	0.15	0.14	0.14					
	11.59									1.09	1.09	1.09	1.09	1.09	1.09	1.09	1.09	1.09	1.09					
128-D2															65	58	53	48	43	39	35	31		
	2.92														2.45	2.46	2.49	2.47	2.45	2.38	2.29	2.20		
															3.37	3.54	3.74	3.94	4.14	4.32	4.50	4.70		
															0.05	0.05	0.05	0.05	0.05	0.05	0.05	0.05		
															0.19	0.17	0.17	0.16	0.17	0.16	0.15	0.15		
	11.34														1.09	1.09	1.09	1.09	1.09	1.09	1.09	1.09		
No. of openings		7	7	8	9	9	10	10	11	12	12	12	13	13	14	14	15	15	16	16	16	17	17	18
Draped point, ft		7.0	7.0	7.0	7.0	7.0	7.3	7.7	8.0	8.3	8.7	9.0	9.3	9.7	10.0	10.3	10.7	11.0	11.3	11.7	12.0	12.3	12.7	13.0

The span is the effective span length between the bearings centerline to centerline

Strand pattern designation:108-D2: 10 = number of strands, 8 = diameter of strand in 16ths, D depressed (S = straight), and 2 = number of depression points

Key:
63 Allowable superimposed service load, psf
1.77 Estimated camber at erection, in.
2.49 Estimated long-term deflection (due to self weight and superimposed dead load only), in.
0.05 Required area of steel for shear, in^2
0.17 Required area of steel at each edge of all opening, in^2
1.09 Instantaneous deflection coefficient.

Table A.6. Section DT-08'-24" without topping, strand patterns 68-S, 88-S, and 88-D2.

Strand Pattern	e_s / e_c	Span, ft																		
		30	32	34	36	38	40	42	44	46	48	50	52	54	56	58	60	62	64	66	68
68-S	11.15	179	153	132	114	99	86	75	65	57	79	43	37	32							
		0.23	0.24	0.26	0.28	0.29	0.30	0.31	0.30	0.30	0.28	0.25	0.23	0.18							
		0.49	0.51	0.54	0.54	0.55	0.52	0.50	0.43	0.37	0.25	0.10	-0.04	-0.26							
		0.05	0.05	0.05	0.05	0.05	0.05	0.05	0.05	0.05	0.05	0.05	0.05	0.05							
		0.14	0.13	0.14	0.13	0.14	0.12	0.13	0.12	0.13	0.12	0.11	0.11	0.10							
	11.15	1.13	1.13	1.14	1.14	1.15	1.14	1.15	1.15	1.15	1.15	1.15	1.15	1.15							
88-S	9.15		186	161	140	122	107	94	82	73	64	56	50	43	38	33					
			0.28	0.31	0.32	0.35	0.36	0.37	0.37	0.38	0.37	0.35	0.33	0.29	0.24	0.20					
			0.60	0.64	0.66	0.68	0.66	0.66	0.61	0.56	0.46	0.33	0.21	0.01	-0.23	-0.45					
			0.05	0.05	0.05	0.05	0.05	0.05	0.05	0.05	0.05	0.05	0.05	0.05	0.05	0.05					
			0.17	0.18	0.16	0.18	0.16	0.17	0.16	0.16	0.15	0.14	0.15	0.14	0.13	0.13					
	9.15		1.13	1.14	1.14	1.15	1.14	1.15	1.15	1.15	1.15	1.15	1.15	1.15	1.15	1.15					
88-D2	9.15				199	176	155	138	122	109	97	87	78	70	62	56	50	44	40	35	31
					0.63	0.70	0.75	0.81	0.85	0.90	0.93	0.96	1.00	1.01	1.01	1.03	1.01	0.97	0.96	0.90	0.82
					1.42	1.54	1.62	1.72	1.77	1.84	1.85	1.83	1.84	1.77	1.66	1.58	1.39	1.16	0.96	0.63	0.24
					0.05	0.05	0.05	0.05	0.05	0.05	0.05	0.05	0.05	0.05	0.05	0.05	0.05	0.05	0.05	0.05	0.05
					0.17	0.18	0.16	0.17	0.16	0.17	0.15	0.14	0.15	0.14	0.13	0.13	0.12	0.12	0.12	0.11	0.11
					1.14	1.15	1.14	1.15	1.15	1.15	1.15	1.15	1.15	1.15	1.15	1.15	1.15	1.15	1.15	1.15	.1.15
No. of openings		4	4	5	5	6	7	7	7	8	8	8	9	9	9	10	10	11	11	11	12
Draped point, ft		7.0	7.0	7.0	7.0	7.0	7.0	7.0	7.3	7.7	8.0	8.3	8.7	9.0	9.3	9.7	10.0	10.3	10.7	11.0	11.3

The span is the effective span length between the bearings centerline to centerline

Strand pattern designation:108-D2: 10 = number of strands, 8 = diameter of strand in 16ths, D depressed (S = straight), and 2 = number of depression points

Key: 82 Allowable superimposed service load, psf
0.37 Estimated camber at erection, in.
0.61 Estimated long-term deflection (due to self weight and superimposed dead load only), in.
0.05 Required area of steel for shear, in^2
0.16 Required area of steel at each edge of all opening, in^2
1.15 Instantaneous deflection coefficient.

Table A.7. Section DT-08'-24" without topping, strand patterns 108-D2, 128-D2, and 148-D2.

Strand Pattern	e_e / e_c	Span, ft																						
		44	46	48	50	52	54	56	58	60	62	64	66	68	70	72	74	76	78	80	82	84	86	88
108-D2		158	142	127	114	104	93	84	77	69	62	57	51	46	42	37	33							
	7.15	1.14	1.23	1.29	1.34	1.42	1.46	1.49	1.55	1.56	1.56	1.59	1.57	1.53	1.52	1.45	1.35							
		2.49	2.64	2.72	2.77	2.86	2.87	2.84	2.85	2.75	2.60	2.51	2.27	1.97	1.74	1.32	0.84							
		0.05	0.05	0.05	0.05	0.05	0.05	0.05	0.05	0.05	0.05	0.05	0.05	0.05	0.05	0.05	0.05							
		0.19	0.20	0.19	0.18	0.18	0.17	0.16	0.16	0.15	0.14	0.15	0.14	0.13	0.14	0.13	0.12							
	14.15	1.15	1.15	1.15	1.15	1.15	1.15	1.15	1.15	1.15	1.15	1.15	1.15	1.15	1.15	1.15	1.15							
128-D2									96	88	80	73	66	60	55	50	45	42	38	34	31			
	5.48								2.04	2.09	2.12	2.19	2.21	2.21	2.24	2.21	2.16	2.15	2.06	1.95	1.88			
									4.06	4.05	3.98	3.99	3.84	3.64	3.50	3.19	2.81	2.51	1.98	1.38	0.87			
									0.05	0.05	0.05	0.05	0.05	0.05	0.05	0.05	0.05	0.05	0.05	0.05	0.05			
									0.19	0.18	0.17	0.17	0.16	0.16	0.16	0.15	0.14	0.15	0.14	0.13	0.14			
	13.9								1.15	1.15	1.15	1.15	1.15	1.15	1.15	1.15	1.15	1.15	1.15	1.15	1.15			
148-D2														74	68	63	57	53	48	44	40	37	33	30
	4.29													2.86	2.93	2.94	2.93	2.97	2.92	2.85	2.83	2.72	2.57	2.49
														5.23	5.20	4.98	4.70	4.51	4.09	3.59	3.20	2.54	1.78	1.15
														0.05	0.05	0.05	0.05	0.05	0.05	0.05	0.05	0.05	0.05	0.05
														0.18	0.18	0.18	0.17	0.17	0.16	0.15	0.16	0.15	0.14	0.15
	13.65													1.15	1.15	1.15	1.15	1.15	1.15	1.15	1.15	1.15	1.15	1.15
No. of openings.		7	8	8	8	9	9	9	10	10	11	11	11	12	12	12	13	13	13	13	14	14	14	15
Draped point, ft		7.3	7.7	8.0	8.3	8.7	9.0	9.3	9.7	10.0	10.3	10.7	11.0	11.3	11.7	12.0	12.3	12.7	13.0	13.3	13.7	14.0	14.3	14.7

The span is the effective span length between the bearings centerline to centerline

Strand pattern designation:108-D2: 10 = number of strands, 8 = diameter of strand in 16ths, D depressed (S = straight), and 2 = number of depression points

Key: 55 Allowable superimposed service load, psf
2.24 Estimated camber at erection, in.
3.50 Estimated long-term deflection (due to self weight and superimposed dead load only), in.
0.05 Required area of steel for shear, in^2
0.16 Required area of steel at each edge of all opening, in^2
1.15 Instantaneous deflection coefficient.

Table A.8. Section DT-08'-32" without topping, strand patterns 128-D2, 148-D2, and 168-D2.

Strand	e_s	Span, ft																										
Pattern	e_c	50	52	54	56	58	60	62	64	66	68	70	72	74	76	78	80	82	84	86	88	90	92	94	96	98	100	
128-D2	12.04	200	181	164	148	136	124	113	103	95	86	78	71	66	60	54	49	45	40	36	32							
		0.81	0.84	0.87	0.90	0.95	0.97	0.98	0.98	1.02	1.01	1.00	0.97	0.99	0.95	0.89	0.82	0.81	0.72	0.61	0.49							
		1.77	1.82	1.85	1.86	1.94	0.93	1.89	1.84	1.86	1.75	1.62	1.46	1.40	1.18	0.92	0.62	0.44	0.06	-0.37	-0.85							
		0.06	0.06	0.06	0.06	0.06	0.06	0.06	0.06	0.06	0.06	0.06	0.06	0.06	0.06	0.06	0.06	0.06	0.06	0.06	0.06							
		0.22	0.20	0.19	0.18	0.19	0.18	0.17	0.16	0.17	0.16	0.15	0.14	0.15	0.15	0.14	0.13	0.06	0.06	0.06	0.06							
	17.96	1.14	1.14	1.14	1.14	1.14	1.14	1.14	1.14	1.14	1.14	1.14	1.14	1.14	1.14	1.14	1.14	0.14	0.13	0.13	0.12							
148-D2	9.71		215	196	178	164	150	137	125	116	106	97	89	83	76	69	63	59	54	49	44	43	37	33				
			1.03	1.08	1.12	1.19	1.22	1.25	1.27	1.33	1.34	1.34	1.34	1.38	1.35	1.32	1.27	1.29	1.22	1.14	1.04	1.01	0.88	0.74				
			2.28	2.35	2.40	2.53	2.55	2.56	2.54	2.61	2.56	2.47	2.36	2.35	2.18	1.97	1.72	1.61	1.28	0.91	0.49	0.24	-0.28	-0.85				
			0.06	0.06	0.06	0.06	0.06	0.06	0.06	0.06	0.06	0.06	0.06	0.06	0.06	0.06	0.06	0.06	0.06	0.06	0.06	0.06	.0.06	0.06				
			0.23	0.22	0.20	0.22	0.21	0.19	0.18	0.20	0.19	0.18	0.17	0.18	0.17	0.16	0.15	0.16	0.15	0.15	0.14	0.15	0.14	0.14				
	17.71		1.14	1.14	1.14	1.14	1.14	1.14	1.14	1.14	1.14	1.14	1.14	1.14	1.14	1.14	1.14	1.14	1.14	1.14	1.14	1.15	1.14	1.14				
168-D2	8.21				207	191	175	161	147	137	126	116	107	99	92	84	77	72	67	61	56	52	48	43	39	37	33	
					1.34	1.42	1.47	1.52	1.56	1.64	1.66	1.69	1.70	1.76	1.76	1.75	1.72	1.76	1.71	1.65	1.58	1.58	1.48	1.36	1.22	1.17	1.00	
					2.94	3.10	3.17	3.21	3.24	3.36	3.35	3.31	3.24	3.29	3.17	3.01	2.82	2.76	2.5	2.18	1.82	1.63	1.17	0.66	0.09	-0.27	-0.96	
					0.06	0.06	0.06	0.06	0.06	0.06	0.06	0.06	0.06	0.06	0.06	0.06	0.06	0.06	0.06	0.06	0.06	0.06	0.06	0.06	0.06	0.06	0.0	
					0.23	0.25	0.23	0.22	0.21	0.22	0.21	0.20	0.19	0.20	0.19	0.18	0.17	0.18	0.17	0.17	0.16	0.17	0.16	0.15	0.15	0.15	0.15	
	17.46				1.14	1.14		1.14	1.14	1.14	1.14	1.14	1.14	1.14	1.14	1.14	1.14	1.14	1.14	1.14	1.14	1.15	1.14	1.14	1.14	1.15	1.14	
No. of openings		6	6	6	6	7	7	7	7	8	8	8	8	9	9	9	9	10	10	10	10	11	11	11	11	12	12	
Draped point, ft		8.3	8.7	9.0	9.3	9.7	10.0	10.3	10.7	11.0	11.3	11.7	12.0	12.3	12.7	13.0	13.3	13.7	14.0	14.3	14.7	15.0	15.3	15.7	16.0	16.3	16.7	

The span is the effective span length between the bearings centerline to centerline

Strand pattern designation:108-D2: 10 = number of strands, 8 = diameter of strand in 16ths, D depressed (S = straight), and 2 = number of depression points

Key: 89 Allowable superimposed service load, psf
1.34 Estimated camber at erection, in.
2.36 Estimated long-term deflection (due to self weight and superimposed dead load only), in.
0.06 Required area of steel for shear, in^2
0.17 Required area of steel at each edge of all opening, in^2
1.14 Instantaneous deflection coefficient.

Table A.9. Section DT-08'-32" without topping, strand patterns 188-D2, 208-D2, and 228-D2.

Strand	e_s	Span, ft																									
Pattern	e_c	60	62	64	66	68	70	72	74	76	78	80	82	84	86	88	90	92	94	96	98	100	102	104	106	108	110
188-D2	6.82	200	183	169	157	145	134	124	116	107	99	91	85	79	73	67	63	58	53	49	46	42	38				
		1.71	1.77	1.82	1.92	1.97	2.00	2.04	2.12	2.14	2.14	2.14	2.20	2.17	2.13	2.08	2.11	2.03	1.93	1.82	1.80	1.66	1.49				
		3.74	3.83	3.89	4.06	4.09	4.09	407	4.17	4.09	3.98	3.83	3.84	3.62	3.36	3.05	2.93	2053	2.07	1.56	1.27	0.64	-0.05				
		0.06	0.06	0.06	0.06	0.06	0.06	0.06	0.06	0.06	0.06	0.06	0.06	0.06	0.06	0.06	0.06	0.06	0.06	0.06	0.06	0.06	0.06				
		0.26	0.25	0.23	0.25	0.23	0.22	0.21	0.22	0.21	0.20	0.19	0.20	0.19	0.19	0.18	0.19	0.18	0.17	0.06	0.17	0.17	0.16				
	17.21	1.14	1.14	1.14	1.14	1.14	1.14	1.14	1.14	1.14	1.14	1.14	1.14	1.14	1.14	1.14	1.15	1.14	1.14	1.14	1.15	1.14	1.14				
208-D2	5.71						151	140	131	122	113	104	98	91	84	78	74	68	63	58	55	51	47	43	40		
							2.32	2.37	2.47	2.51	2.53	2.55	2.63	2.63	2.61	2.58	2.63	2.57	2.50	2.41	2.42	2.30	2.16	1.99	1.95		
							4.86	4.88	5.03	5.00	4.94	4.84	4.90	4.73	4.52	4.26	4.20	3.86	3.46	3.00	2.78	2.22	1.58	0.88	0.46		
							0.06	0.06	0.06	0.06	0.06	0.06	0.06	0.06	0.06	0.06	0.06	0.06	0.06	0.06	0.06	0.06	0.06	0.06	0.06		
							0.24	0.23	0.25	0.23	0.22	0.21	0.22	0.21	0.20	0.20	0.21	0.20	0.19	0.18	0.18	0.18	0.18	0.17	0.18		
	16.96						1.14	1.14	1.14	1.14	1.14	1.14	1.14	1.14	1.14	1.14	1.15	1.14	1.14	1.14	1.15	1.14	1.14	1.14	1.15		
228-D2	4.80										126	117	110	103	96	89	84	78	72	67	63	59	54	50	47	44	40
											2.91	2.94	3.05	3.06	3.07	3.06	3.13	3.10	3.05	2.98	3.02	2.92	2.80	2.66	2.64	2.47	2.26
											5.86	5.81	5.92	5.80	5.64	5.44	5.44	5.12	4.80	4.40	4.25	3.74	3.16	2.52	2.17	1.40	0.54
											0.06	0.06	0.06	0.06	0.06	0.06	0.06	0.06	0.06	0.06	0.06	0.06	0.06	0.06	0.06	0.06	0.06
											0.24	0.23	0.25	0.23	0.22	0.21	0.22	0.22	0.21	0.20	0.21	0.20	0.19	0.18	0.19	0.19	0.17
	16.71										1.14	1.14	1.14	1.14	1.14	1.14	1.15	1.14	1.14	1.14	1.15	1.14	1.14	1.14	1.15	1.14	1.14
No. of openings		7	7	7	8	8	8	8	9	9	9	9	10	10	10	10	11	11	11	11	12	12	12	12	13	13	13
Draped point, ft		10.0	10.3	10.7	11.0	11.3	11.7	12.0	12.3	12.7	13.0	13.3	13.7	14.0	14.3	14.7	15.0	15.3	15.7	16.0	16.3	16.7	17.0	17.3	17.7	18.0	18.3

The span is the effective span length between the bearings ceterline to centerline

Strand pattern designation:108-D2: 10 = number of strands, 8 = diameter of strand in 16ths, D depressed (S = straight), and 2 = number of depression points

Key: 84 Allowable superimposed service load, psf
2.61 Estimated camber at erection, in.
4.52 Estimated long-term deflection (due to self weight and superimposed dead load only), in.
0.06 Required area of steel for shear, in^2
0.20 Required area of steel at each edge of all opening, in^2
1.14 Instantaneous deflection coefficient.

Table A.10. Section DT-08'-20" with topping, strand patterns 48-S, 68-S, and 68-D2.

Strand Pattern	e_c	e_s 24	26	28	30	32	34	Span, ft 36	38	40	42	44	46	48
48-S	11.59	183	148	120	98	80	65	52	41	33				
		0.16	0.18	0.20	0.22	0.23	0.24	0.24	0.24	0.23				
		0.35	0.39	0.40	0.41	0.41	0.40	0.35	0.29	0.20				
		0.05	0.05	0.05	0.05	0.05	0.05	0.05	0.05	0.05				
		0.08	0.09	0.08	0.09	0.10	0.10	0.09	0.09	0.09				
	11.59	1.09	1.10	1.10	1.11	1.12	1.13	1.12	1.13	1.13				
68-S	8.59		198	163	135	113	94	78	65	54	43	35		
			0.22	0.24	0.26	0.28	0.30	0.30	0.31	0.31	0.29	0.28		
			0.47	0.49	0.52	0.54	0.54	0.51	0.46	0.40	0.29	0.16		
			0.05	0.05	0.05	0.05	0.05	0.05	0.05	0.05	0.05	0.05		
			0.14	0.12	0.13	0.14	0.14	0.13	0.13	0.14	0.12	0.13		
	8.59		1.10	1.10	1.11	1.12	1.13	1.12	1.13	1.13	1.13	1.13		
68-D2	8.59				178	150	127	108	91	78	66	55	46	38
					0.43	0.47	0.52	0.55	0.59	0.62	0.65	0.67	0.67	0.67
					0.93	1.01	1.07	1.11	1.14	1.16	1.15	1.11	1.01	0.90
					0.05	0.05	0.05	0.05	0.05	0.05	0.05	0.05	0.05	0.05
					0.13	0.14	0.14	0.13	0.13	0.14	0.14	0.14	0.13	0.13
	12.09				1.11	1.12	1.13	1.12	1.13	1.13	1.13	1.14	1.13	1.14
No. Of openings		3	4	4	5	6	7	7	8	9	9	10	10	11
Draped point, ft		7.0	7.0	7.0	7.0	7.0	7.0	7.0	7.0	7.0	7.0	7.3	7.7	8.0

The span is the effective span length between the bearings centerline to centerline

Strand pattern designation:108-D2: 10 = number of strands, 8 = diameter of strand in 16ths, D depressed (S = straight), and 2 = number of depression points

Key: 113 Allowable superimposed service load, psf
0.28 Estimated camber at erection, in.
0.54 Estimated long-term deflection (due to self weight and superimposed dead load only), in.
0.05 Required area of steel for shear, in^2
0.14 Required area of steel at each edge of all opening, in^2
1.12 Instantaneous deflection coefficient.

Table A.11. Section DT-08'20" with topping, strand patterns 88-D2, and 108-D2.

Strand Pattern	e_s / e_c	Span, ft												
		34	36	38	40	42	44	46	48	50	52	54	56	58
88-D2	6.59	182	157	135	117	102	88	76	66	56	48	41	34	
		0.75	0.81	0.88	0.95	1.02	1.07	1.11	1.15	1.17	1.19	1.19	1.19	
		1.64	1.75	1.86	1.96	2.05	2.10	2.09	2.08	1.99	1.90	1.72	1.53	
		0.05	0.05	0.05	0.05	0.05	0.05	0.05	0.05	0.05	0.05	0.05	0.05	
		0.19	0.17	0.17	0.18	0.18	0.18	0.17	0.17	0.15	0.15	0.14	0.14	
	11.59	1.13	1.12	1.13	1.13	1.13	1.14	1.13	1.14	1.13	1.14	1.13	1.14	
108-D2	4.59								91.50	80.00	70.50	61.00	53.50	46.00
									1.61	1.66	1.73	1.76	1.81	1.82
									3.19	3.20	3.21	3.13	3.04	2.86
									0.05	0.05	0.05	0.05	0.05	0.05
									0.21	0.19	0.19	0.18	0.18	0.17
	11.59								1.14	1.13	1.14	1.13	1.14	1.13
No. of openings		7	7	8	9	9	10	10	11	12	12	12	13	13
Draped point, ft		7.0	7.0	7.0	7.0	7.0	7.3	7.7	8.0	8.3	8.7	9.0	9.3	9.7

The tension stresses at final is governed by 12 f_c after the double line
The span is the effective span length between the bearings centerline to centerline
Strand pattern designation:108-D2: 10 = nu after the do number of strands, 8 = diameter of strand in 16ths, D depressed (S = straight), and 2 = number of depression points

Key: 102 Allowable superimposed service load, psf
1.02 Estimated camber at erection, in.
2.05 Estimated long-term deflection (due to self weight and superimposed dead load only), in.
0.05 Required area of steel for shear, in^2
0.18 Required area of steel at each edge of all opening, in^2
1.13 Instantaneous deflection coefficient.

Table A.12. Section DT-08'-24" with topping, strand patterns 48-S, 68-S, and 68-D2.

Strand Pattern	e_s / e_c	Span, ft																		
		26	28	30	32	34	36	38	40	42	44	46	48	50	52	54	56	58	60	62
48-S		211	176	150	127	110	94	81	70	61	53	45	38	33						
	14.15	0.15	0.17	0.19	0.21	0.23	0.24	0.26	0.26	0.28	0.29	0.28	0.27	0.26						
		0.34	0.36	0.40	0.42	0.45	0.45	0.45	0.43	0.41	0.38	0.30	0.20	0.10						
		0.05	0.05	0.05	0.05	0.05	0.05	0.05	0.05	0.05	0.05	0.05	0.05	0.05						
		0.10	0.08	0.10	0.09	0.10	0.09	0.09	0.08	0.09	0.09	0.09	0.08	0.08						
	14.15	1.19	1.18	1.21	1.20	1.23	1.22	1.23	1.23	1.24	1.25	1.24	1.24	1.25						
68-S				205	175	152	132	115	100	88	77	68	60	52	46	40	35	30		
	11.15			0.26	0.28	0.31	0.33	0.36	0.38	0.41	0.41	0.43	0.44	0.43	0.43	0.42	0.39	0.37		
				0.56	0.59	0.65	0.67	0.71	0.71	0.72	0.69	0.67	0.60	0.51	0.43	0.28	0.09	-0.07		
				0.05	0.05	0.05	0.05	0.05	0.05	0.05	0.05	0.05	0.05	0.05	0.05	0.05	0.05	0.05		
				0.14	0.13	0.14	0.13	0.14	0.12	0.13	0.12	0.13	0.12	0.11	0.11	0.10	0.10	0.10		
	11.15			1.21	1.20	1.23	1.22	1.23	1.23	1.24	1.23	1.24	1.24	1.24	1.24	1.24	1.24	1.24		
68-DS						185	161	142	124	110	97	87	76	68	60	53	47	42	37	32
	11.15					0.42	0.45	0.50	0.53	0.57	0.60	0.64	0.65	0.67	0.69	0.69	0.69	0.70	0.67	0.64
						0.91	0.96	1.04	1.08	1.13	1.14	1.17	1.14	1.09	1.06	0.96	0.83	0.72	0.51	0.27
						0.05	0.05	0.05	0.05	0.05	0.05	0.05	0.05	0.05	0.05	0.05	0.05	0.05	0.05	0.05
						0.14	0.13	0.14	0.12	0.13	0.12	0.13	0.12	0.11	0.11	0.10	0.10	0.10	0.09	0.09
	14.65					1.23	1.22	1.23	1.23	1.24	1.23	1.24	1.24	1.24	1.24	1.24	1.24	1.24	1.24	1.24
No. of openings		4	4	5	6	7	7	8	9	9	10	10	11	11	12	12	13	13	14	14
Draped point, ft		7.0	7.0	7.0	7.0	7.0	7.0	7.0	7.0	7.0	7.3	7.7	8.0	8.3	8.7	9.0	9.3	9.7	10.0	10.3

The span is the effective span length between the bearings centerline to centerline

Strand pattern designation:108-D2: 10 = number of strands, 8 = diameter of strand in 16ths, D depressed (S = straight), and 2 = number of depression points

Key: 88 Allowable superimposed service load, psf
0.41 Estimated camber at erection, in.
0.72 Estimated long-term deflection (due to self weight and superimposed dead load only), in.
0.05 Required area of steel for shear, in^2
0.13 Required area of steel at each edge of all opening, in^2
1.24 Instantaneous deflection coefficient.

Table A.13. Section DT-08'-24" with topping, strand patterns 88-D2, 108-D2, and 128-D2.

Strand Pattern	e_e / e_c	Span, ft																					
		38	40	42	44	46	48	50	52	54	56	58	60	62	64	66	68	70	72	74	76	78	80
88-D2	9.15	197	174	155	138	124	111	99	90	81	72	66	59	53	48	43							
		0.71	0.76	0.84	0.89	0.95	1.00	1.04	1.10	1.13	1.15	1.20	1.21	1.21	1.23	1.21							
		1.56	1.65	1.78	1.84	1.95	1.98	2.00	2.05	2.02	1.96	1.95	1.83	1.67	1.55	1.31							
		0.05	0.05	0.05	0.05	0.05	0.05	0.05	0.05	0.05	0.05	0.05	0.05	0.05	0.05	0.05							
		0.18	0.16	0.17	0.16	0.17	0.15	0.14	0.15	0.14	0.13	0.13	0.12	0.12	0.12	0.11							
	14.40	1.23	1.23	1.24	1.23	1.24	1.24	1.24	1.24	1.24	1.24	1.24	1.24	1.24	1.24	1.24							
108-D2	7.15				178	160	144	130	118	107	97	88	80	73	66	60	55	50	45	41			
					1.16	1.26	1.33	1.39	1.49	1.55	1.60	1.68	1.72	1.75	1.82	1.83	1.84	1.88	1.86	1.82			
					2.52	2.69	2.79	2.87	3.00	3.05	3.06	3.13	3.09	3.04	2.99	2.84	2.64	2.51	2.21	1.86			
					0.05	0.05	0.05	0.05	0.05	0.05	0.05	0.05	0.05	0.05	0.05	0.05	0.05	0.05	0.05	0.05			
					0.20	0.20	0.19	0.17	0.18	0.17	0.16	0.16	0.15	0.14	0.15	0.14	0.13	0.14	0.13	0.12			
	14.15				1.23	1.24	1.24	1.24	1.24	1.24	1.24	1.24	1.24	1.24	1.24	1.24	1.24	1.24	1.24	1.24			
128-D2	5.48											110	101	92	85	77	71	65	60	54	50	46	42
												2.15	2.22	2.28	2.39	2.44	2.47	2.56	2.57	2.58	2.63	2.61	2.57
												4.27	4.31	4.31	4.38	4.32	4.20	4.17	3.97	3.71	3.53	3.16	2.72
												0.05	0.05	0.05	0.05	0.05	0.05	0.05	0.05	0.05	0.05	0.05	0.05
												0.19	0.18	0.17	0.18	0.17	0.16	0.16	0.15	0.14	0.15	0.14	0.13
	13.90											1.24	1.24	1.24	1.24	1.24	1.24	1.24	1.24	1.24	1.24	1.24	1.24
No. of openings		6	7	7	7	8	8	8	9	9	9	10	10	11	11	11	12	12	12	13	13	13	13
Draped point, ft		7.0	7.0	7.0	7.3	7.7	8.0	8.3	8.7	9.0	9.3	9.7	10.0	10.3	10.7	11.0	11.3	11.7	12.0	12.3	12.7	13.0	13.3

The span is the effective span length between the bearings centerline to centerline
Strand pattern designation:108-D2: 10 = number of strands, 8 = diameter of strand in 16ths, D depressed (S = straight), and 2 = number of depression points

Key: 80 Allowable superimposed service load, psf
1.72 Estimated camber at erection, in.
3.09 Estimated long-term deflection (due to self weight and superimposed dead load only), in.
0.05 Required area of steel for shear, in^2
0.15 Required area of steel at each edge of all opening, in^2
1.24 Instantaneous deflection coefficient.

Table A.14. Section DT-08'-32" with topping, strand patterns 108-D2-128-D2, and 148-D2.

Strand Pattern	e_e / e_c	Span, ft																							
		44	46	48	50	52	54	56	58	60	62	64	66	68	70	72	74	76	78	80	82	84	86	88	90
108-D2	15.31	236	211	189	171	154	139	125	114	103	93	84	76	69	62	55	50	45	40						
		0.52	0.55	0.58	0.62	0.64	0.66	0.68	0.71	0.72	0.72	0.72	0.74	0.73	0.71	0.68	0.67	0.62	0.57						
		1.14	1.19	1.22	1.29	1.31	1.32	1.31	1.33	1.29	1.24	1.16	1.12	1.00	0.85	0.68	0.55	0.31	0.05						
		0.06	0.06	0.06	0.06	0.06	0.06	0.06	0.06	0.06	0.06	0.06	0.06	0.06	0.06	0.06	0.06	0.06	0.06						
		0.20	0.18	0.17	0.18	0.17	0.16	0.15	0.16	0.15	0.14	0.13	0.14	0.14	0.13	0.12	0.13	0.12	0.12						
	18.21	1.21	1.21	1.21	1.22	1.22	1.21	1.21	1.22	1.22	1.21	1.21	1.22	1.22	1.22	1.21	1.22	1.22	1.22						
128-D2	12.04			234	212	192	174	158	145	132	120	109	100	91	83	75	69	63	57	51	47	42			
				0.73	0.79	0.83	0.86	0.89	0.94	0.96	0.98	1.00	1.03	1.04	1.04	1.03	1.04	1.02	0.98	0.94	0.92	0.86			
				1.60	1.71	1.76	1.80	1.82	1.89	1.89	1.87	1.83	1.87	1.77	1.66	1.54	1.46	1.27	1.06	0.81	0.61	0.27			
				0.06	0.06	0.06	0.06	0.06	0.06	0.06	0.06	0.06	0.06	0.06	0.06	0.06	0.06	0.06	0.06	0.06	0.06	0.06			
				0.20	0.22	0.20	0.19	0.18	0.19	0.18	0.17	0.16	0.17	0.16	0.15	0.14	0.15	0.15	0.14	0.13	0.14	0.13			
	17.96			1.21	1.22	1.22	1.21	1.21	1.22	1.22	1.21	1.21	1.22	1.22	1.22	1.21	1.22	1.22	1.22	1.21	1.22	1.22			
148-D2	9.71					229	209	190	175	160	146	134	123	113	103	95	87	80	73	67	62	56	51	46	42
						1.00	1.05	1.09	1.16	1.20	1.24	1.27	1.32	1.34	1.36	1.37	1.40	1.40	1.38	1.36	1.37	1.32	1.27	1.20	1.17
						2.19	2.26	2.32	2.43	2.47	2.49	2.49	2.55	2.51	2.45	2.37	2.34	2.21	2.04	1.84	1.70	1.43	1.12	0.77	0.48
						0.06	0.06	0.06	0.06	0.06	0.06	0.06	0.06	0.06	0.06	0.06	0.06	0.06	0.06	0.06	0.06	0.06	0.06	0.06	0.06
						0.23	0.22	0.20	0.22	0.21	0.19	0.18	0.20	1.09	0.18	0.17	0.18	0.17	0.16	0.15	0.16	0.15	0.15	0.14	0.15
	17.71					1.22	1.21	1.21	1.22	1.22	1.21	1.21	1.22	1.22	1.22	1.21	1.22	1.22	1.22	1.21	1.22	1.22	1.22	1.22	1.22
No. of openings		5	5	5	6	6	6	6	7	7	7	7	8	8	8	8	9	9	9	9	10	10	10	10	11
Draped point, ft		7.3	7.7	8.0	8.3	8.7	9.0	9.3	9.7	10.0	10.3	10.7	11.0	11.3	11.7	12.0	12.3	12.7	13.0	13.3	13.7	14.0	14.3	14.7	15.0

The span is the effective span length between the bearings centerline to centerline

Strand pattern designation:108-D2: 10 = number of strands, 8 = diameter of strand in 16ths, D depressed (S = straight), and 2 = number of depression points

Key: 120 Allowable superimposed service load, psf
0.98 Estimated camber at erection, in.
1.87 Estimated long-term deflection (due to self weight and superimposed dead load only), in.
0.06 Required area of steel for shear, in^2
0.17 Required area of steel at each edge of all opening, in^2
1.21 Instantaneous deflection coefficient.

Table A.15. Section DT-08'-32" with topping, strand patterns 168-D2, 188-D2, and 208-D2.

Strand	e_c	Span, ft																									
Pattern	e_c	56	58	60	62	64	66	68	70	72	74	76	78	80	82	84	86	88	90	92	94	96	98	100	102	104	106
		221	204	187	171	157	146	134	123	114	105	97	89	82	76	70	64	59	55	50	45	41					
168-D2	8.21	1.29	1.38	1.43	1.48	1.53	1.60	1.67	1.67	1.70	1.76	1.77	1.77	1.77	1.80	1.78	1.75	1.70	1.70	1.63	1.55	1.45					
		2.81	2.97	3.07	3.09	3.13	3.24	3.24	3.22	3.18	3.21	3.12	3.00	2.84	2.76	2.54	2.28	1.98	1.76	1.38	0.94	0.46					
		0.06	0.06	0.06	0.06	0.06	0.06	0.06	0.06	0.06	0.06	0.06	0.06	0.06	0.06	0.06	0.06	0.06	0.06	0.06	0.06	0.06					
		0.23	0.25	0.24	0.22	0.21	0.22	0.21	0.20	0.19	0.20	0.19	0.18	0.17	0.18	0.17	0.17	0.16	0.17	0.16	0.15	0.15					
	17.46	1.21	1.22	1.22	1.21	1.21	1.22	1.22	1.22	1.21	1.22	1.22	1.22	1.21	1.22	1.22	1.22	1.22	1.22	1.22	1.22	1.22					
				213	196	181	167	155	143	132	123	113	105	97	90	84	77	71	66	61	56	52	48	44	40		
188-D2	6.82			1.66	1.72	1.78	1.88	1.93	1.98	2.02	2.10	2.13	2.15	2.17	2.22	2.22	2.21	2.18	2.21	2.16	2.10	2.03	2.00	1.90	1.78		
				3.59	3.68	3.76	3.91	3.95	3.97	3.97	4.05	4.00	3.93	3.82	3.90	3.63	3.42	3.17	3.01	2.68	2.30	1.87	1.54	1.01	0.42		
				0.06	0.06	0.06	0.06	0.06	0.06	0.06	0.06	0.06	0.06	0.06	0.06	0.06	0.06	0.06	0.06	0.06	0.06	0.06	0.06	0.06	0.06		
				0.26	0.25	0.23	0.25	0.24	0.22	0.21	0.22	0.21	0.20	0.19	1.20	0.20	1.09	0.18	0.19	0.18	0.17	0.17	0.17	0.17	0.16		
	17.21			1.22	1.21	1.21	1.22	1.22	1.22	1.21	1.22	1.22	1.2.	1.21	1.22	1.22	1.22	1.22	1.22	1.22	1.22	1.22	1.22	1.22	1.22		
									162	150	140	129	120	111	104	97	90	83	78	72	67	62	58	53	49	45	42
208-D2	5.71								2.28	2.33	2.43	2.48	2.52	2.55	2.63	2.65	2.66	2.65	2.70	2.68	2.64	2.58	2.59	2.51	2.41	2.30	2.25
									4.70	4.74	4.87	1.86	4.83	4.77	4.80	4.68	4.52	4.32	4.22	3.94	3.61	3.24	2.98	2.50	1.97	1.37	0.90
									0.06	0.06	0.06	0.06	0.06	0.06	0.06	0.06	0.06	0.06	0.06	0.06	0.06	0.06	0.06	0.06	0.06	0.06	0.06
									0.25	0.23	0.25	0.23	0.22	0.21	0.23	0.22	0.21	0.20	0.21	0.20	0.19	0.18	1.09	0.18	0.18	0.17	0.18
	16.96								1.22	1.21	1.22	1.22	1.22	1.21	1.22	1.22	1.22	1.22	1.22	1.22	1.22	1.22	1.22	1.22	1.22	1.22	1.22
No. of openings		6	7	7	7	7	8	8	8	8	9	9	9	9	10	10	10	10	11	11	11	11	22	1.22	1.22	1.22	1.22
Draped point, ft		9.3	937	10.0	10.3	10.7	11.0	11.3	11.7	12.0	12.3	12.7	13.0	133.	13.4	14.0	14.3	14.7	15.0	15.3	15.7	16.0	16.3	16.7	17.0	17.3	17.7

The span is the effective span length between the bearings centerline to centerline

Strand pattern designation:108-D2: 10 = number of strands, 8 = diameter of strand in 16ths, D depressed (S = straight), and 2 = number of depression points

Key: 123 Allowable superimposed service load, psf
2.10 Estimated camber at erection, in.
4.05Estimated long-term deflection (due to self weight and superimposed dead load only), in.
0.06 Required area of steel for shear, in^2
0.22 Required area of steel at each edge of all opening, in^2
1.22 Instantaneous deflection coefficient.

Table A.16. (B-1) DT-08-24 single tee section properties with and without web openings

Properties	Solid section		Openings section	
cross-section area, in^2	A_s	201	A_o	140
distance from bottom, in.	y_{bs}	17.15	y_{bo}	18.41
distance from top, in.	y_{ts}	6.85	y_{to}	5.59
moment of inertia, in^4	I_s	10492.5	I_o	9032
bottom section modulus, in^3	Z_{bs}	612	Z_{bo}	491
top section modulus, in^3	Z_{ts}	1532	Z_{to}	1615
weight of the beam, plf	W_s	214	W_o	146
weight of the beam, psf	W_s	52	W_o	37
V/S		1.41		

Table A.17. Section properties of single tee for solid and with openings sections.

Properties	Solid section			Openings section		
		untopped	topped		untopped	topped
cross-section area, in^2	A_s	182	278	A_o	141	237
distance from bottom, in.	y_{bs}	14.59	16.81	y_{bo}	15.30	17.61
distance from top, in.	y_{ts}	5.41	5.19	y_{to}	4.70	4.39
moment of inertia, in^4	I_s	6276	8890	I_o	5740	7626
bottom section modulus, in^3	Z_{bs}	430	529	Z_{bo}	375	433
top section modulus, in^3	Z_{ts}	1160	1713	Z_{to}	1221	1738
weight of the beam, plf	W_s	189	289	W_o	147	247
weight of the beam, psf	W_s	52	72	W_o	37	62
V/S		1.41			1.19	

Table A.18. B-4 Bending moment at different sections (ft-kips).

	due to self weight	due to topping	due to SIDL	due to L.L.	Ultimate
At transfer	7.72	4.57	2.74	9.14	37
At draping	24.92	14.75	8.85	29.49	118
At midspan	44.70	26.45	15.87	52.90	212

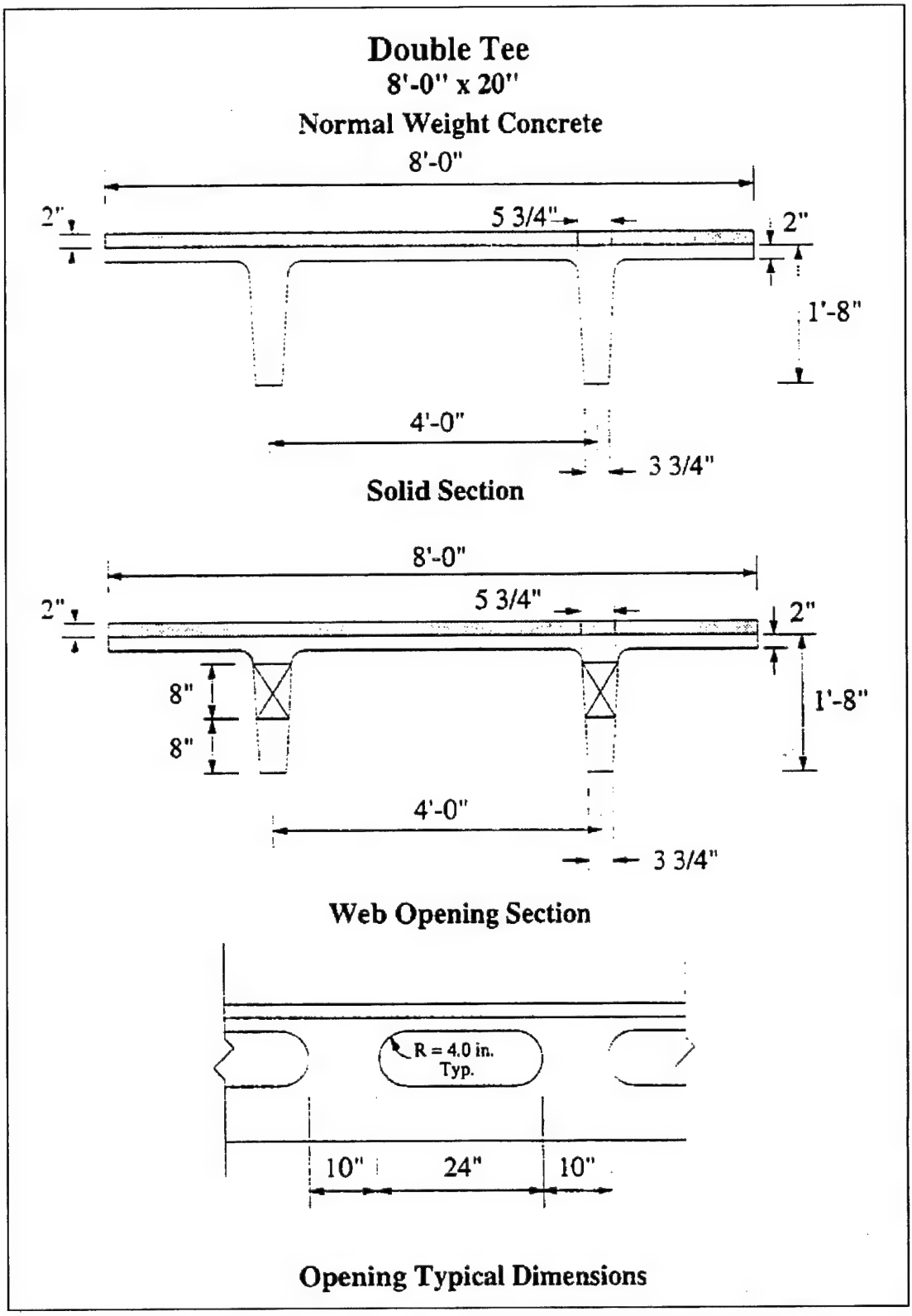

Figure A.1. Cross-section details of DT-8'-20".

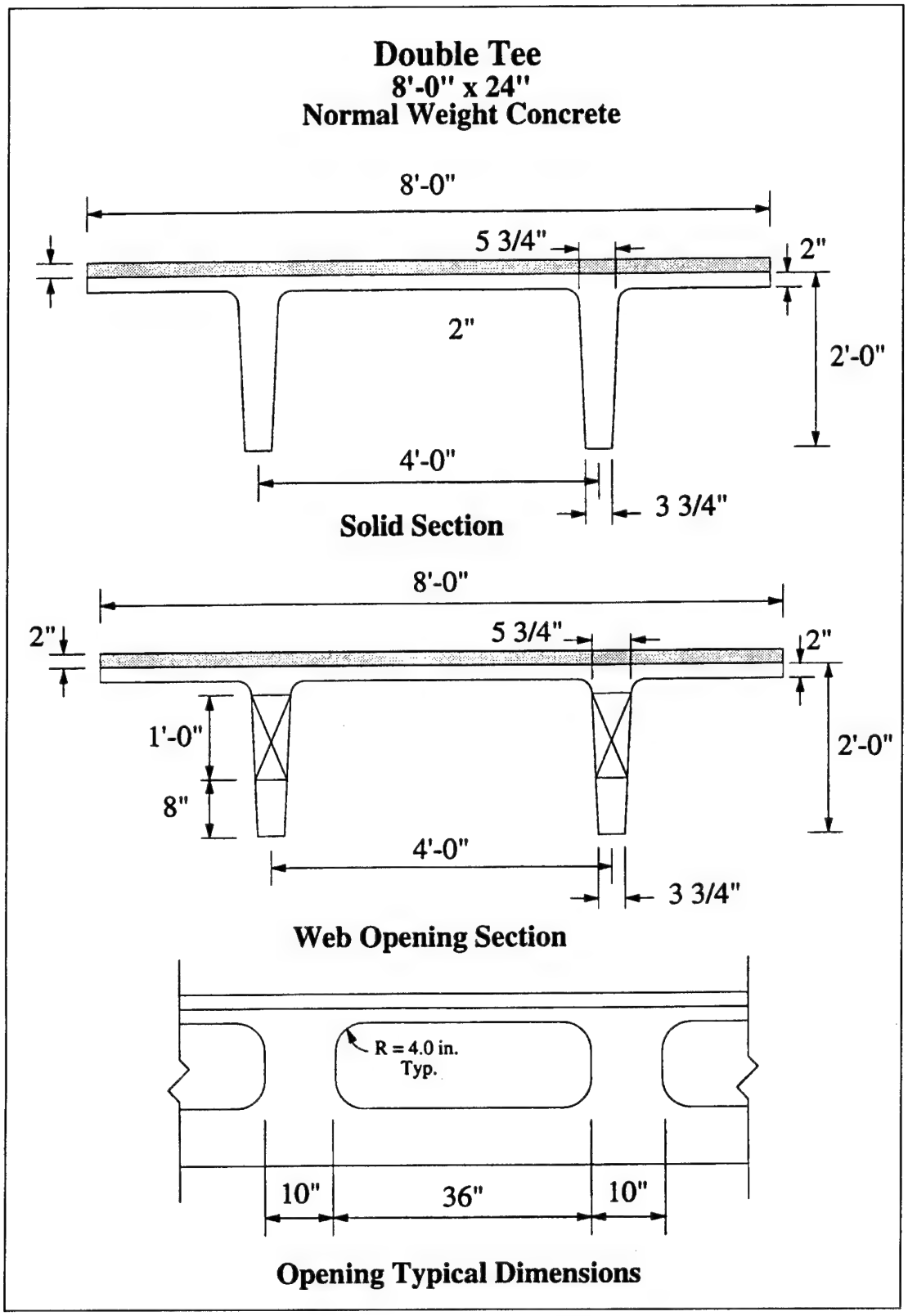

Figure A.2. Cross-section details of DT-8'-24".

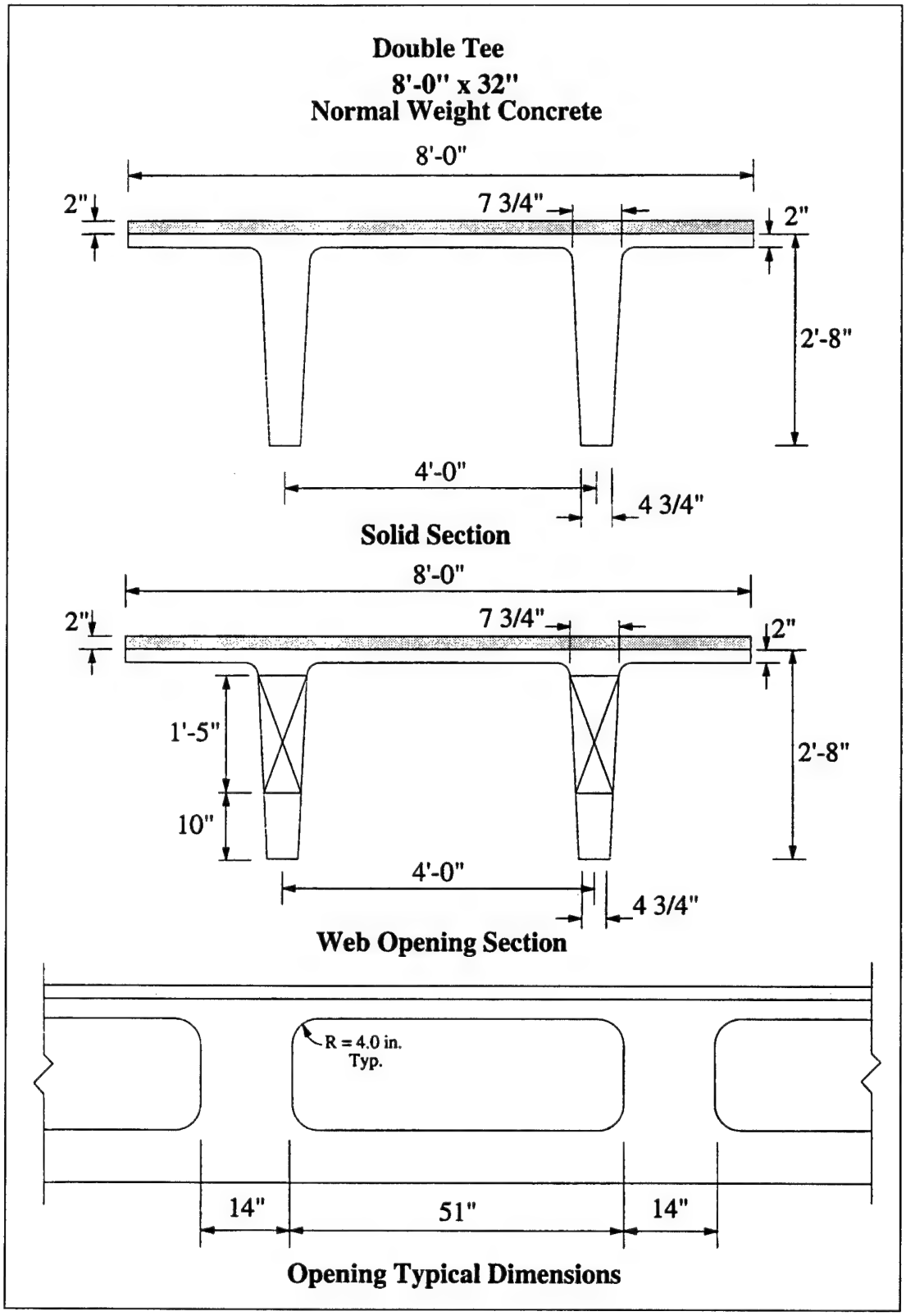

Figure A.3. Cross-section detail of DT 8'-32".

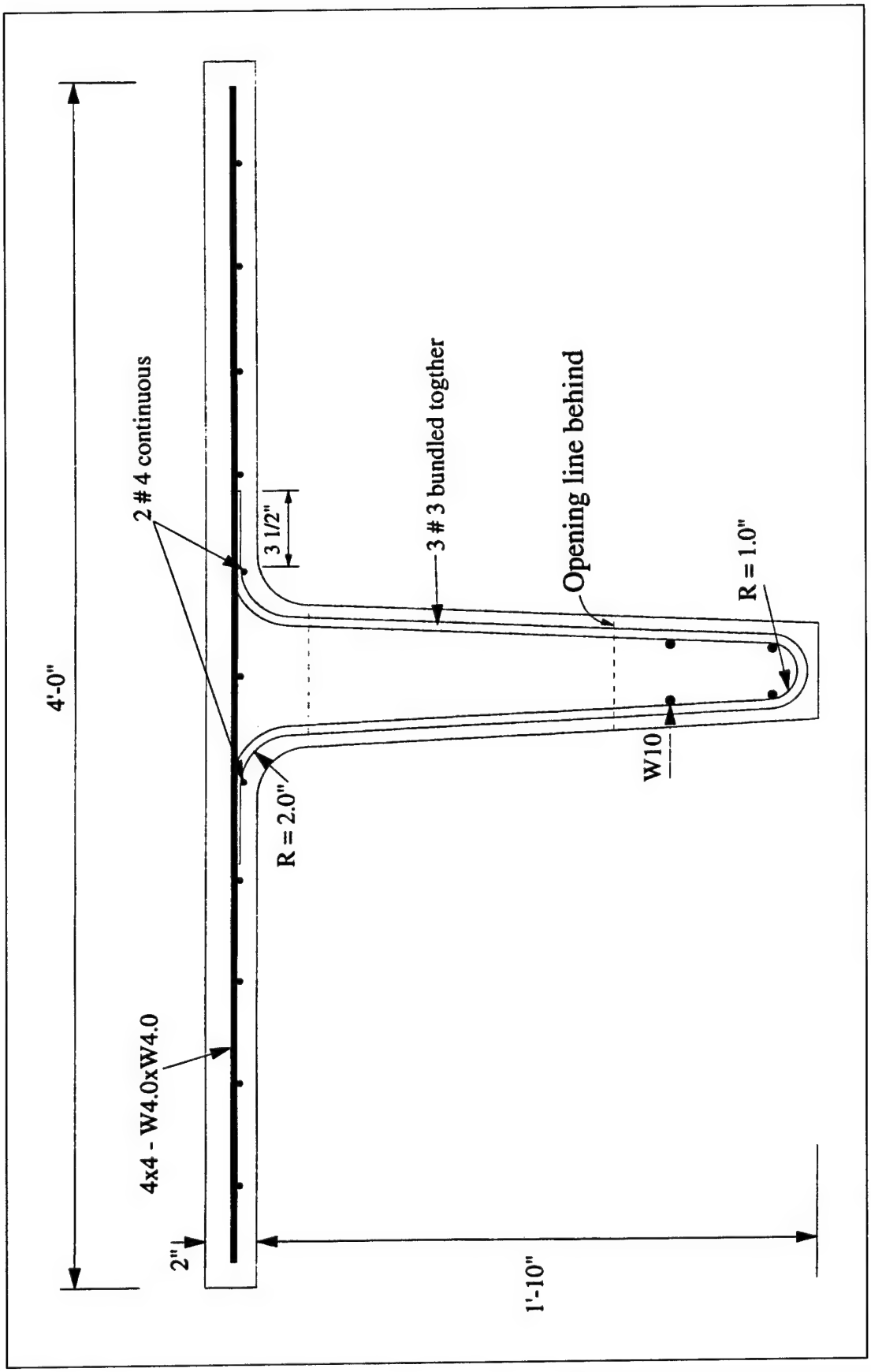

Figure A.4. Details of the reinforcement at the edge of the opening.

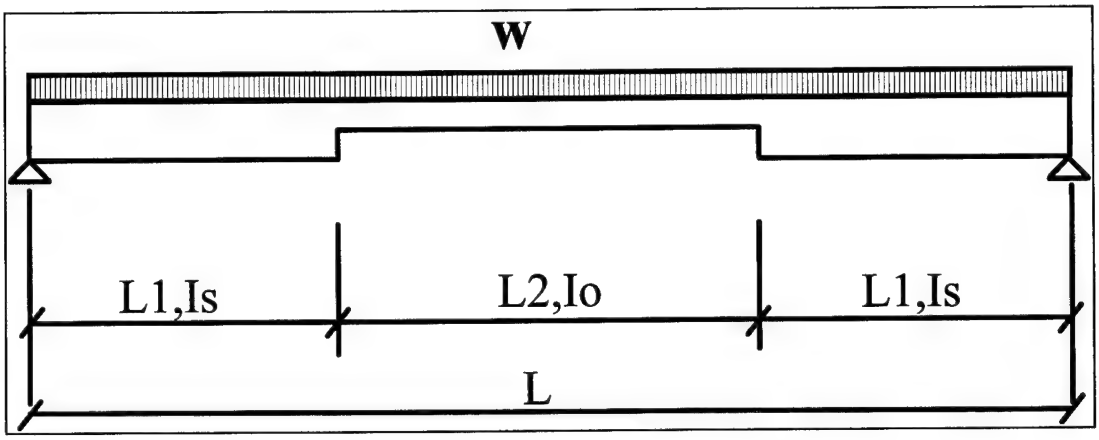

Figure A.5. Idealized double-tee beam with varying moment of inertia.

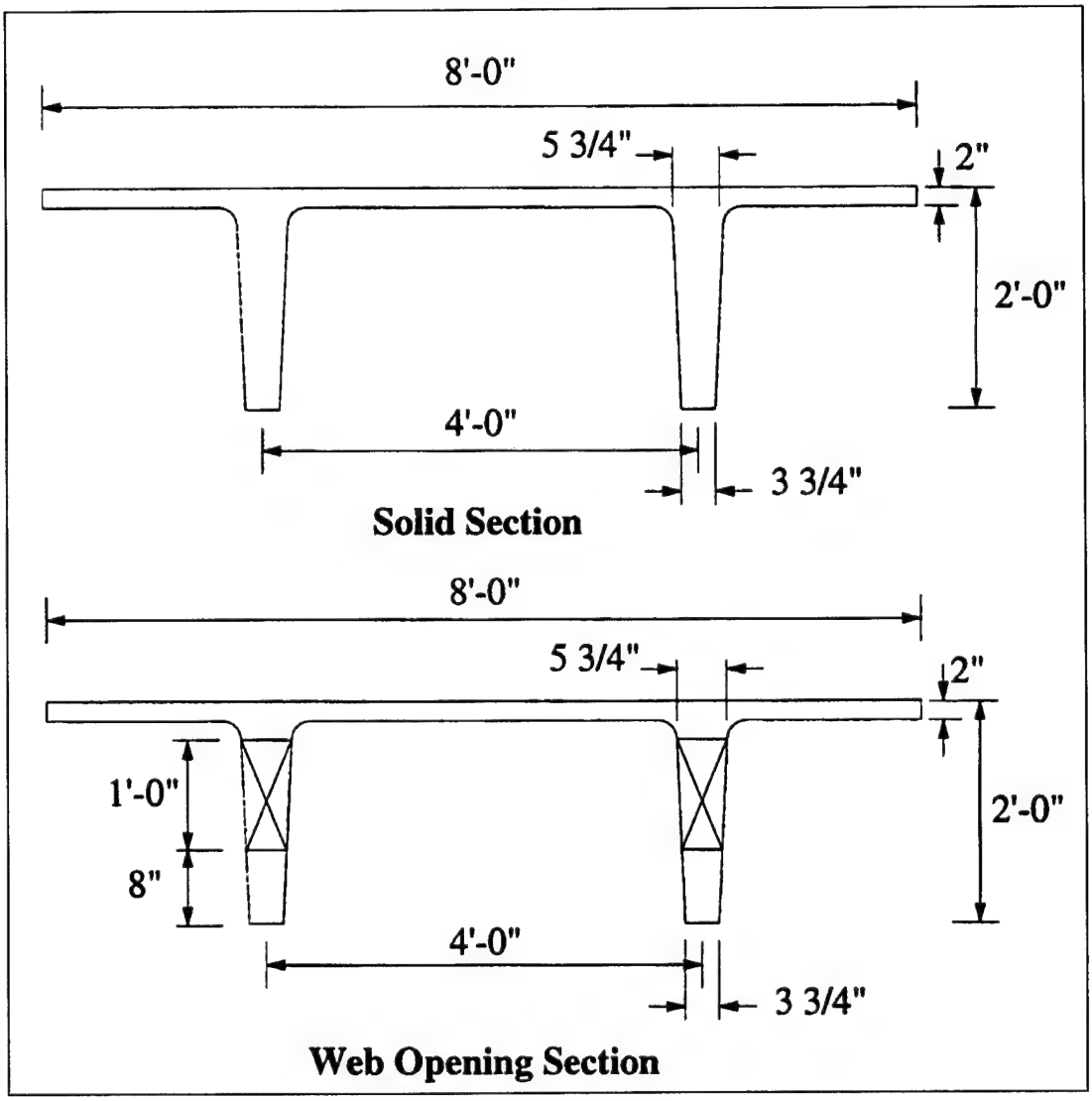

Figure A.6. Cross-section dimensions for solid and with web opening sections.

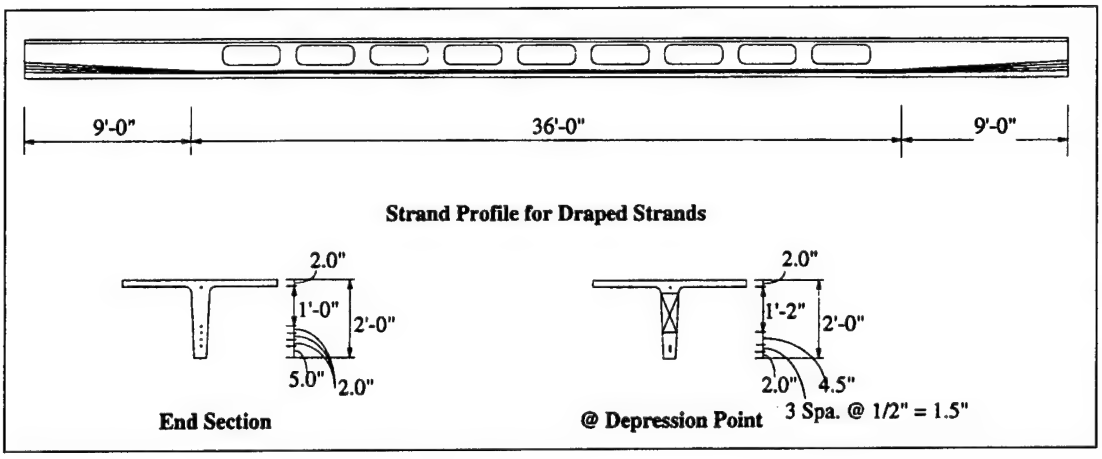

Figure A.7. Strand pattern and eccentricity.

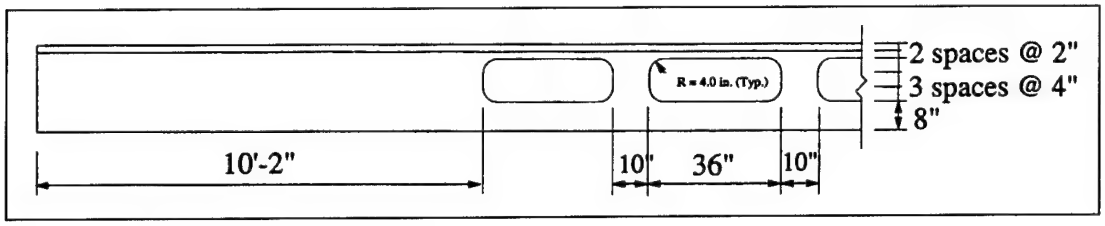

Figure A.8. Typical opening dimensions.

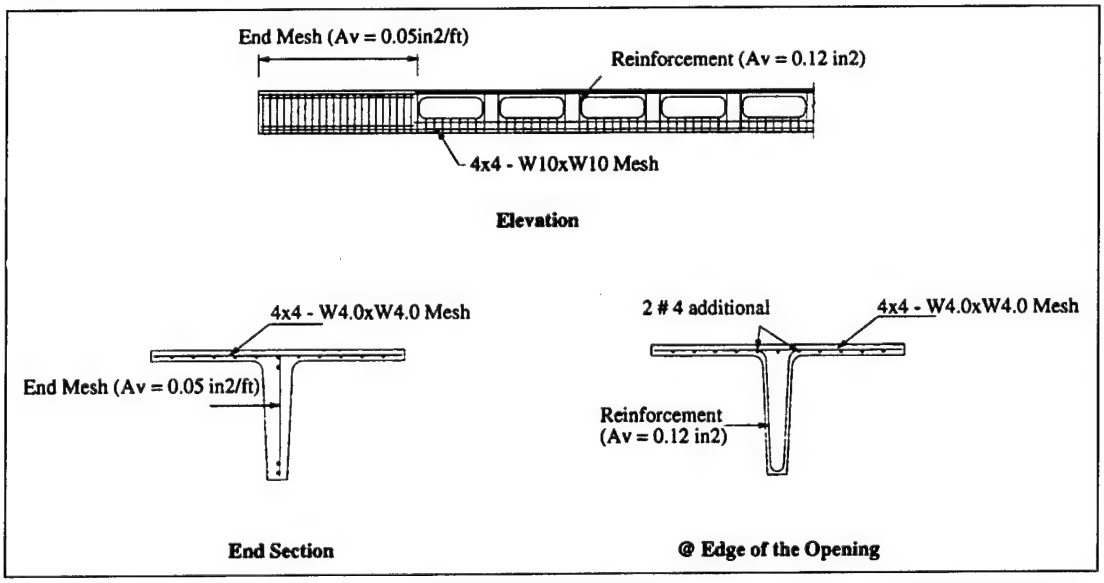

Figure A.9. Reinforcement details.

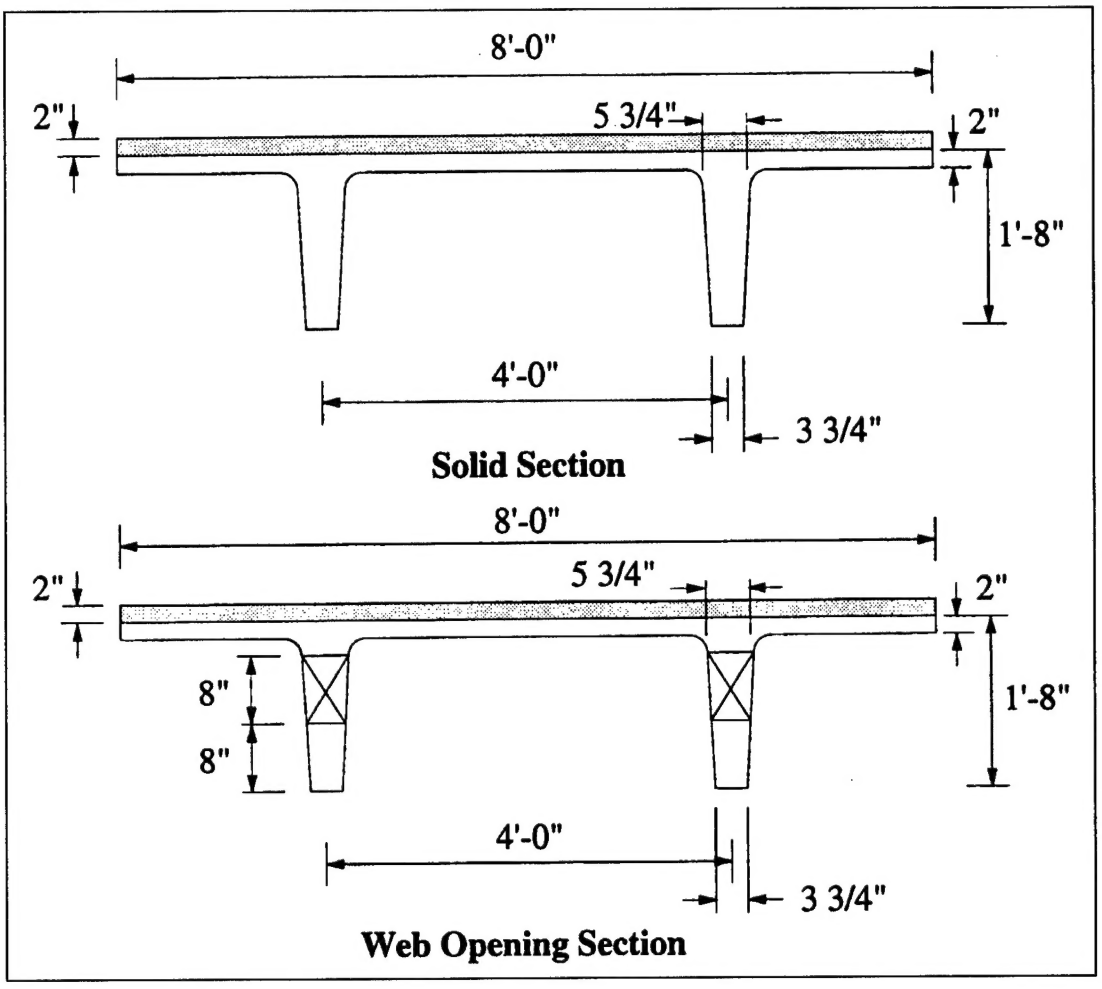

Figure A.10. Cross-section dimensions for solid and web opening sections.

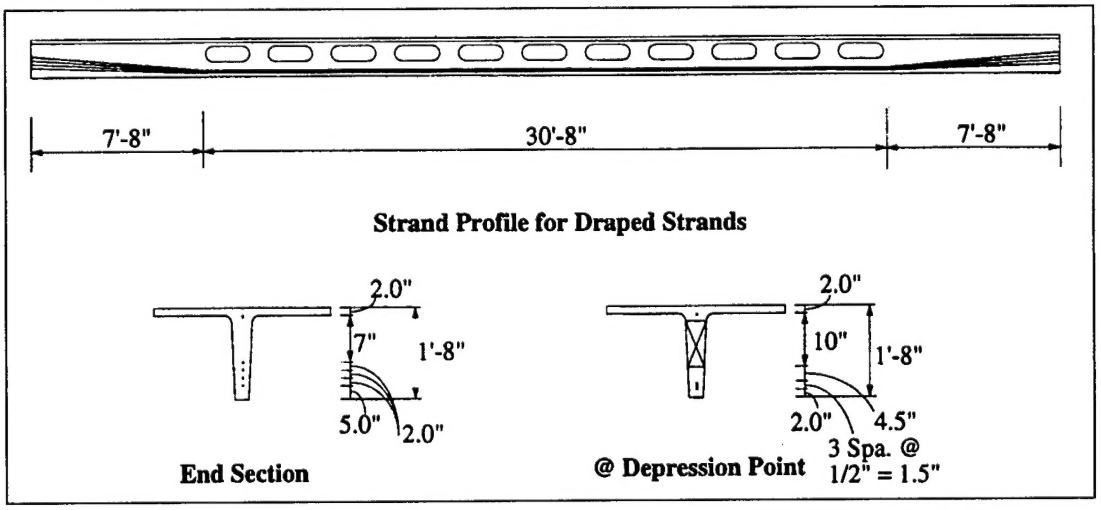

Figure A.11. Strand pattern and eccentricity.

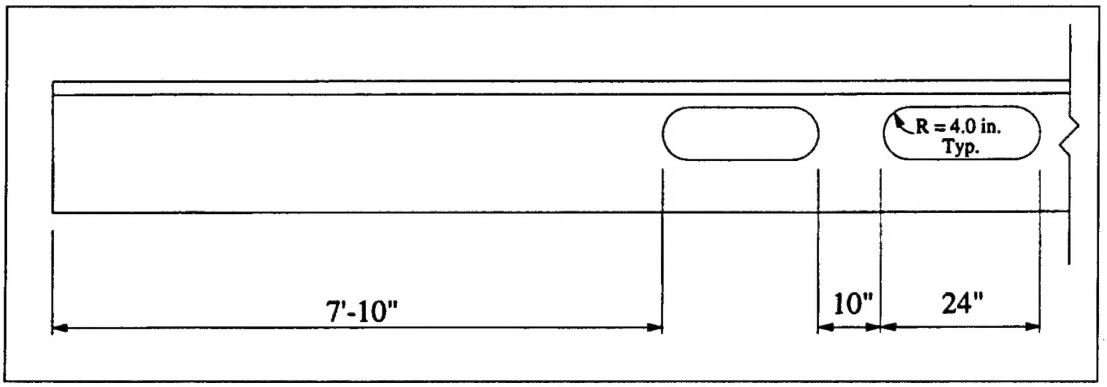

Figure A.12. Typical opening dimensions.

Abbreviations and Acronyms

ASCII	American Standard Code for Information Interchange
CIP	cast-in-place
kip	kilopound
ksi	kilopounds per square inch
OWSJ	open web steel joist
PCI	Prestressed Concrete Institute
plf	pounds per linear foot
psi	pounds per square inch
psf	pounds per square foot
USACE	U.S. Army Corps of Engineers
USACERL	U.S. Army Construction Engineering Research Laboratories

USACERL DISTRIBUTION

Chief of Engineers
ATTN: CEHEC-IM-LH (2)
ATTN: CEHEC-IM-LP (2)
ATTN: CEMP-CE
ATTN: CEMP-ET
ATTN: CERD-C (2)
ATTN: CERD-L
ATTN: CERD-M

Fort Belvoir 22060
ATTN: CECC-R

US Army Engineer District
ATTN: Library (40)

US Army Engineer Divisions
ATTN: Library (11)

Defense Tech Info Center 22304
ATTN: DTIC-O (2)

64
11/97